Master Thesis in Geographical Information Science nr 66

Study of spatial and temporal variation of atmospheric optical parameters and their relation with PM 2.5 concentration over Europe using GIS technologies

Panagiotis Symeonidis

2017
Department of
Physical Geography and Ecosystem Science
Centre for Geographical Information Systems
Lund University
Sölvegatan 12
S-223 62 Lund
Sweden

Panagiotis Symeonidis (2017). Study of spatial and temporal variation of atmospheric optical parameters and their relation with PM 2.5 concentration over Europe using GIS technologies
Master degree thesis, 30/ credits in Master in Geographical Information Science
Department of Physical Geography and Ecosystem Science, Lund University

Study of spatial and temporal variation of atmospheric optical parameters and their relation with PM 2.5 concentration over Europe using GIS technologies

---

Panagiotis Symeonidis

Master thesis, 30 credits, in Geographical Information Sciences

Dr. Thomas Holst
Department of Physical Geography and Ecosystem Science
Centre for GeoBiosphere Science
Lund University

Exam committee:

Prof. David Tenenbaum
Department of Physical Geography and Ecosystem Science
Centre for GeoBiosphere Science
Lund University

As. Prof. Cecilia Akselsson
Department of Physical Geography and Ecosystem Science
Centre for GeoBiosphere Science
Lund University

Abstract

The purpose of this study was to examine the use of remote sensing aerosol data as an estimator of ground level fine particulate matter concentration (PM 2.5). In order to examine this possible relation, daily MODIS Aerosol Optical Depth (AOD) data were used, collected for an entire year. The analysis involved manipulation of pollution and meteorological data, such as the PM 2.5 concentration which resulted from a regional photochemical model and meteorological parameters like wind speed, mixing height and humidity, which in turn resulted from the application of a prognostic meteorological model for the whole of Europe. Statistical regression analysis was performed for the aforementioned data in several locations of big urban agglomerations all over Europe, where the problem of particulate matter air pollution is higher, as well as its impact on man and the environment. Furthermore, the relation of AOD with PM 2.5 and meteorological parameters was also examined using PM 2.5 measurements of two operational air pollution stations located in Attica, Greece.

The study confirmed a conclusion reached by other relevant studies, that the relationship between AOD and PM 2.5 is highly variable for different regions and for different time scales (Engel-Cox, 2004; Hu et al, 2013). A strong correlation of AOD – PM 2.5 was established for winter and autumn in most locations. During spring and especially summer the regression models did not produce good results for most of the places that were applied.

The study also confirmed that the use of meteorological data can improve the PM 2.5 to AOD correlation. AOD or AOD/PBL was the most dominant factor in the regression analysis only in 40 % of the cases with good results. In 60 % of cases, one of the meteorological factors (RH, WS or PBL) was the most important factor in the regression equation.

Περίληψη

Σκοπός της συγκεκριμένης εργασίας είναι να εξετάσει την πιθανή σχέση ανάμεσα στα σωματίδια που μετρούνται με μεθόδους τηλεπισκόπισης και τα αιωρούμενα σωματίδια της κατώτερης ατμόσφαιρας (PM 2.5). Για το σκοπό αυτό χρησιμοποιείται το οπτικό βάθος (Aerosol Optical Depth) του MODIS σε ημερήσια βάση και για ένα ολόκληρο έτος. Για τις συγκεντρώσεις των σωματιδίων χρησιμοποιούνται τα αποτελέσματα ενός φωτοχημικού μοντέλου. Η περιοχή αναφοράς είναι η Ευρώπη. Στην εξεταζόμενη σχέση λαμβάνονται επιπλέον υπόψη και μετεωρολογικές παράμετροι όπως η υγρασία, η ταχύτητα ανέμου και το ύψος ανάμιξης όπως αυτά έχουν προκύψει από την εφαρμογή ενός προγνωστικού μετεωρολογικού μοντέλου. Η στατιστική ανάλυση πραγματοποιείται σε επιλεγμένα σημεία που αφορούν μεγάλα αστικά κέντρα της Ευρώπης, όπου το πρόβλημα τη σωματιδιακής αέριας ρύπανσης είναι μεγαλύτερο όπως και οι επιπτώσεις της στον άνθρωπο και στο περιβάλλον. Η σχέση αυτών των παραμέτρων εξετάζεται επίσης με βάση τα δεδομένα μετρήσεων δύο σταθμών ατμοσφαιρικής ρύπανσης στην Αττική.

Τα αποτελέσματα της εργασίας επιβεβαίωσαν ότι, η συσχέτιση της συγκέντρωσης των αιωρούμενων σωματιδίων με το οπτικό βάθος που προκύπτει από τις δορυφορικές παρατηρήσεις, είναι ιδιαίτερα μεταβλητή για διαφορετικές περιοχές και χρονικές κλίμακες. Επομένως η σχέση μεταξύ αυτών των παραμέτρων μπορεί να εξεταστεί μόνο τοπικά και λαμβάνοντας υπόψη την εποχική μεταβλητότητα.

Η εργασία επιβεβαίωσε επίσης ότι η χρήση μετεωρολογικών παραμέτρων μπορεί να βελτιώσει τη συσχέτιση μεταξύ PM 2.5 και AOD. Αυτό προκύπτει από το γεγονός ότι, στις περιπτώσεις που εξετάστηκαν, μόνο στο 40% αυτών το AOD ήταν η πιο σημαντική παράμετρος συσχέτισης, ενώ στο υπόλοιπο 60% ως πλέον σημαντική παράμετρος εμφανίζεται μία εκ των μετεωρολογικών παραμέτρων όπως η υγρασία, η ταχύτητα ανέμου και το ύψος ανάμιξης.

Table of Contents

FIGURES

TABLES

Chapter 1: Introduction

1.1 Summary

The purpose of this study was to examine the possible relation between the aerosols measured using remote sensing methods and the air pollution levels of suspended particles (PM 2.5) in the lower atmosphere. For this purpose, the daily MODIS Aerosol Optical Depth (AOD) data have been used for an entire year (2009). For the same period, concentrations of particulate matter which resulted from the application of a regional photochemical model have been used in order to provide air pollution data for the whole of Europe. In the examined relation, meteorological parameters such as wind speed, mixing height and humidity, resulting from a prognostic meteorological model, have been taken also into consideration. Statistical regression analysis was performed on selected points at the locations of big urban agglomerations in Europe, where usually particulate matter concentration is higher, as well as its impact on man and the environment. In addition, the relation of these parameters was also examined using the measurements of two operational air pollution stations located in Attica, Greece.

- In **Chapter 1** of this study, the scope of work with a brief description of my personal motivation in this research area is presented.
- **Chapter 2** presents the scientific background related to air pollution, air quality modeling and use of remote sensing data for environmental monitoring and especially in atmospheric research.
- **Chapter 3** presents the data used in this study as well as the methodology.
- **Chapter 4** presents the results of this study that are the spatial and temporal distribution of aerosols and PM 2.5 over Europe and the AOD-PM 2.5 relation in several locations in Europe based on air quality and meteorological modeling data but also on measurements of 2 monitoring stations located in Attica, Greece. The results of this study supported the statement that the relationship between AOD and PM 2.5 is highly variable for different regions and for different time scales and thus a localized method is most appropriate for the examination of their relation in comparison to a uniform statistical regression analysis. It was also confirmed that the use of meteorological parameters, in addition to AOD, can improve the relationship between AOD and PM 2.5, since, in several cases, the dominant parameter in the regression equation was one

of the meteorological parameters such as boundary layer height, wind speed or relative humidity.

- Finally, **Chapter 5** summarize the findings of the study while, **Chapter 6**, has a brief discussion on the most important parameters that should be considered for the evaluation of the results.

1.2 Scope of Work

Aerosols have important role in the atmosphere since they affect the Earth's weather and climate. Aerosols can affect the energy balance of the atmosphere, directly, through their interaction with solar and terrestrial radiation, and indirectly, through their effect on cloud particle size, cloud composition (liquid / ice water content), cloud lifetime and cloud optical parameters (George et al, 2006). Their effect on clouds has also impact on weather, mostly through modification of precipitation patterns (Twomey, 1977; Albrecht, 1989).

According to the Intergovernmental Panel on Climate Change (IPCC), aerosol effects represent some of the most uncertain aspects of the climate system and so, their study is one of the most active research areas in climatic studies (IPCC, 2001; IPCC 2007; IPCC 2013).

The study of global aerosols patterns is a challenging task because of their high spatial and temporal variability. Spatial and temporal variations in the aerosol optical parameters are relatively high compared to that of other atmospheric components, like greenhouse gases (Kaufman et al, 2002). So distribution of aerosols should be accurately estimated, in order to be able to understand their origin, their transport, and their impact on weather and climate, on both regional and global scales. To facilitate this task, space based observations can be used to provide quantitative information on aerosols and their variability over time and space.

In this study, the spatial and temporal variation of different atmospheric optical parameters over Europe was examined. The study was based on MODIS remote sensing data and the spatial analysis was performed using Geographic Information Systems.

The study tried to analyze the aerosol spatial patterns in order to investigate a possible relation of atmospheric aerosol concentration of particulate matter of less than 2.5 μm (PM 2.5) diameter, in Europe. PM 2.5 is defined as particle matter with an aerodynamic diameter of less than 2.5μm. It is evidenced from a large number of epidemiological studies that exposure to fine particles can increase the incidence of heart disease, cardiovascular disease, and lung cancer (Pope, 2000; Peters et al, 2001; Hu, 2009). In order to monitor particulate matter, air

pollution ground-based air quality measuring stations are operating worldwide in order to provide continuous and accurate air quality data. However, ground stations are usually sparse and located mostly in urban areas. Thus, the study of regional particulate matter pollution is difficult or even impossible in areas with lack of availability of ground station data.

Several research studies found that remote sensing aerosol data, and especially the satellite-derived aerosol optical depth (AOD), is closely related to the surface PM 2.5 concentration; thus this parameter can be used to predict PM 2.5 concentration at the regional scale (Chu et al, 2003; Engel-Cox et al, 2004; Gupta et al, 2006; Van Donkelaar et al, 2010). It is important to understand that satellite AOD measures the total amount of particles over a vertical column, while PM 2.5 is the mass concentration of particles near the surface. The AOD-PM 2.5 relationship is influenced by several factors, such as the vertical distribution of the aerosols, aerosol composition, and size of particles (Gupta et al, 2009). These influences have been studied in several research studies in order to estimate a reliable AOD-PM 2.5 relationship (Toth et al, 2014; Wang et al, 2010). In order to overcome the lack of the required data, statistical models were also used to eliminate these influences and to obtain a more accurate AOD-PM 2.5 relationship (Liu et al, 2004). Most studies are focused upon establishing a simple relationship between AOD-PM 2.5, in the form of a simple linear regression equation (Liu et al, 2005). In order to improve the correlation between AOD and PM 2.5, meteorological and environmental parameters were also used (Gupta et al, 2009).

In most of the AOD-PM 2.5 estimation studies, AOD from the MODerate Resolution Imaging Spectroradiometer (MODIS) instrument was used because of its daily global coverage and consistent accuracy, as well as PM 2.5 concentration data from air quality monitoring stations. In this study, MODIS AOD data was also used, but instead was compared with datasets from numerical models, both for meteorological and for air quality. The reason for this choice was the need to avoid the problems associated with the scarcity of PM 2.5 data in areas where air quality monitoring stations are not available, and to examine if such a relation can be established using model data.

All data was analyzed using GIS techniques. Working with remote sensing and model data was a difficult task since the type and the size of data required special handling and techniques suitable for big data analysis.

Overall the project was a very challenging task since it required very good knowledge of:

- Use of Remote sensing data and software (BEAM, ERDAS)
- GIS Analysis tools (ArcGIS)
- GIS programming (Python, GDAL)
- Statistical analysis (SPSS)

The idea to work with remote sensing and model data for air quality purposes using GIS technologies was also very closely related to my personal scientific interests. I had worked in the past both in air quality modeling (my Ph.D was related to the development of emission inventories systems as well as use of air quality modeling and GIS as environmental impact assessment tools) and remote sensing data (mostly post processing and visualization in web interfaces) and thus the idea to couple all these with GIS was very challenging and interesting to me.

Chapter 2: Scientific background

2.1 Air Quality Modeling

2.1.1 The air pollution problem

Air pollution is one of the most important environmental problems, since it causes diseases or even death in humans, it damages other living organisms like animals and plants, and generally it is harmful for the natural or even the built environment. Air pollution can be caused due to natural or anthropogenic sources. Nevertheless, most of the recent (after 1950) air pollution episodes are results of increased anthropogenic economic activities such as industry, transport, energy and agriculture, as well as some domestic household activities, like heating.

The main air pollutants are:

- **Particulate matter** (PM) is generally defined as a mixture of solid and/or liquid particles suspended in the air. There are natural sources of PM (like sea, deserts, volcanos) and anthropogenic sources like vehicles, shipping, power generation and households. PM vary in size from a few nanometers to several tenths of micrometers. Exposure to increased PM concentration is linked to human health problems like asthma, lung cancer and cardiovascular issues, the severity of which depends on the size, shape and the chemical composition of the particles (Dockery and Stone, 2007; Perez et al, 2009).
- **Sulphur dioxide** (SO_2) is emitted by natural sources like volcanos and manmade activities including power generation, industry, shipping and households. It is harmful for people and the environment since it is related to acidification of soil and inland waters.
- **Nitrogen oxides** (NO_x) are mostly emitted by anthropogenic activities related to combustion of fuels. They can harm human health and also contribute to acidification and eutrophication. Nitrogen oxides are involved in the photochemical processes of ground-level ozone (O_3) production.
- **Volatile organic compounds** (VOC) are emitted by the use of solvents in products and industry, road vehicles, household heating and power generation. VOCs are also involved in the production of ground-level ozone. They are also significant greenhouse gasses affecting the Earth's climate.

- **Ground-level ozone** (O_3) is a secondary pollutant produced by photochemical reactions of NO_x and VOCs. It harms both human and the natural ecosystems, including plants, crops and buildings.

Among the effects of air pollution are:

- **Health problems** include serious effects on the cardiovascular (Miller et al, 2007) and respiratory systems, leading to reduced lung function, asthma, chronic bronchitis and premature death (Dockery, 1993; Pope, 1995).
- **Acidification** of soil and water damages plants and animals in natural ecosystems (Fabry et al, 2008; Orr et al, 2005) as well as buildings and historical sites (Kucera, et al, 1995).
- **Eutrophication** is the excess of nutrients in water or soil. It threatens biodiversity through the excessive growth of simple plants that damage other plants and animals in soils, rivers and lakes (Chislock et al, 2013).
- **Physical damage** to buildings and monuments, due to corrosion and soiling of their surfaces as a result of particulates and acidification (Saiz-Jimenez, 2004).
- **Ozone depletion**. The ozone layer that protects the earth from harmful ultra-violet radiation has become thinner and thinner over the last decades. The reason for the ozone depletion is the anthropogenic emissions of compounds that can harm the ozone in the stratosphere (Solomon, 1999).

In Europe, European Union **policy** on air quality aims to develop and implement appropriate instruments to improve air quality. These measures and policies include control of emissions from stationary and mobile sources, improving fuel quality and promoting the use or renewable energy sources. The implementation of these actions resulted in improvement of air quality in Europe. Nevertheless, air pollution is still one of the most important environmental issues since even now it is the most significant environmental cause of death in the EU (over 400.000 premature deaths per year). It is well known that long-term exposure to very fine particles (PM 2.5) can harm human health. According to the European Environmental Agency (EEA, 2015), "more than 80% of the EU's urban population is exposed to PM levels above the 2005 WHO Air Quality Guidelines, depriving citizens of more than eight months of life on average – with life expectancy reduced by up to two years in the most pollute places". At the same time, air pollution still continues to harm natural ecosystems, as more than half of the EU territory is

exposed to high concentrations of ozone and excess of nitrogen deposition, which causes reduced biodiversity, crop yields and other material damage.

EU environmental policy (European Commission, 2016a) focusses on developing and implementing a **clean air policy framework.** EU policies also aim at implementing the Union's international obligations in the field of air pollution, and on integrating environmental protection requirements into different sectors of activities like transport, industry and agriculture.

There are two main EU instruments related to air pollution. The first is the EU Ambient Air Quality Directive (revised and adopted in 2008), with aim to develop a long-term, strategic and integrated policy to protect humans and natural ecosystems against the significant effects of air pollution. It also sets pollutant concentration limit values and air quality standards for ground level ozone, CO, SO_2, PM, NOx, heavy metals and other pollutants. The second is the National Emissions Ceilings Directive (NEC) that was adopted in 2001, and set limit to the overall emissions of SO_2, NH_3, NOx and VOCs.

The new Directive **2008/50/EC** of the European Parliament and of the Council of 21 May 2008 on **ambient air quality and cleaner air for Europe (CAFE)** entered into force on 11 June 2008 with the following key elements (European Commission, 2016b):

- The merging of most of existing legislation into a single directive (except for the Directive 2004/107/EC, known also as the fourth daughter directive) with no change to existing air quality objectives
- New air quality objectives for PM 2.5, including the limit value and exposure related objectives – exposure concentration obligation and exposure reduction target
- The possibility to discount natural sources of pollution when assessing compliance against limit values
- The possibility for time extensions of three years (PM10) or up to five years (NO_2, benzene) for complying with limit values, based on conditions and the assessment by the European Commission.

Other EU legislation related to air pollution (European Commission, 2016b) are:

1. Council Directive **96/62/EC** on ambient air quality assessment and management is commonly referred to as the **Air Quality Framework Directive**. It describes the basic principles as to how air quality should be assessed and managed in the Member States. It lists the pollutants for which air quality standards and objectives will be developed and specified in legislation.
2. Council Directive **1999/30/EC** relating to limit values for SO_2, NO_2 and NO_x, PM and lead in ambient air. This directive was the so-called "**First Daughter Directive**". The directive describes the numerical limits and thresholds required to assess and manage air quality for the pollutants mentioned. It addresses both PM10 and PM 2.5 but only establishes monitoring requirements for fine particles.
3. Directive **2000/69/EC** of the European Parliament and of the Council relating to limit values for benzene and CO in ambient air. This was the **Second Daughter Directive.**
4. Directive **2002/3/EC** of the European Parliament and of the Council relating to O_3 in ambient air. This was the **Third Daughter Directive** and established target values and long-term objectives for the concentration of O_3 in air. The directive also describes certain monitoring requirements relating to VOCs and NO_2 in the air.
5. Directive **2004/107/EC** of the European Parliament and of the Council relating to arsenic, cadmium, mercury, nickel and polycyclic aromatic hydrocarbons in ambient air. This is the **Fourth Daughter Directive** and completes the list of pollutants initially described in the Framework Directive. Target values for all pollutants except mercury are defined for the listed substances, though for PAHs, the target is defined in terms of concentration of benzo(a)pyrene which is used as a marker substance for PAHs generally. Only monitoring requirements are specified for mercury.
6. Council Decision **97/101/EC** establishing a reciprocal exchange of information and data from networks and individual stations measuring ambient air pollution within the Member States.
7. Commission Decision **2004/461/EC** presents a questionnaire for annual reporting on ambient air quality assessment under Council Directives 96/62/EC and 1999/30/EC and under Directives 2000/69/EC and 2002/3/EC of the European Parliament and of the Council.

8. Commission Decision **2004/224/EC** specifies the obligation of Member States to submit within two years so-called Plans and Programs for those air quality zones where certain assessment thresholds set in the Directives are exceeded.
9. Council Directive **80/779/EEC** of 15 July 1980 on air quality limit values and guide values for SO_2 and suspended particulates, as last amended by Directive 89/427/EEC
10. Council Directive **85/203/EEC** of 7 March 1985 on air quality standards for nitrogen dioxide, as last amended by Council Directive 85/580/EEC

Most European countries have set up air quality monitoring networks to assess ambient air quality with respect to several pollutants. The networks in each state may be national, regional or local in area coverage. Most countries operate the networks the entire year, except for Norway and Sweden, where the air quality monitoring is concentrated within the six winter months, as this is the period when the highest concentrations occur.

The total number of European stations for which 2010 data have been collected in the European air quality database system (AirBase) was 4533. In general, the largest European countries have the most stations, for instance France with close to 900 sites, Germany with more than 500 sites, and Spain with almost 1000 sites. On the other hand, Albania has 23 urban sites, Greece has 32 sites, Croatia has 41 sites, and Norway has 45 sites (ETC/ACM, 2013).

The sites in which monitoring stations have been established are classified by the European Environment Agency using the following types: urban, traffic hot spots, industrial hot spots (urban or rural), and regional. In most European countries, all categories are represented, while the total traffic sites are 754, the urban industrial sites are 130, and the rural industrial sites are 93. However, air quality monitoring stations are not distributed equally across Europe so as to assess air quality throughout the European territory as required from the Air Quality Directives (2004/107/EC and 2008/50/EC). This is presented in the following map (Figure 1) showing the location of stations for which 2011 air quality data for PM 2.5 were reported to AirBase (Malherbe et al, 2013). The spatial distribution of the location of the stations shows that **most European countries do not have an efficient monitoring network that measures air quality levels throughout the whole country.**

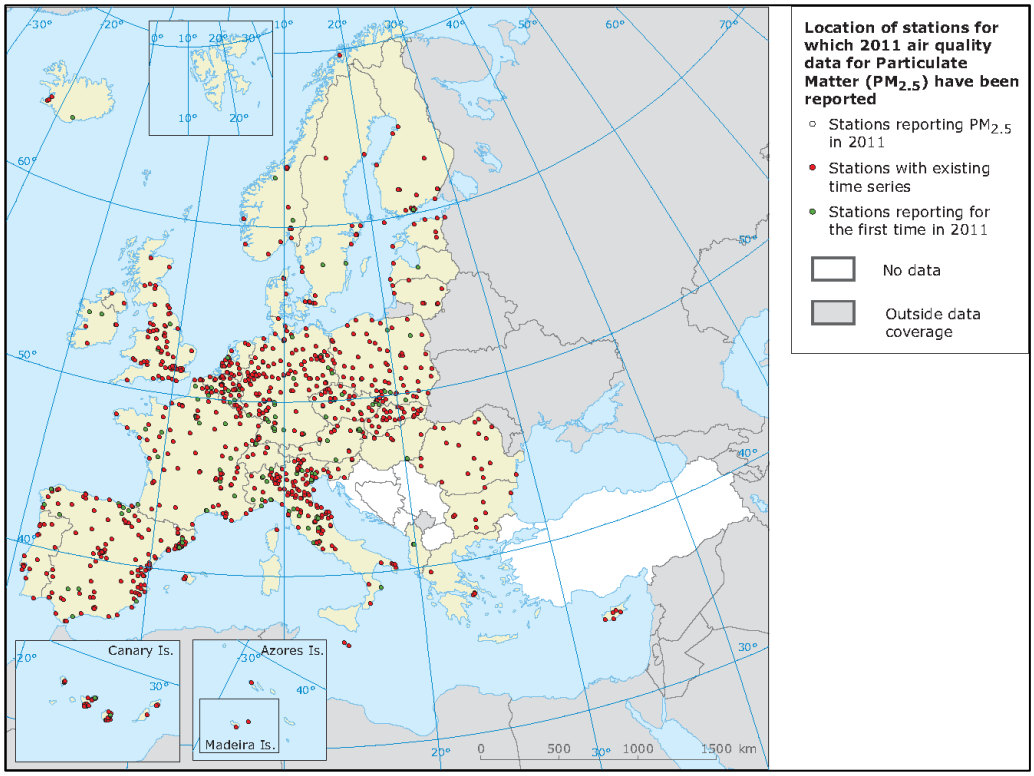

Figure 1: Location of stations for which 2011 air quality data for particulate matter (PM 2.5) have been reported.

Another crucial issue regarding mainly urban environments is the phenomenon of microclimate. Microclimate is the set of meteorological parameters that characterize a localized area. The main factors that comprise microclimate are surface temperature, relative humidity, wind speed, solar insolation and precipitation (Hogan, 2012).

Microclimate is closely linked to air pollution, as it determines air pollutant dispersal. In some cases, microclimates have a critical influence on altering air pollutant dispersal, changing local air pollution levels dramatically. Urban physical design makes a large contribution to create microclimatic conditions that largely affect air quality (Edussuriya, 2000).

Air quality in urban areas depends mainly on the amount of emitted pollutants and the direction and speed of the wind. Wind has the ability to disperse urban air pollution, although the surrounding topography and sea breezes determine wind characteristics. Tall buildings affect winds, as narrow streets created between them can funnel winds, causing dust and air pollutants to irritate passers-by in the street. However, average height buildings create only friction with wind moderating moving air and decreasing air pollution's dispersion.

Moreover, urban vegetation can affect local air quality by altering the urban microclimate. In general, urban trees are considered to contribute to lower air temperatures during summer, although in some cases they may have the opposite effect. However, reduced air temperature

is believed to improve air quality, as emissions of many pollutants are temperature dependent. Among others, vegetation can reduce air pollutants' concentration up taking them via leaf stomata or plant surface (Nowak, 1994).

Determining the air pollution profile within a region is a very complex procedure depending on various meteorological and topographical factors, indicators of land use and emissions information. All the above determine the required number of air monitoring stations so as to obtain sufficient air quality data from the entire domain of interest. Directive 2008/50/EC requires that "air quality shall be assessed throughout the entire territory of Member States". However, according to EEA, because setting up a monitoring station is costly, **other techniques, such as satellite imagery and air quality models, have been entered into forced so as to obtain deeper knowledge of Europe's air quality** (EEA, 2013).

Use of mathematical models can simulate the atmospheric and photochemical processes and provide estimates of pollution concentration over a wider area. Of course this is a challenging and complicated task since weather, landscape characteristics and emission sources play a significant role in the models results. Thus, air quality modelling comes with the drawback of uncertainty, as models cannot accurately simulate all the factors linked to formation, dispersion and deposition of pollutants.

The use of remote sensing data would be an alternative solution in order to provide air quality information for the entire European territory. Nevertheless, since the various substances that the European policy requires monitoring are not measured directly using the satellite instruments, a relation between them should be established. This study aims to investigate this alternative for air quality assessment / monitoring.

2.1.2 Mathematical modeling of air quality

2.1.2.1 Meteorological Models

Meteorological models are computer programs that simulate atmospheric processes in order to predict meteorological conditions for future times at given locations (domains) and altitudes (pressures). They are using mathematical models of the atmosphere, land and oceans in order to predict the weather based on current weather conditions. This is performed by solving a set of equations, known as the primitive equations, which, along with the ideal gas law, can predict the future state of the atmosphere. The parameters that meteorological models are able to simulate are the air density and pressure, the potential temperature scalar fields as well as the wind vector field (wind speed and direction) of the atmosphere through time.

Depending on the prediction scale, meteorological models are classified as Global Forecast Models and Mesoscale models.

A brief description of the most well-known models (OpenWeatherMap, 2016) is provided below.

- **Global Models**
  - Integrated Forecast System (IFS)

    The Integrated Forecast System (IFS) is an operational global meteorological forecasting model. IFS is developed and maintained by the **European Centre for Medium-Range Weather Forecasts (ECMWF)** based in Reading, England. Information from the IFS is proprietary and copyrighted. Nevertheless, a limited amount of the model's most important outputs are public available.
  - Global Forecast System (GFS)

    The Global Forecast System (GFS) is a global numerical weather prediction computer model run by the U.S. National Oceanic and Atmospheric Administration (NOAA). The model is run in two parts: the first part with a higher resolution runs an 8 day forecast, while the second part runs a 16 day forecast at a lower resolution.
  - The Global Environmental Multiscale Model (GEM)

    The Global Environmental Multiscale Model (GEM) is an integrated forecasting and data assimilation system developed in the Recherche en Prévision Numérique (RPN), Meteorological Research Branch (MRB), and the Canadian Meteorological Centre (CMC).
- **Mesoscale Models**
  - MM5

    The MM5 (Fifth-Generation Penn State/NCAR Mesoscale Model) is a regional mesoscale model used for creating weather forecasts and climate projections. It is a community model maintained by Penn State University and the National Center for Atmospheric Research (UCAR, 2016).

- WRF

  WRF (Weather Research and Forecasting) Model is an advanced mesoscale forecasting system (Michalakes et al, 2001; Michalakes et al, 2004). The first version of the model was available in year 2000 and it is continuously supported since then. It is available in two different core codes: ARW (Advanced Research WRF) at National Center for Atmospheric Research (NCAR) and NMM (Non-Hydrostatic Mesoscale Model) at National Oceanic and Atmospheric Administration (NCEP). WRF is a fully compressible, non-hydrostatic model. Among its features are a data assimilation module and the ability to run in nested domains (with different detail analysis and resolution). Since WRF is a relatively new model, it supports also advanced IT features like distributed memory and parallel computing.

  WRF can be used both in research and in operations. It is currently the primary meteorological forecast model in several meteorological agencies all around the world, including NCEP, AFWA, and ECMWF. It was also used in this study by the Aristotle University of Thessaloniki in order to simulate the weather conditions during year 2009.

2.1.2.2 Pollution dispersion models

Air quality models (AQM) are computer applications that simulate the physical (transport, diffusion, deposition) and chemical (photochemical reactions) processes in the atmosphere. AQM can be used for operational forecasting of air quality or for the assessment of the environmental impacts to air quality of specific activities (Macdonald, 2003) or the evaluation of different emission reduction policies and measures (Afshar et al, 2007; Sharma et al, 2004). They can be applied at multiple spatial scales including local, regional, national, and global scales (Daly, 2007).

Simple AQM can simulate only non-reactive, primary pollutants (which are emitted directly into the atmosphere), while **photochemical models** can also predict the concentration of reactive, secondary pollutants, like O_3, which are produced as a result of chemical reactions in the atmosphere. Air quality modelling is a challenging task since it requires several, sometimes difficult to provide, input data like meteorological data, topography, and emission characteristics in order to produce results (concentrations) of different air pollutants.

Depending on the mathematical method applied in the models in order to simulate the physical processes and the perspective of atmospheric motion, we can categorize AQM models as:

- **Lagrangian** models (also known as trajectory models) that examines air parcels as they move over space and time
- **Eulerian** models that use a gridded reference system in which atmospheric conditions are calculated.

The Lagrangian method is easier to mathematically represent, thus there are a lot of models that use this method in order to simulate air pollutants dispersion. Nevertheless, this approach is considered incomplete and as a result, currently, most air quality models are using the **three-dimensional** Eulerian grid approach. This method is more computationally demanding, but the recent advantages in IT systems (more processing power) made possible the adaptation of this approach.

There are several AQM available to be used in air quality studies. Among the most widely used photochemical models are:

- **Comprehensive Air quality Model with extensions (CAMx):** The model can be used from regional to local scales. It estimates the concentration of different primary and secondary pollutants, like CO, NO_x, PM, O_3 and heavy metals. CAMx can be coupled with many meteorological models, that can provide the necessary meteorological data (WRF, MM5, and RAMS are supported) and emission models, that can provide the biogenic and anthropogenic emission data (SMOKE, CONCEPT, EPS, EMS). One of the most useful feature of the model is the source apportionment tool that estimates the contribution of the different emission sources to the estimated concentration of O_3, PM and air toxics. Other advanced supported features are: two-way and flexi grid nesting, multiple supported gas phase chemistry mechanism options (CB6, CB05, SAPRC99) and dry deposition options (Wesely89, Zhang03), subgrid space point sources plumes, and parallel processing capabilities on both shared and distributed memory systems (Ramboll Environ, 2016).

  The CAMx model was also used in this study by the Aristotle University of Thessaloniki in order to simulate the air quality over Europe during year 2009.

- **Community Multi-scale Air Quality (CMAQ):** CMAQ is an open source photochemical AQM developed by the U.S. EPA Atmospheric Science Modeling Division. It is continuously supported by the CMAS Center. It can be used also from regional to local scales. It provides several state-of-the-art functionalities like gas-phase chemical reactions, aqueous-phase reactions and aerosol dynamics and chemistry (UNC, 2016).
- **Regional Modeling System for Aerosols and Deposition (REMSAD)**: REMSAD is another U.S. EPA photochemical model. It was developed in order to estimate the concentration of both reactive and non-reactive primary and secondary pollutants in regional scales.
- **Urban Airshed Model Variable Grid (UAM-V):** The model was developed by Systems Applications International (SAI) in early 1970s. UAM is one of the most widely used photochemical AQM with active maintenance and support for over 4 decades. It can be used from regional to local scales in order to estimate the concentration of inert and reactive compounds. The model was extensively used for the simulation of ozone episodes, all over the world, in cities like Los Angeles, Mexico and Athens. Among its capabilities we should mention the two-way grid nesting, the variable vertical layer number and spacing and the ability to include subgrid space photochemical plumes (ICF International, 2016).

2.2 Remote sensing data

2.2.1 Use of remote sensing data in environmental studies

The use of remote sensing data for natural resources mapping and environmental monitoring has been very popular during the last decades. Several different sensors installed in several different satellites with a wide range of spatiotemporal, radiometric and spectral resolutions has made remote sensing the best source of data for large-scale applications and studies (Melesse et al, 2007).

Remote sensing data can be used in environmental application related to:

- *Land Use Planning and Change*

  Passive optical sensors like those onboard the Sentinel, Landsat, SPOT, IKONOS, GeoEye and other satellites can be used for land use planning and change detection applications (Hegazy et al, 2015). These sensors provide panchromatic or multi-spectral images of the earth surface which can reveal information about land use classification, vegetation / crop type and condition or even soil type. Based on time series of these images scientists can monitor land use change over time that is related to global environmental problems like deforestation (Beuchle et al, 2015) or desertification (Zanchetta et al, 2016).

- Agriculture

  Precision agriculture uses satellite data to monitor plants and vegetation conditions, as well as water and nutrient levels in the soil, in order to support efficient use of resources like water, pesticides, and fertilizers (El-Sharkawy et al, 2016). The most commonly used remote sensing product for agricultural use is the Normalized Difference Vegetation Index (NDVI), which estimates the vegetation biomass density (Liakos et al, 2015). More complex products can measure the primary plant production and leaf stress (Li, 2013). Usually these products derive from the combination of remote sensing data in different wavelengths (in the optical or infrared bands).

- *Water Resources and Fisheries*

  Remote sensing data like those from SeaWiFS or MODIS or from the new sensors onboard Sentinel 3, can be used to monitor oceans. This include measurements of the hydrodynamics of the water, like sea surface temperature, water elevation and sea currents, but also the water quality, with measurements of the concentration of chlorophyll-a, the water color (expressed as the diffused attenuation of light), the primary production of phytoplankton etc (Copernicus, 2016). The information derived from the remote sensing images can be used for better coastal zone management as well as in fisheries. For example, scientists can predict the existence and the transport of harmful algal blooms (Shen et al, 2012)), or they can identify areas suitable for fishing, both in terms of fish quantity but also related to the protection of sensitive species (Nammalwar et al, 2013).

- *Wetlands and Watersheds*

  Remote Sensing data can support the protection of the sensitive environment of wetlands (Corcoran et al, 2013). Using sensors suitable for monitoring the land and the marine environment like Sentinel 2 and 3, or even Radar sensors like those in Sentinel 1, we can monitor the changing ecosystem environment in these areas, examine topography or land use changes, detect illegal activities or monitor pollution of water and land.

- *Climate Change*

  There are various satellites in orbit that provide data suitable for the study of global climate variations. NASA's Earth Observing System (EOS) started in 1999 and since then, through different satellites, monitors the Earths land, sea and atmosphere, including the observation of aerosols, cloud cover, fires, ocean productivity, pollution, solar radiation, sea ice, and snow cover (King et al, 2000). Among these satellites are ADEOS I, Aura and Toms for monitoring the Ozone Layer, AQUA, AQUARIUS, ERS-1, SeaWiFS monitoring the oceans, ICESat measuring the ice mass and ERBS, Cloudsat, OCO-2, Terra, Meteor-3M-1, and CALIPSO monitoring the atmosphere. European Space Agency (ESA) had a similar project. ERS 1 launched in 1991, ERS 2 launched in 1995 and Envisat launched in 2002, were equipped with different sensors capable to monitor the complex Earths system. Among them are MERIS, AATSR, SCIAMACHYMWR, GOMOS and MIPAS.

- *Disaster Management and Emergency Response*

  Remote sensing data can facilitate disaster management and emergency response (Boccardo et al, 2014) throughout the emergency management cycle (Readiness, Response, Recovery, Reduction). They can assist decision makers with the risk identification for various natural phenomena like flood, fire, earthquakes or erosion, or even technological accidents like oil spills or industrial accidents. During the event, the images provided by the satellites, can show the size and the extent of the consequences of the event, like for example the spread of the smoke plume during a volcano eruption (Prata et al, 2015), or the trajectory of a hurricane (Tourville et al, 2015). They can also provide information about the affected areas allowing policy makers and emergency personnel to act immediately, focusing on the areas that require more attention. Finally, by monitoring spatial activity patterns like for example the occurrence of hurricanes during an El Niño event, or by providing information to prediction models, they can

also reduce the risk and the consequences of such events by allowing the involved actors to take the necessary measures, preventing loss of lives and damages (Park et al, 2016).

2.2.1.1 The TERRA and AQUA satellites

Two of the most commonly used satellites in environmental applications are the NASA's TERRA and AQUA satellites. These are part of the NASA-centered international Earth Observing System (EOS). TERRA satellite was launched on December 18, 1999 while AQUA satellite was launched on May 4, 2002.

Terra collects data about the Earth's bio-geochemical and energy systems using five sensors that observe the atmosphere, land surface, oceans, snow and ice, and energy budget. Each sensor has unique features that enable scientists to meet a wide range of science objectives.

The five sensors onboard **Terra** (NASA, 2016a) are:

- **ASTER,** or Advanced Spaceborne Thermal Emission and Reflection Radiometer
- **CERES,** or Clouds and Earth's Radiant Energy System
- **MISR,** or Multi-angle Imaging SpectroRadiometer
- **MODIS,** or Moderate-resolution Imaging Spectroradiometer
- **MOPITT,** or Measurements of Pollution in the Troposphere

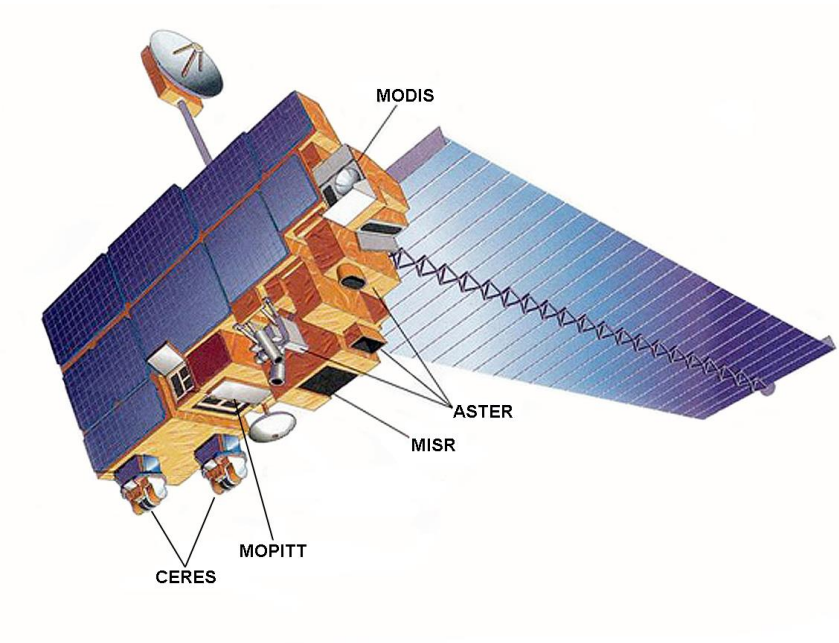

Figure 2: Instruments on board TERRA satellite (Source: NASA, 2016b)

The AQUA satellite is focusing on precipitation, evaporation and cycling of water. **AQUA** carries six instruments (NASA, 2016c), which are:

- **AMSR-E**, or Advanced Microwave Scanning Radiometer-EOS
- **MODIS**, or Moderate Resolution Imaging Spectroradiometer
- **AMSU-A**, or Advanced Microwave Sounding Unit
- **AIRS**, or Atmospheric Infrared Sounder
- **HSB**,or Humidity Sounder for Brazil
- **CERES**, or Clouds and the Earth's Radiant Energy System

Among the parameters measured by the above instruments are: cloud and atmospheric aerosol properties, radiative energy flux, land and sea temperature, and atmospheric temperature and humidity.

Because all sensors share a common platform, they collect complementary observations of Earth's surface and atmosphere. These varying perspectives of the same event can yield unique insights into the processes that connect Earth's systems.

Moderate Resolution Imaging Spectroradiometer

The MODIS instrument (NASA, 2016e) is onboard both the TERRA and AQUA satellites. The instrument has a 2,330km wide viewing swath. The observation frequency is about 1-2 days (complete earth coverage). It provides measurements in 36 discrete spectral bands (ranging in mean wavelength from 0.4 μm to 14.4 μm and at varying spatial resolutions (2 bands at 250 m, 5 bands at 500 m and 29 bands at 1 km). It is designed to provide measurements of large-scale global dynamics including changes in Earth's cloud cover, radiation budget and processes occurring in the oceans, on land, and in the lower atmosphere.

MODIS data can provide valuable insights to scientists about the role of clouds and aerosols on the Earth’s energy and radiative budget. MODIS not only provide an image of the spatial and temporal distribution of clouds but also provide information about cloud characteristics and composition like water vapor and ice size and distribution. In addition, it provides information about aerosols like concentration, size, composition and vertical distribution. All these parameters affect the atmosphere and thus have a significant role in Earth’s climate system (Chylek et al, 1995; Chin, 2009; Levin, 2008).

2.2.2 Use of remote sensing data for air quality monitoring

2.2.2.1 Atmospheric aerosols

Atmospheric aerosols are defined as a colloid of fine solid particles or liquid droplets in the air (Hinds, 1999). Atmospheric aerosols are caused by several different processes and are emitted to the atmosphere from different natural or anthropogenic sources. Natural aerosols include desert and soil dust, the suspended sea salt, the volcano ash, or the soot and ash from natural fires. Anthropogenic aerosols are those emitted from manmade activities like particles from fossil fuel burning for energy production or other industrial activities, central heating, transport or agricultural activities.

Aerosol optical depth (AOD) or **optical thickness** (AOT) is a *fundamental measurement of the quantity and distribution of aerosols* in the atmosphere. It is defined as the extinction of the solar radiation due to aerosols. There are two physical processes that can block sunlight in the atmosphere; absorption and scattering. AOD tells us how much direct sunlight is prevented from reaching the ground by the aerosol particles. It is a dimensionless number that is related to the amount of aerosol in the vertical column of atmosphere over the observation location. A value of 0.01 corresponds to an extremely clean atmosphere, and a value of 0.4 would correspond to a very hazy condition. Optical depths above 2 or 3 represent very high concentrations of aerosols.

There are many applications for aerosol optical thickness data, including:

1 Air Quality (Chin, 2007)
2 Health and Environment (Carmichael et al, 2009)
3 Earth Radiation Budget (Chylek et al, 1995)
4 Climate Change (Chin, 2009; Levin, 2008)
5 Monitoring of volcanic eruptions and forest fires (Koren, 2004)

The first satellite instrument capable of monitoring aerosol optical depth from space was the **Advanced Very High Resolution Radiometer** (AVHRR), which first was operational in the late 1970s. It retrieved optical depth from measurements in the visible and near-infrared spectrum. AVHRR was a passive radiometer, measuring the intensity of sunlight as it was reflected by the aerosols, using the dark ocean as the background. Thus it was able to measure AOD only over the water (Zhao, 2014).

Over the next decades, the instruments have grown more sophisticated and made it possible to study aerosols over the land as well (Petrenko et al, 2013). Newer radiometers such as the Multi-angle Imaging Spectroradiometer (**MISR**) and the Moderate Resolution Imaging Spectroradiomer (**MODIS**) were capable of viewing aerosols at many more angles and wavelengths, providing more accurate results (Qie et al, 2015). Other instruments used to monitor AOD are the Cloud Aerosol Lidar and Infrared Pathfinder Satellite Observer (**CALIPSO**), the Polarization and Directionality of the Earth's Reflectances (**POLDER**) and the Aerosol Polarimetery Sensor (**APS**).

Although satellites provide a global perspective of aerosol concentration and characteristics, ground based measurements are also necessary in order to validate the results and to calibrate the instruments. AERONET is a global network of ground-based stations (more than 200) which are measuring AOD (Holben, 2001).

2.2.2.2 AOD as a PM indicator

AOD offers indirect estimates of particulate matter. Previous research showed a significant positive correlation between satellite-based measurements of AOD and ground-based measurements of particulate matter with aerodynamic diameter less than or equal to 2.5 μm and aerodynamic diameter less than or equal to 10 μm, (correlation coefficient of 0.96) (Chu, 2006; Gupta et al, 2006; Li et al, 2003; Engel-Cox et al, 2004; Wang and Christopher, 2003 and Liu et al, 2007).

To explore the quantitative relationship between satellite-derived AOD and ground-measured PM 2.5, various models were developed, such as:

1) General linear or nonlinear regression models (Donkelaar et al, 2010; Liu et al, 2007; Song et al, 2014)
2) A semi-empirical model (Koelemeijer et al, 2006),
3) Mixed effects models (Lee et al, 2011 and Yap and Hashim, 2013),
4) A generalized additive model (Paciorek et al, 2008),
5) An alternating Conditional Expectation (ACE) model (Benas et al, 2013), and
6) An artificial Neural Network (ANN) model (Gupta and Christopher, 2009)

Linear regression models were examined in most of the research projects. As an example, Wang and Christopher (2003) explored the relationship between the columnar aerosol optical thickness (AOT) derived from the MODIS on the Terra/Aqua satellites and the hourly fine

particulate mass (PM 2.5) measured at the surface at seven locations in Jefferson County, Alabama for 2002. The results indicated that there was a good correlation between the satellite-derived AOT and PM 2.5 (linear correlation coefficient, R = 0.7) indicating that most of the aerosols were in the well-mixed lower boundary layer during the satellite overpass times. There was also excellent agreement between the monthly mean PM 2.5 and MODIS AOT (R > 0.9), with maximum values during the summer months due to enhanced photolysis. PM 2.5 has a distinct diurnal signature, with maxima in the early morning (6:00 - 8:00AM) due to increased traffic flow, and restricted mixing depths during these hours. Using simple empirical linear relationships derived between the MODIS AOT and 24hr mean PM 2.5 they showed that the MODIS AOT can be used quantitatively to estimate air quality categories as defined by the U.S. Environmental Protection Agency (EPA) with an accuracy of more than 90% **in cloud-free conditions**. However, **they have outlined several factors that could affect the relationship between PM 2.5 and satellite-derived AOT and further research is needed to quantify these effects**.

Research shows that the correlation between AOD and ground PM 2.5 is affected by a combination of many factors, including inherent characteristics of satellite observations in aerosol optical depth algorithms, errors of estimate of regression models, **terrain**, **cloud cover**, height of the **mixing layer (or Planetary Boundary Layer - PBL)**, **relative humidity (RH)**, **wind speed (WS)**, **temperature**, **aerosol chemical composition**, and sea-level **atmospheric pressure** conditions (Kumar et al, 2007; Gupta et al, 2006; Schaap et al, 2009 and Liu et al, 2007). Therefore, the corrections may vary widely in different regions, different seasons, and even on different days in one location.

For example, Engel-Cox (2004) found that the correlation was stronger in the eastern half of the United States, while it was weaker in the western United States. They believe that some of the general variation between AOD and PM measurements is caused by artifacts of linear analysis, different terrain conditions, and inherent differences in the data sets. Gupta (2006) found that the relationship between AOD and PM 2.5 was higher **for cloud-free conditions, low boundary layer heights, and low relative humidity**. The highest correlation between MODIS AOT and PM 2.5 mass was found under clear sky conditions with less than 40–50% RH and when PBL ranges from 100 to 200 m. Pelletier (2007) also suggested that meteorological variables improved the relationship between AOD and PM 10. Other atmospheric physical scientists concluded that the effect of meteorological conditions, such as wind velocity, relative humidity, temperature, and atmospheric pressure, can confound the

AOD–PM 2.5 association (Kumar et al, 2007; Liu et al, 2007), demonstrating that surface level wind speed, surface air temperature, and mixing layer height are significant predictors in PM 2.5–AOD models. (Li et al, 2009).

Global chemical transport models (CTMs) resolve atmospheric composition at a resolution of hundreds of kilometers horizontally by hundreds of meters vertically, with a temporal frequency of tens of minutes. Liu (2004) first estimated surface-level PM 2.5 from MISR observations by using CTM output to represent local AOD–PM 2.5 conversion factors over the contiguous United States. Van Donkelaar (2006) extended the approach used by Liu et al (2004) to estimate PM 2.5 from both MODIS and MISR observations. They used a global chemical transport model (GEOS-CHEM) to simulate the factors affecting the relation between AOD and PM 2.5. AERONET AOD was used to evaluate the method ($r = 0.71$, $N = 48$, slope = 0.69). They found significant spatial variation of the annual mean ground-based measurements with PM 2.5 determined from MODIS ($r = 0.69$, $N = 199$, slope = 0.82) and MISR ($r = 0.58$, $N = 199$, slope = 0.57). Excluding California significantly increased the respective slopes and correlations. The relative vertical profile of aerosol extinction was the most important factor affecting the spatial relationship between satellite and surface measurements of PM 2.5; neglecting this parameter would reduce the spatial correlation to 0.36. In contrast, temporal variation in AOD was the most influential parameter affecting the temporal relationship between satellite and surface measurements of PM 2.5; neglecting daily variation in this parameter would decrease the correlation in eastern North America from 0.5–0.8 to less than 0.2. Other simulated aerosol properties, such as effective radius and extinction efficiency were found to have a minor role temporally, but did not influence the spatial correlation.

The **characteristics of the particles** was also examined while evaluating AOD – PM 2.5 relationship. For example, Liu (2007) used MISR-retrieved spherical versus non-spherical particle fraction, in addition to model-derived vertical distribution, to separate mineral dust from other aerosol species. More recently, Paciorek (2009) probed the limitations of using AOD without accounting for vertical distribution or speciation and concluded that agreement with ground-based monitors based on this approach might depend on factors other than satellite observations.

Furthermore, **meteorological and geographical factors** were recommended to be integrated to the AOD–PM 2.5 relationship to improve models' performance (Guo et al, 2009; Liu et al,

2009; Tian and Chen, 2010). However, the estimation accuracy of the above models still has room to improve. The spatial variability of the AOD–PM 2.5 relationship is not fully taken into account, or in other words, the strength of the AOD–PM 2.5 correlation should not be constant across space and it should change with spatial context (Hu et al, 2013). The spatial variability and nonstationarity can be examined by GWR model, which is based on local regression techniques (Zhao et al, 2010; and Hu et al, 2013).

To estimate the daily concentration of ground-level PM 2.5 coincident to satellite overpass at regional scale, a satellite-based **geographically weighted regression** (GWR) model was developed by Song (2014). The model enhances PM 2.5 estimation accuracy by considering spatial variation and non-stationarity that might introduce significant biases into PM 2.5 estimation. The model was evaluated and validated against the PM 2.5 data collected over the Pearl River Delta (PRD) region, China for the period of May 2012 to September 2013. The evaluation evidenced that, with meteorological parameters assimilated, the GWR model is able to explain 73.8% of the variability in ground-level PM 2.5 concentration, a better performance than the two conventional statistical models (a general linear regression model Model-I, 56.4% and a semi-empirical model Model-II, 52.6%, respectively). The vertical correction on satellite-derived AOD and relative humidity significantly improve the AOD–PM 2.5 correlative relationship. The findings from the study demonstrated the great potential and value of the GWR model for regional PM 2.5 estimation.

Chapter 3: Methodology and Data

3.1 Description of datasets

In this study the following data was used:

1. MODIS Level 3 Global Daily Atmospheric Data
2. Meteorological Data over Europe from the WRF modeling system
3. PM 2.5 concentration data over Europe from the CAMx modeling system
4. PM 2.5 concentration data from two air quality monitoring stations located in Attica, Greece

All datasets were for the year 2009.

In the next paragraphs, a short description of these datasets will be provided.

3.1.1 Remote sensing data from MODIS

All MODIS data have been downloaded from the NASA's website:

ftp://ladsftp.nascom.nasa.gov/allData/5/MOD08_D3/

MODIS (Moderate Resolution Imaging Spectroradiometer) is a key instrument aboard the Terra (EOS AM) and Aqua (EOS PM) satellites. Terra MODIS and Aqua MODIS are viewing the entire Earth's surface every 1 to 2 days, acquiring data in 36 spectral bands, or groups of wavelengths.

The Level-3 MODIS Atmosphere Daily Global Product contains roughly 600 statistical datasets that are derived from approximately 80 scientific parameters from four Level-2 MODIS Atmosphere Products: Aerosol, Water Vapor, Cloud, and Atmosphere Profile. There are two MODIS Daily Global data product files: **MOD08_D3**, containing data collected from the Terra platform; and **MYD08_D3**, containing data collected from the Aqua platform.

A range of statistical summaries (like mean, minimum, maximum, standard deviation, histograms etc.) are computed, depending on the parameter being considered. Statistics are sorted into 1 by 1 degree cells on an equal-angle grid that spans a 24-hour (0000 to 2400 Greenwich Mean Time) interval and are then summarized over the globe (NASA, 2016d).

From the available **atmospheric parameters**, in this study we used:

- Aerosol **Optical Depth** and
- Aerosol **Angstrom exponent**

3.1.1.1 Aerosol Optical Depth

Aerosol Optical Depth or Thickness is the degree to which aerosols prevent the transmission of light by absorption or scattering of light.

The aerosol optical depth (usually expressed as τ) is defined as the integrated extinction coefficient over a vertical column of unit cross-section.

Extinction coefficient is the fractional depletion (attenuation) of radiance per unit path length. The optical thickness along the vertical direction is also called normal optical thickness (compared to optical thickness along slant path length).

The Aerosol Optical Depth in a wavelength (λ) can be expressed as (IUPAC, 1997):

$$\tau_\lambda = \ln\left(\frac{\Phi^{i}_{e,\lambda}}{\Phi^{t}_{e,\lambda}}\right) = -\ln T_\lambda,$$

Where:

$\Phi^{t}_{e,\lambda}$ is the spectral radiant flux in wavelength transmitted;

$\Phi^{i}_{e,\lambda}$ is the spectral radiant flux in wavelength received;

T_λ is the spectral transmittance in wavelength λ.

A AOD value of 0.01 corresponds to an extremely clean atmosphere, while a value of 0.4 corresponds to very hazy condition.

3.1.1.2 Aerosol Angstrom Exponent

The Aerosol Angstrom Exponent (α) expresses the spectral dependence of aerosol optical thickness (τ) with the wavelength of incident light (λ).

The spectral dependence of aerosol optical thickness can be approximated (depending on size distribution) by the formula (GES DISC, 2016):

$\tau_a = \beta \lambda^{\alpha}$

where:

β = aerosol optical thickness at 1 μm.

Thus, the Angstrom exponent, which can be computed from Optical Depth measurements on two different wavelengths, can be used to find the Optical Depth on another wavelength using the relation:

$$\tau_{\lambda} = \tau_{\lambda_0}\left(\frac{\lambda}{\lambda_0}\right)^{-\alpha}$$

The Angstrom exponent is very useful in the interpretation of aerosol characteristics since it provides information on the particle size, aerosol phase function and the relative magnitude of aerosol radiances at different wavelengths. Large values of the exponent indicate smaller particle sizes (GES DISC, 2016).

3.1.2 Air quality data

PM 2.5 daily average concentrations over Europe were used in this study. The data was produced from the CAMx modeling system as part of the EU FP7 project MACC, and was provided by the Laboratory of Atmospheric Physics of the Aristotle University of Thessaloniki (MACC Project, 2009). Their spatial extent was the whole of Europe in a 0.3 Degrees spatial resolution grid presented in the Geographic WGS84 projection.

The image below (Figure 3) presents the CAMx air quality-modeling domain:

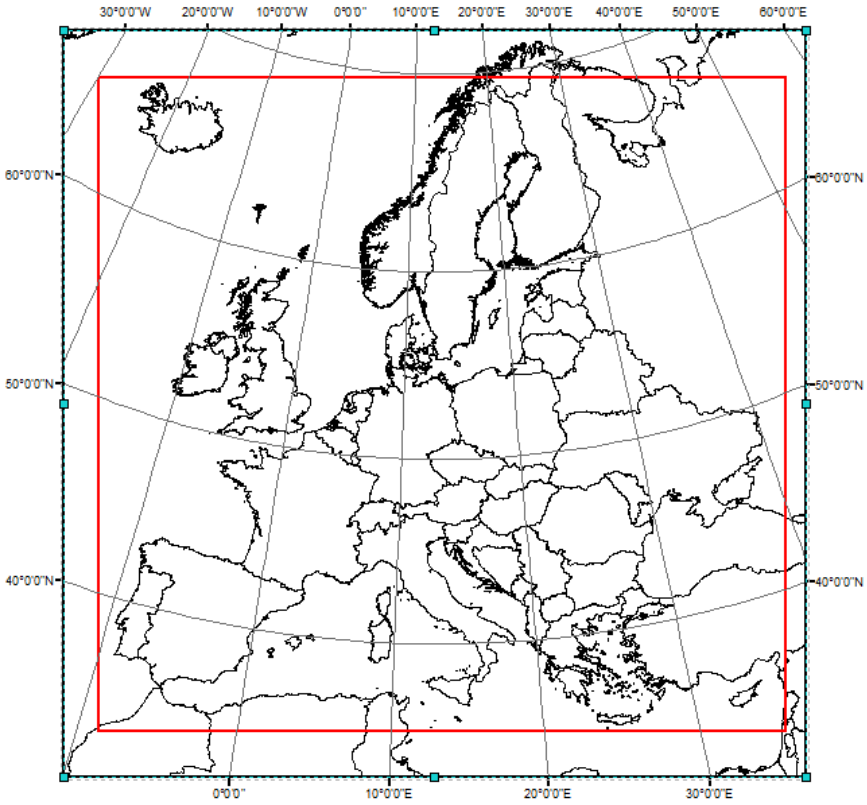

Figure 3: The CAMx modeling domain over Europe

3.1.3 Meteorological data

Meteorological data (Planetary Boundary Layer Height (PBL), wind speed and relative humidity) were also used. The data was produced from the WRF modeling system. They were also produced as part of the EU FP7 project MACC, and was provided by the Laboratory of Atmospheric Physics of the Aristotle University of Thessaloniki (MACC Project, 2009).

Their spatial coverage was the whole Europe in a 30km spatial resolution presented in the Lambert Conformal Conic projection. The time step (temporal resolution) of the data was 1 hour, but for this study 24 hours, daily average values were used.

The image below (Figure 4) presents the WRF modeling domain:

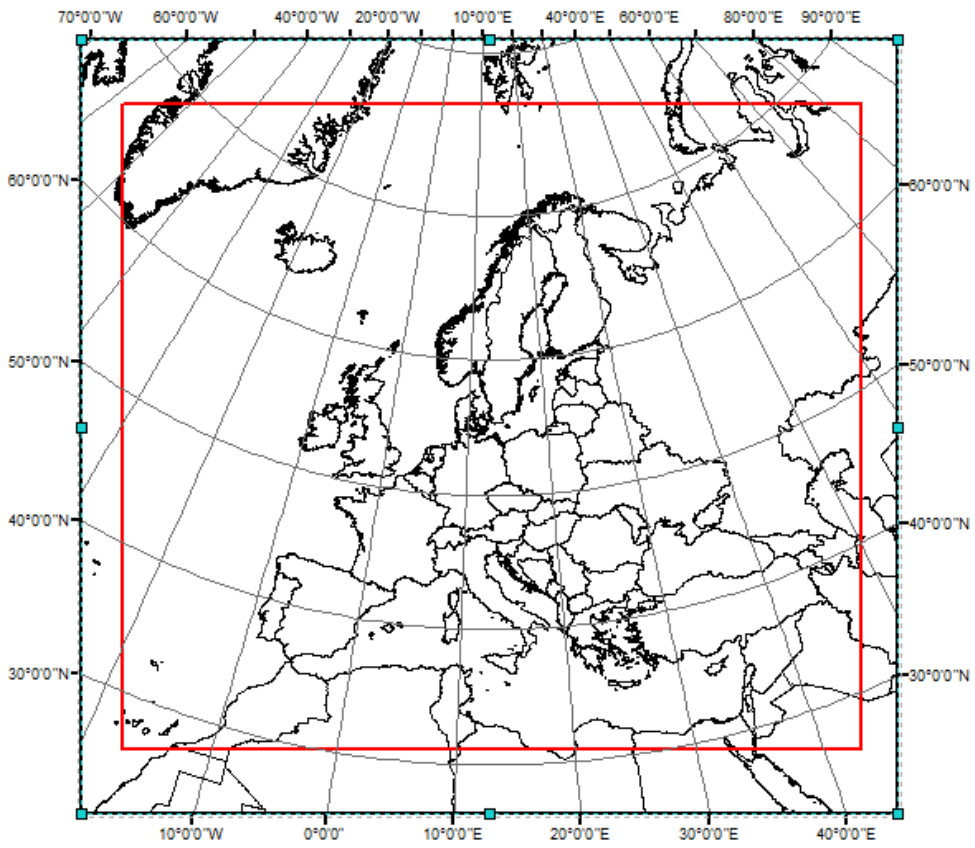

Figure 4: The WRF modeling domain over Europe

3.1.4 On site PM measurements

For the evaluation of the possible relation between remote sensing data and PM concentration, measurements from 2 air quality stations were used. The stations were located in the Greater Athens Area in Greece. These stations are part of the Greek National Air Quality Measurements Network. The stations are:

- **Lykovrisi** (**LYK** - ΛΥΚΟΒΡΥΣΗ): Longitude: 23.7871, Latitude: 38.0652
- **Agia Paraskevi** (**AGP** - ΑΓΙΑ ΠΑΡΑΣΚΕΥΗ): Longitude: 23.8177, Latitude: 37.9925

The location of these stations is presented in the map below (Figure 5).

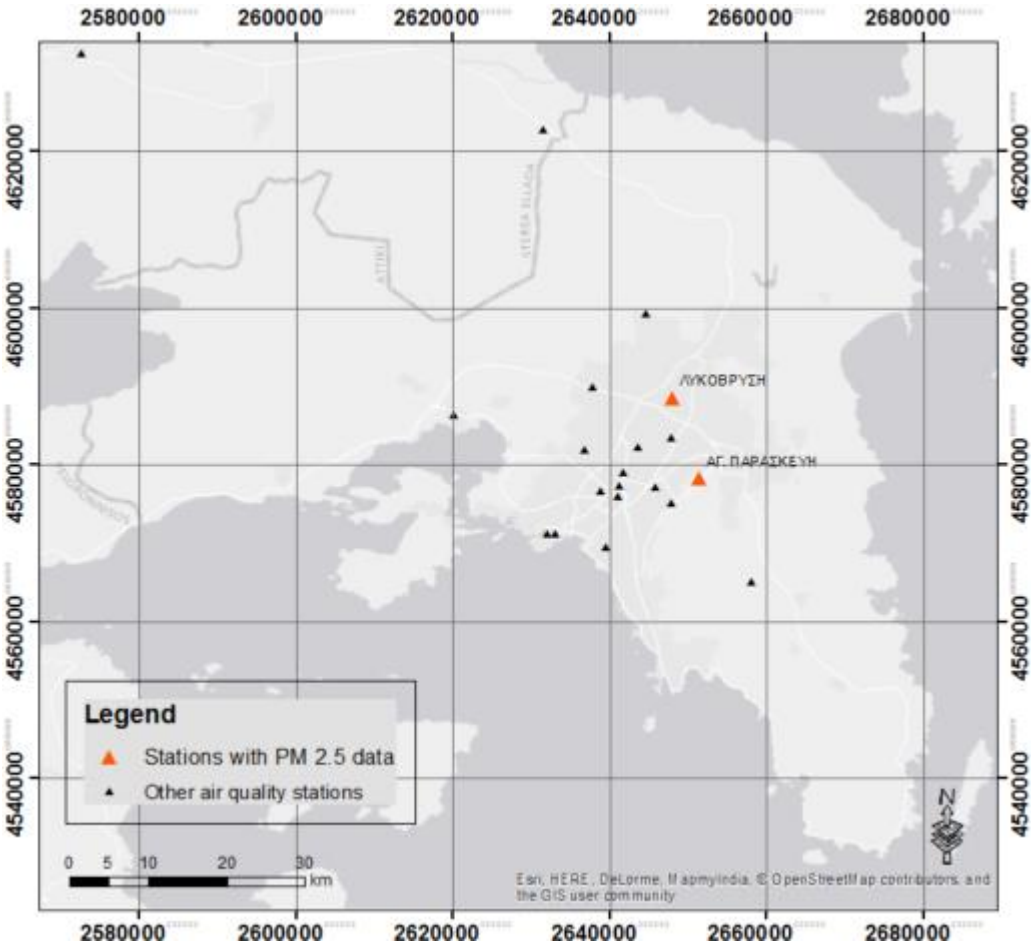

Figure 5: Location of PM 2.5 stations

Station Lykovrisi represents suburban conditions, while station Agia Paraskevi represents suburban / background conditions.

These stations are selected since only they had PM 2.5 measurements for the requested period (year 2009).

The data (daily average concentrations) was available through the web portal of the Greek Ministry of Environment and Energy: http://www.ypeka.gr/Default.aspx?tabid=495

3.1.5 Data preprocessing

MODIS data were provided in HDF format. Each file included all the atmospheric parameters measured by the MODIS instrument. Thus extraction of the AOD and AE datasets was performed. The resulting GeoTiFFs were ready to be used in GIS software like ArcGIS.

PM and **meteorological** variables were provided in NetCDF format. There were different files for each parameter. The files contained the average daily concentration of the parameters in all

the horizontal layers of the model. Thus the extraction of data for the closest to the ground level was required which was performed using python scripts. The data files were exported to GeoTiff format using custom python scripts that utilize the open source geospatial library GDAL. The data was also resampled to 1-degree resolution, in order to match the resolution of the MODIS images.

Station PM **data** were in standard ASCII format, and thus no preprocessing was necessary.

3.2 Tools and methods

The GIS datasets that were used in this study were analyzed and visualized using various GIS software and tools. The data preprocessing was mostly performed using custom python scripts and open source libraries for spatial data processing like GDAL and scientific data (HDF, NC).

The resulting data were analyzed and visualized in ArcGIS. Thus ArcGIS was used in order to produce the monthly or seasonal averages (using the Spatial Analyst geoprocessing tools) or in order to extract the raster pixel values at the desired locations. In order to automate the processes. Model Builder as well as python programming using Arcpy were used.

Finally, statistical analysis was performed using the IBM's SPSS software. SPSS provides several advanced statistical tools including tools for descriptive statistics, correlations and regression analysis.

The overall process workflow is presented in the image below (Figure 6):

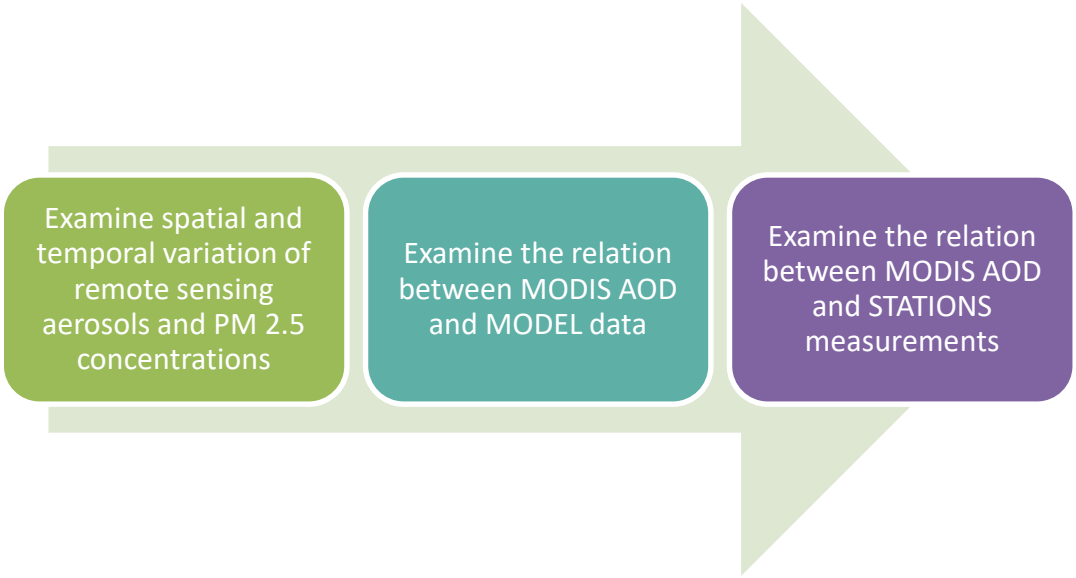

Figure 6: Methodology workflow

3.2.1 Spatial and temporal variation of remote sensing aerosols and PM concentration

Monthly and / or seasonal datasets were produced from the daily raster data of the above parameters (using the Spatial Analyst toolbox *Cell Statistics* geoprocessing tool). Using these datasets, monthly AOD and PM 2.5 maps were produced which are presented in the next chapter of this study. These maps show the spatial and temporal variability of these parameters over Europe.

3.2.2 Creation of regression models between atmospheric aerosol parameters and model data

In this study, the correlation between MODIS AOD and PM 2.5 concentration was examined. In case of a good correlation, the remote sensing data would be used in order to provide an estimation of the particulate matter air quality conditions in Europe.

This hypothesis was tested in a number of locations that were major cities all over Europe. The selection criteria were a) Spanning location across the whole of Europe coverage and b) the population nearby would be affected by high air pollution concentration. PM 2.5 concentration is greater in big urban agglomerations due to higher pollutant emissions. In these areas, all over Europe, very often pollutants concentration exceeds the regulation limits and a large population is affected by air pollution. Thus, monitoring of air quality levels in these areas is of crucial importance. These locations are presented in the map below (Figure 7).

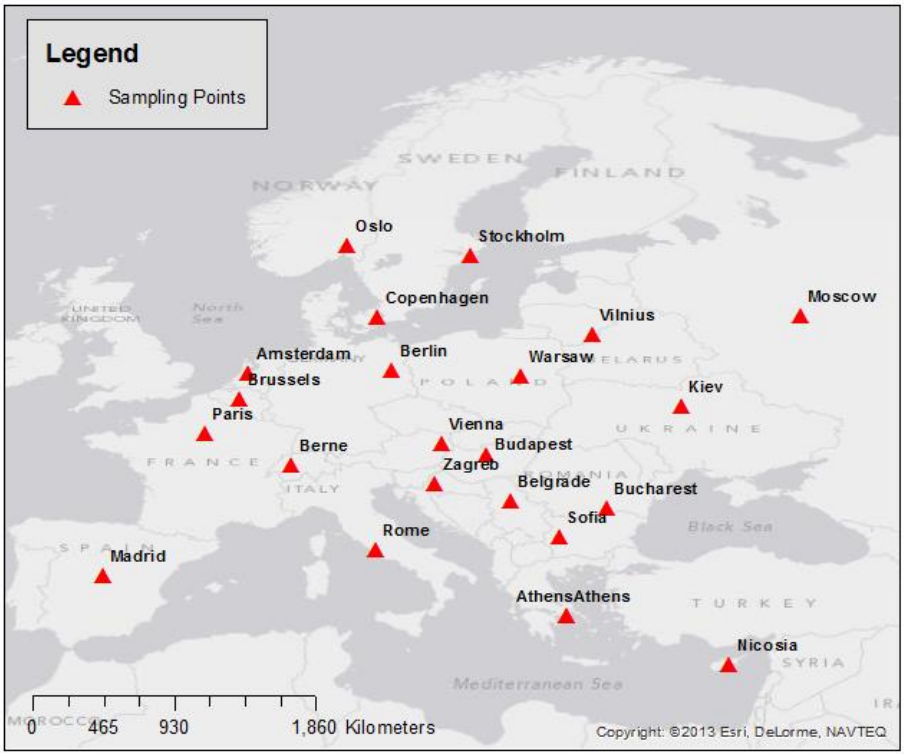

Figure 7: Location of regression analysis points

Based on these points, the relevant values from the MODIS, CAMx air quality and WRF meteorological raster files were extracted (using the Spatial Analyst toolbox *Extract Multi Values to Points* geoprocessing tool).

For each location, the available data was then compiled in a statistical software (SPSS) package, where regression analysis was performed. Two different conditions were examined. One with PM 2.5 as the dependent variable and AOD, AE, wind speed, PBL and relative humidity as independent variables, and one with PM 2.5 as the dependent variable, and **AOD/PBL**, AE, wind speed, and relative humidity as independent variables.

The second condition was selected to be examined since, PM concentration can be expressed as a function of AOD/PBL (Seo et al, 2015):

$$PM = \frac{AOD}{PBL} \frac{4\,\rho\,R_{eff}}{f(RH)3\,Q_{ext}}$$

Where RH is the relative humidity, ρ is the particle mass density, R_{eff} is the particle effective radius and Q_{ext} is the average of the extinction efficiency over the size distribution.

The result of these analyses show:

- if a significant relation exists between these variables,
- which was the most dominant factor in this relationship and
- the mathematical relationship between them.

Since a seasonal variability was expected, the analysis was performed separately for each season (Winter: December-January-February, Spring: March-April-May, Summer: June-July-August, Autumn: September-October-November).

3.2.3 Creation of regression models between atmospheric aerosol parameters, model data and PM 2.5 station data

The correlation between MODIS variables and PM 2.5 concentration in two air quality measurement stations located in Attica, Greece was also examined.

Since both stations were located relatively close to each other (approximately 10 km) and both were within the same AOD cell, their data were compared by correlation analysis.

Then, for each station and for all seasons, regression analysis was performed between PM 2.5 measurements as the dependent variable and AOD, AE from MODIS, as well as the meteorological parameters derived from the model PBL, wind speed, and relative humidity, as independent variables.

This statistical analysis was again performed using the SPSS software package.

Chapter 4: Results

4.1 Spatial and temporal distribution of aerosols

This section will provide information about the spatial and temporal distribution of aerosols in Europe, based on the AOD derived from MODIS datasets for year 2009.

Figure 8 presents the monthly average of AOD in the study area. Regarding the temporal variation of AOD, the highest values over Europe were during spring (March, April, May) while the lowest values were during autumn (September, October, November).

During winter, December AOD values are relatively low (below 0.1) while during January and February, higher values are observed, especially over the sea in the Eastern Mediterranean area. These high values might occur due to sea salt particles suspended in the atmosphere. Some high values are also present over populated or highly industrial areas like the valley of Po in Northern Italy or Paris in France.

During spring high AOD values are observed all over Europe (over 0.2). There is still evidence of high AOD values over populated or industrial areas in Northern Italy, Germany, Poland or even Russia (over Moscow area during April), while high AOD values are also detected over sea areas in the Mediterranean, especially during March and April.

Lower AOD values are generally observed during summer. Higher AOD values are over Poland (June and July), Holland (July), the Balkan area (especially during August) and during the entire summer period in northern Italy.

During autumn, higher AOD values are observed during September and lower during October and November. The highest AOD values are over sea areas in Mediterranean and the Black Sea, while over land the higher values are observed over Turkey.

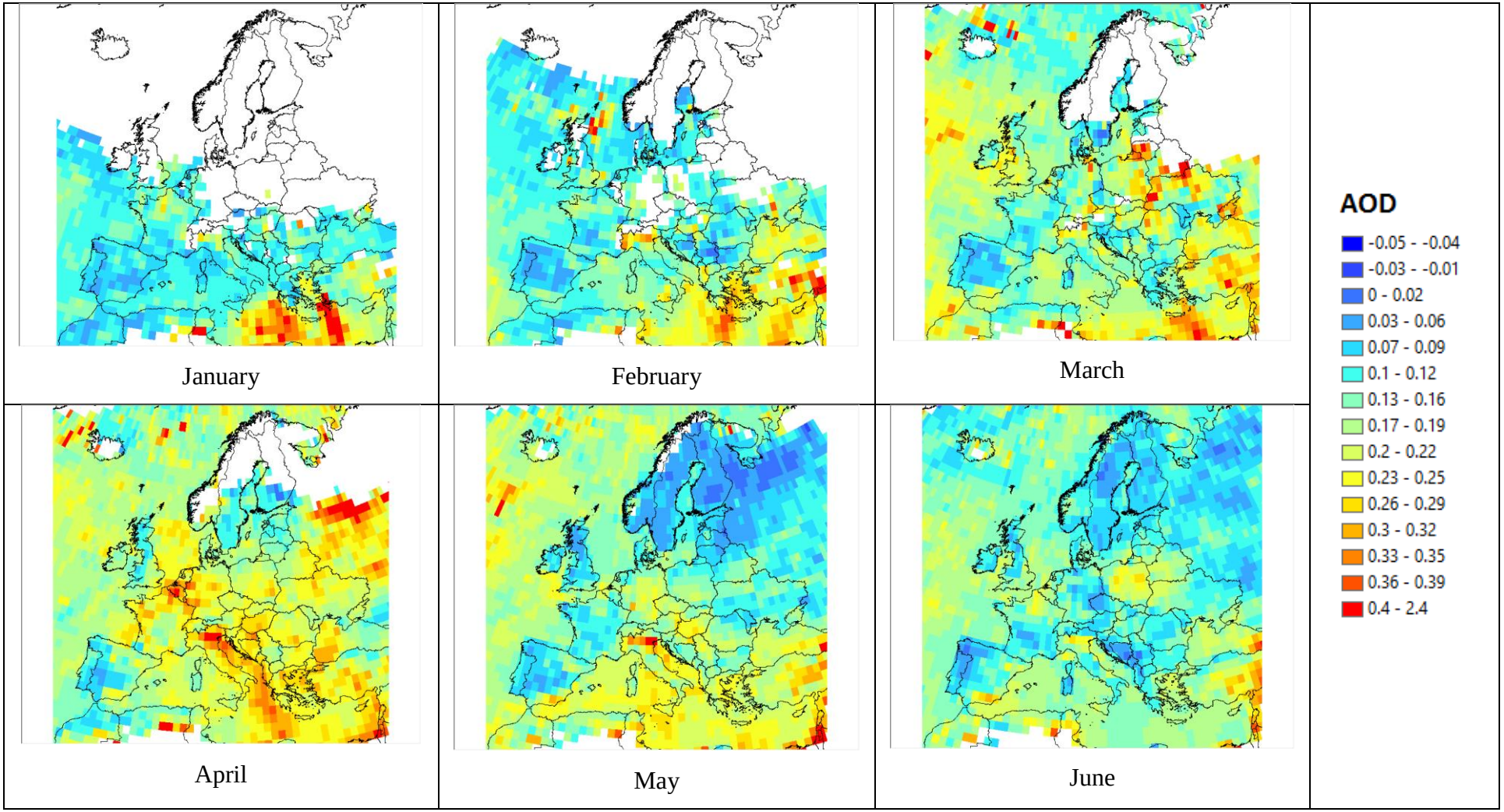
January
February
March
April
May
June
AOD
-0.05 - -0.04
-0.03 - -0.01
0 - 0.02
0.03 - 0.06
0.07 - 0.09
0.1 - 0.12
0.13 - 0.16
0.17 - 0.19
0.2 - 0.22
0.23 - 0.25
0.26 - 0.29
0.3 - 0.32
0.33 - 0.35
0.36 - 0.39
0.4 - 2.4

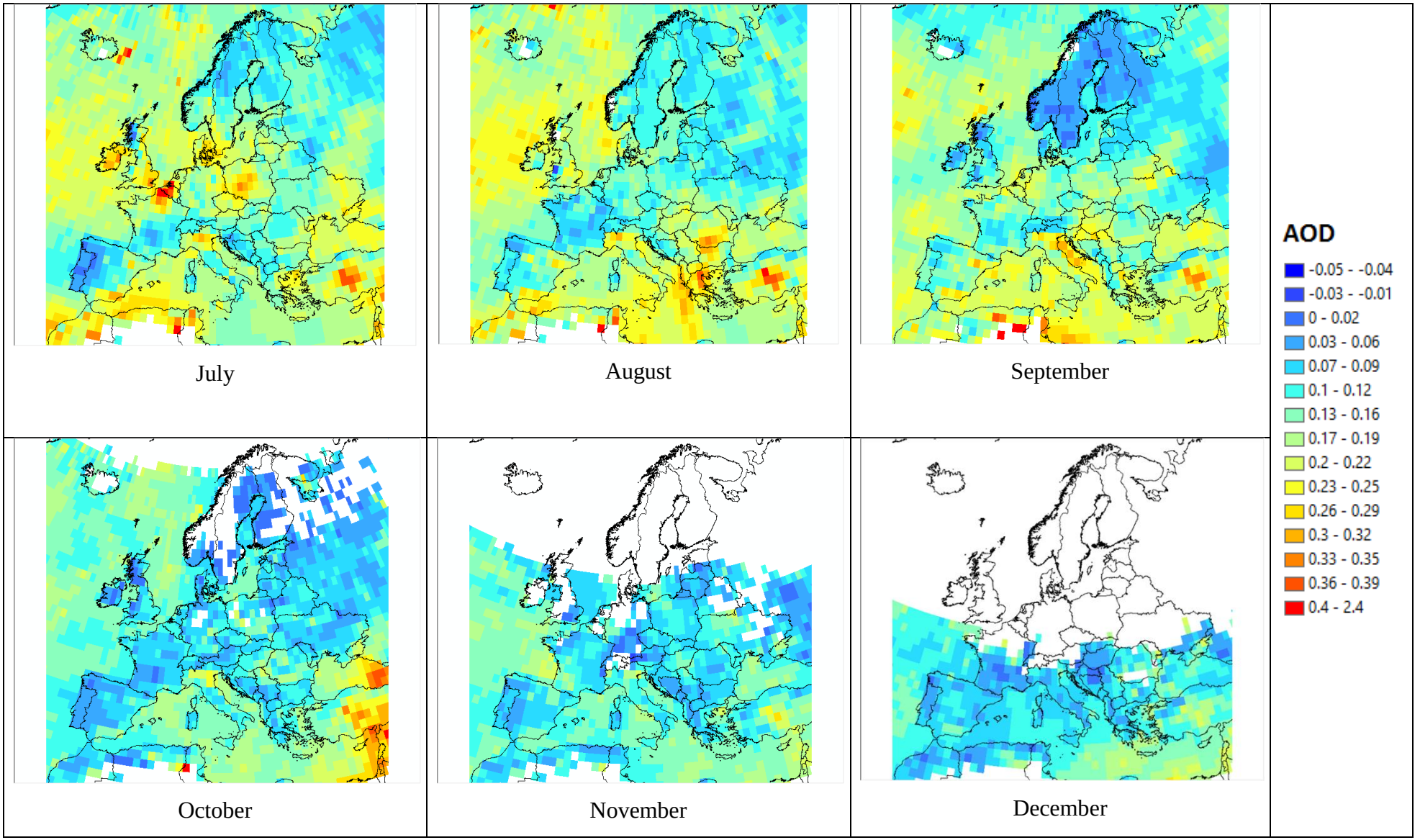

Figure 8: Monthly MODIS AOD values over Europe

4.2 Spatial and temporal distribution of PM 2.5 concentration

This section will provide information about the spatial and temporal distribution of PM 2.5 concentration in Europe. The data was from the CAMx photochemical model, which simulated air pollution levels in Europe for year 2009.

Figure 9 presents the seasonal variation of the PM 2.5 concentration resulting from the model. The results show a significant impact of the boundaries conditions, especially in the western boundary of the model (Liora et al, 2013) as well as to the natural sea salt emissions, especially over the Atlantic Ocean area (Manders et al, 2010; Sofiev et al, 2011). In these areas, the PM 2.5 concentration calculated by the model is over 36 μg/m3, with high values up to 70 μg/m3. The high sea salt emissions probably result in higher PM 2.5 values also in countries like Ireland, UK, France or Portugal (with values up to 40 μg/m3 during winter, spring and autumn).

Over the rest of Europe, higher PM 2.5 values are estimated during winter and autumn due to higher emissions from central heating and other manmade activities, as well as the meteorological conditions and especially the thickness of the PBL during that period. The lower PM 2.5 values are calculated during summer where PM 2.5 are below 20 μg/m3 almost all over Europe.

Figure 10 presents the monthly average concentrations over Europe. The monthly averages allow us to observe several cases were anthropogenic emission are the dominant factor of the PM 2.5 concentration. For example, the maps for October or December show areas with higher PM 2.5 concentration over densely populated / industrialized areas as Northern Italy, central Europe (Belgium, Holland, Germany) or over Poland and Russia.

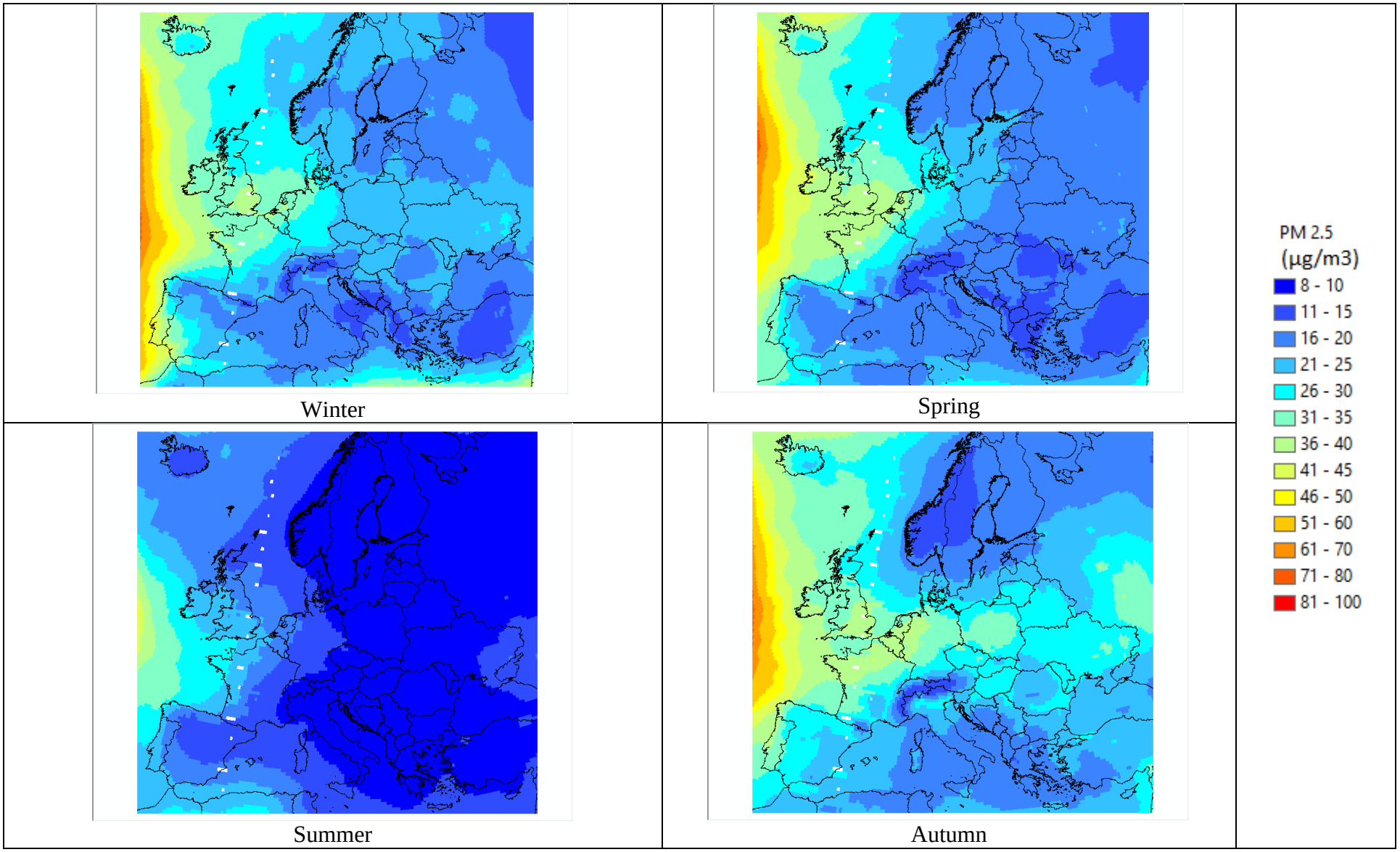

Figure 9: Seasonal PM 2.5 average concentration, based on the CAMx model data, over Europe

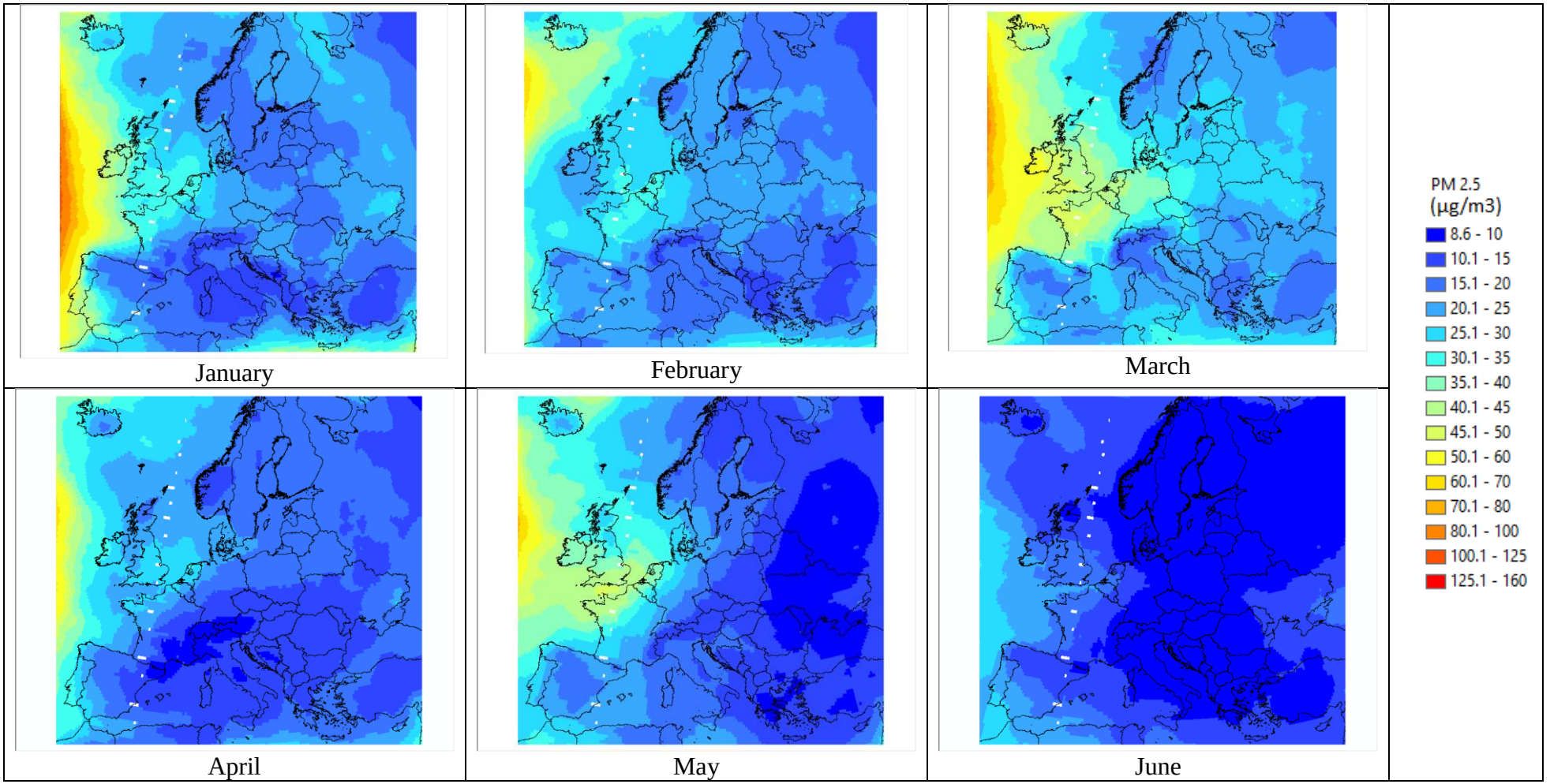
January
February
March
April
May
June
PM 2.5
(µg/m3)
8.6 - 10
10.1 - 15
15.1 - 20
20.1 - 25
25.1 - 30
30.1 - 35
35.1 - 40
40.1 - 45
45.1 - 50
50.1 - 60
60.1 - 70
70.1 - 80
80.1 - 100
100.1 - 125
125.1 - 160

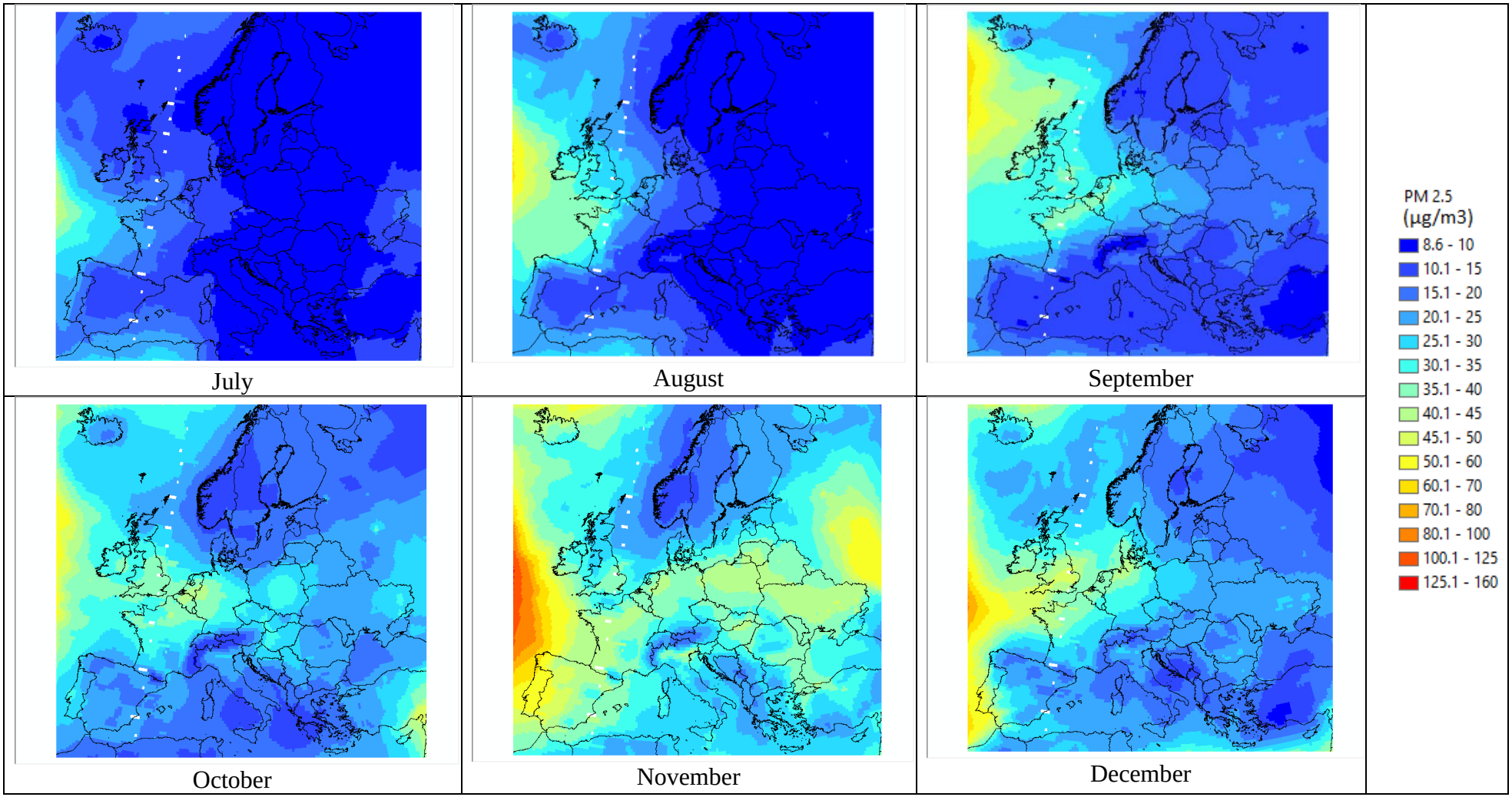

Figure 10: Monthly PM 2.5 average concentration, based on the CAMx model data, over Europe

4.3 Statistical analysis of the relation of AOD – CAMx PM Concentration

The statistical analysis of the relation between PM 2.5 and AOD was examined in 22 locations spread all over Europe. A detailed presentation of the results in 5 locations (Athens, Belgrade, Nicosia, Paris, Zagreb) is given in the following sections. These locations were in the Central / South parts of Europe and, as a result, they had less missing AOD values during autumn and, especially, the winter period. Thus the regression analysis, in these locations, was performed with a higher sample size in relation to other location in the northern Europe. Also, these locations had different characteristics (location, population size / density, pollution levels) and for that reason they were all selected to be presented in details.

4.3.1 Athens

The following figure (Figure 11) presents the seasonal average of PM 2.5, AOD and AOD/PBL in Athens.

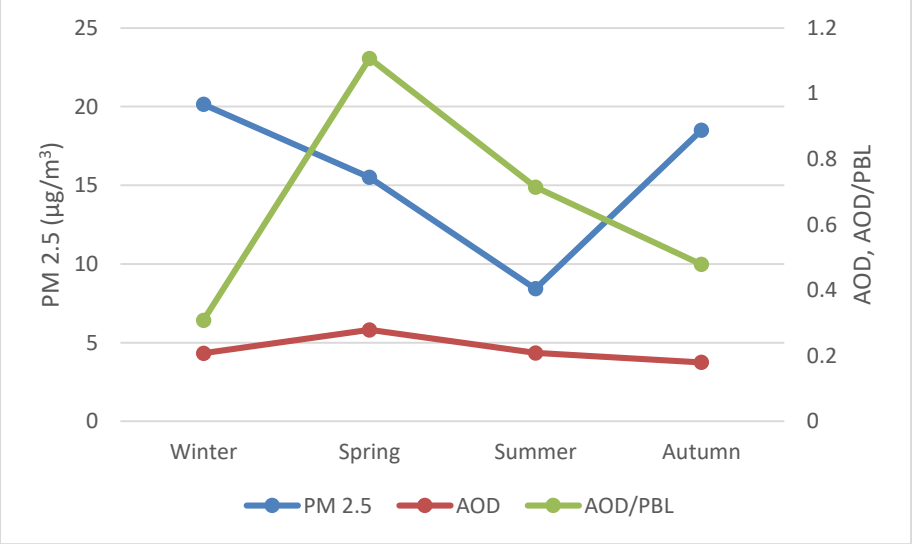

Figure 11: Time series of seasonal average of PM 2.5, AOD, AOD/PBL in Athens

While PM 2.5 concentration shows a maximum during winter, due probably to the increased emissions of central heating, and a minimum during summer, MODIS AOD, which shows a small variability, and AOD/PBL have a maximum during spring and a minimum during autumn.

The Pearson correlation coefficients (R) between PM 2.5 and AOD, AOD/PBL for each season are presented in Table 1 below. These coefficients illustrate a quantitative measure of the statistical relationship between these variables. Greater values show stronger correlations. In

Table 1, values in bold demonstrate the higher correlation for each season and group of variables.

Table 1: correlation coefficients between PM 2.5, AOD and AOD/PBL in Athens

Season	Correlation coefficient of PM 2.5 with AOD	Correlation coefficient of PM 2.5 with AOD/PBL
Winter	0.713	**0.793**
Spring	**0.056**	-0.013
Summer	0.033	**0.146**
Autumn	0.015	**-0.088**

It is clear that both AOD and AOD/PBL have a good correlation with PM 2.5 only during winter in Athens, with correlation coefficients of 0.713 and 0.793, respectively.

The correlation of PM 2.5 with AOD is also illustrated in the seasonal scatter plots in Figure 12 below. A linear regression equation was also calculated and the coefficient of determination, R^2, is displayed for each case. It is clear that PM 2.5 and AOD correlation is significant in Athens only during winter.

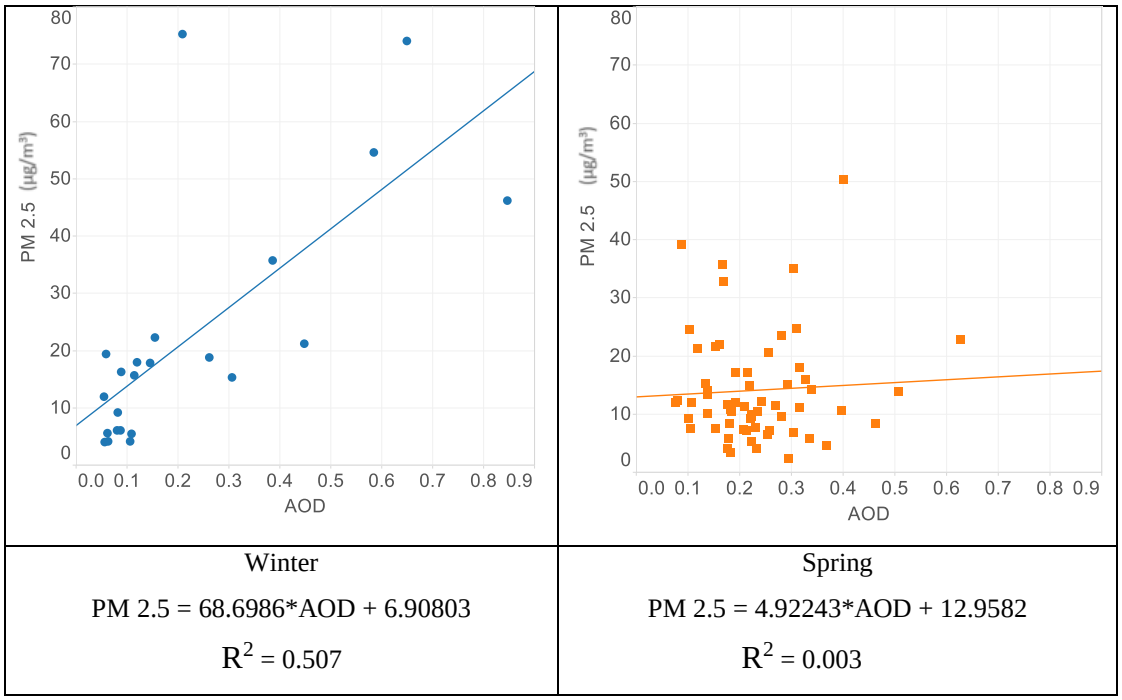

Winter	Spring
PM 2.5 = 68.6986*AOD + 6.90803	PM 2.5 = 4.92243*AOD + 12.9582
R^2 = 0.507	R^2 = 0.003

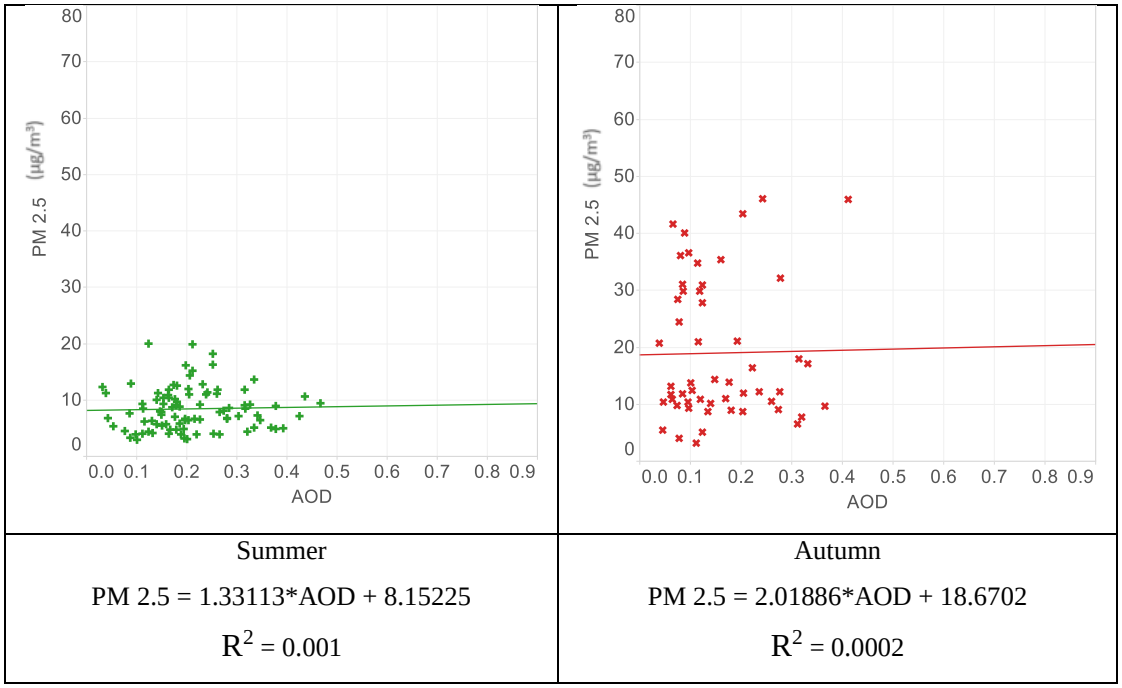

Summer	Autumn
PM 2.5 = 1.33113*AOD + 8.15225	PM 2.5 = 2.01886*AOD + 18.6702
R^2 = 0.001	R^2 = 0.0002

Figure 12: Seasonal Scatter Plots of PM 2.5 and AOD values in Athens

Table 2 presents the regression results and coefficients for the two cases examined.

The first one was with PM 2.5 as the dependent variable and AOD/PBL, Angstrom Exponent (AE), Relative Humidity (RH) and Wind Speed (WS) as independent variables.

The regression equation is expressed as:

Equation 1: $PM\ 2.5 = a_0 + a_1 * AOD/PBL + a_2 * AE + a_3 * RH + {}_a4 * WS$ **(1)**

In the second case, PM 2.5 was again the dependent variable, but in this case the independent variables were AOD, PBL, AE, RH and WS.

The regression equation is expressed as:

Equation 2: $PM\ 2.5 = a_0 + a_1 * AOD + a_2 * AE + a_3 * PBL + a_4 * RH + a_5 * WS$ **(2)**

In both cases, the regression performance was measured by the values of the correlation coefficient, R, and the coefficient of determination, R^2.

In Table 2, N is the sample size used in the regression analysis. The other values in the table are the coefficients of the regression equations:

Table 2: Regression results and evaluation in Athens

season	N	R	R^2	a_0	a_1	a_2	a_3	a_4
Winter	23	0.82	0.672	-37.59	52566.577	6.666	0.335	1.274
Spring	61	0.22	0.048	11.967	545.832	5.858	-0.082	0.322
Summer	91	0.347	0.12	-5.138	143.851	-1.448	0.186	0.155
Autumn	53	0.72	0.519	-77.944	-5216.911	7.785	1.124	0.589

season	N	R	R^2	a_0	a_1	a_2	a_3	a_4	a_5
Winter	23	0.809	0.655	-30.203	78.873	9.805	-0.014	0.445	0.053
Spring	61	0.266	0.071	6.481	13.538	5.616	0.006	-0.023	-0.496
Summer	91	0.613	0.376	3.74	-2.906	-2.156	-0.013	0.069	1.368
Autumn	53	0.704	0.496	-86.728	-7.276	8.617	0.006	1.161	0.633

In order to provide a visual interpretation of the regression results the following scale was applied:

Regression results:

- Good: R >= 0.6 ,
- Relatively Good: 0.4 < R < 0.6 ,
- Bad: R <= 0.4

Both methods had the best performance for winter (R=0.82 for AOD/PBL and R=0.809 for AOD, PBL) where a good correlation between AOD and PM 2.5 existed. Nevertheless, there were also good results for autumn, for both cases and also for Summer for AOD, PBL. Both cases failed to provide a good result for spring.

4.3.2 Belgrade

The following figure (Figure 13) presents the seasonal average of PM 2.5, AOD and AOD/PBL in Belgrade.

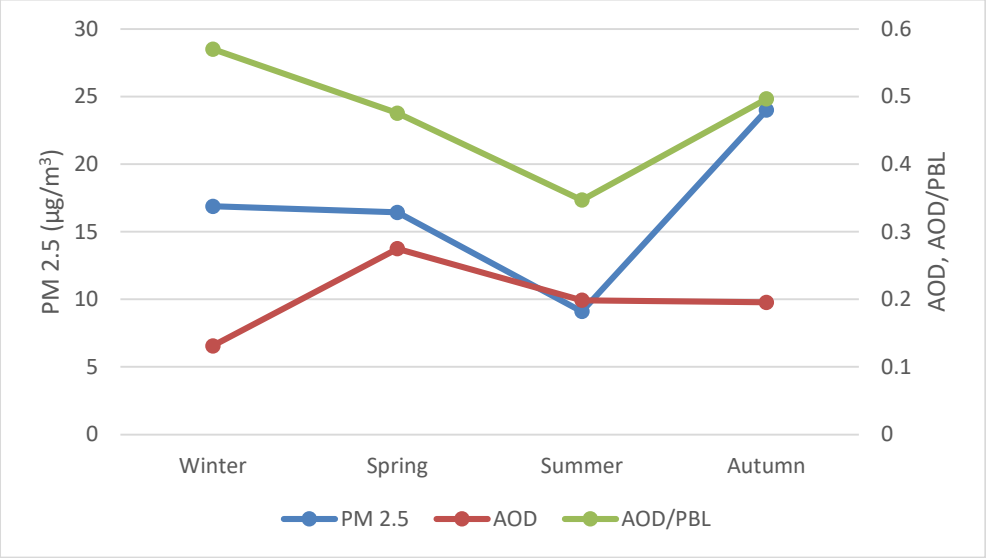

Figure 13: Time series of seasonal average of PM 2.5, AOD, AOD/PBL in Belgrade

PM 2.5 concentration shows a maximum during autumn and a minimum during summer with winter and spring average concentration of about the same magnitude. AOD shows a maximum during spring and a minimum during winter. AOD/PBL shows a similar seasonal variation with PM 2.5 but with maximum during winter.

The seasonal correlation coefficients between PM 2.5, AOD and AOD/PBL for Belgrade are presented in the table below.

Table 3: correlation coefficients between PM 2.5, AOD and AOD/PBL in Belgrade

Season	Correlation coefficient of PM 2.5 with AOD	Correlation coefficient of PM 2.5 with AOD/PBL
Winter	-0.028	**0.336**
Spring	0.407	**0.45**
Summer	0.275	**0.288**
Autumn	-0.169	**0.253**

Overall, the correlation between PM 2.5 and AOD or AOD/PBL was not good in Belgrade, with maximum correlation coefficients 0.407 and 0.45 with AOD and AOD/PBL, respectively, during spring.

This is also illustrated in the seasonal scatter plots of PM 2.5 with AOD for Belgrade in Figure 14 below.

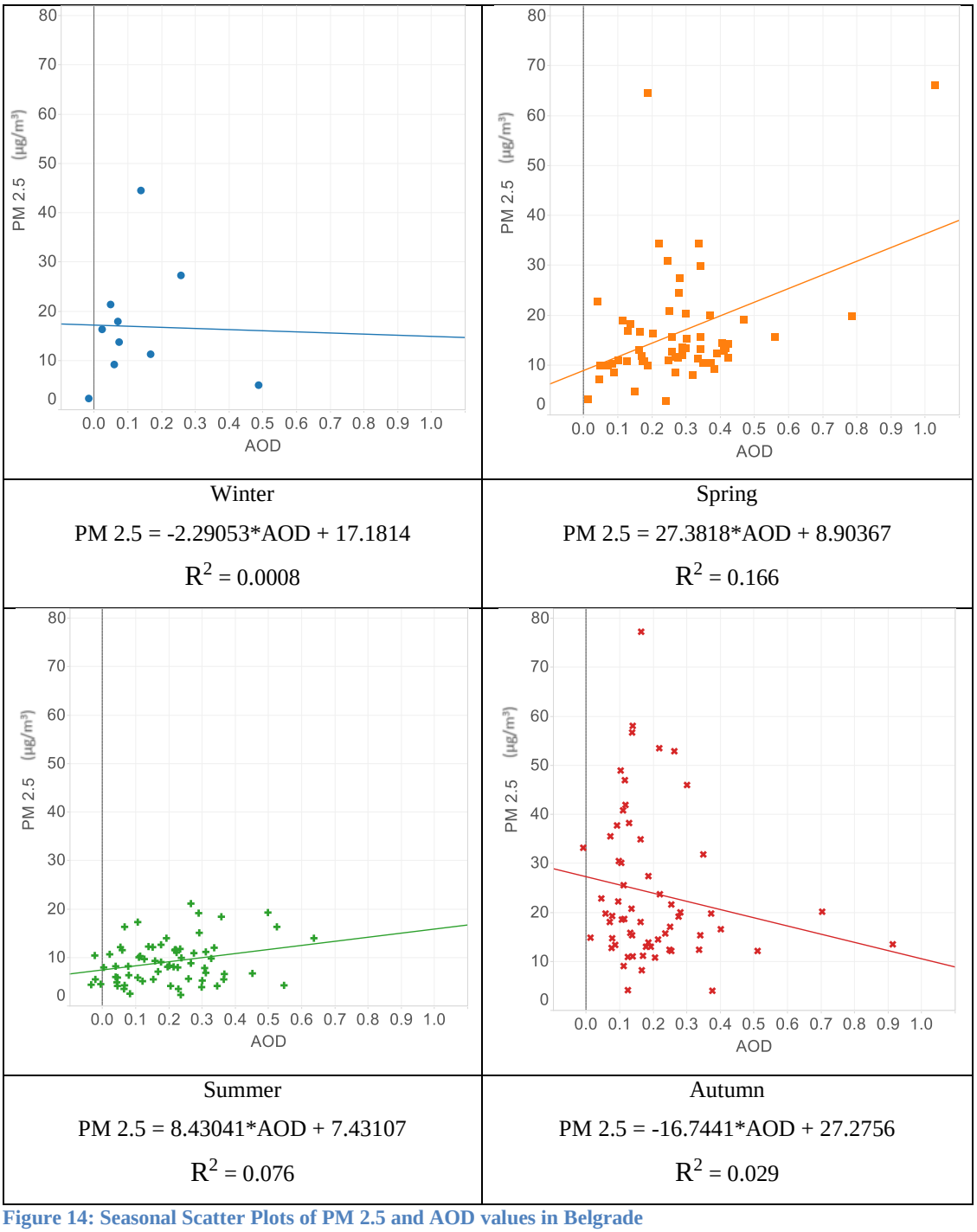

Winter	Spring
PM 2.5 = -2.29053*AOD + 17.1814	PM 2.5 = 27.3818*AOD + 8.90367
R^2 = 0.0008	R^2 = 0.166
Summer	**Autumn**
PM 2.5 = 8.43041*AOD + 7.43107	PM 2.5 = -16.7441*AOD + 27.2756
R^2 = 0.076	R^2 = 0.029

Figure 14: Seasonal Scatter Plots of PM 2.5 and AOD values in Belgrade

The next table presents the regression results and coefficients using AOD/PBL as independent variable as well as both AOD, PBL as independent variables for Belgrade.

The regression equations are those presented in Equation 1 and Equation 2 in the previous paragraph.

For the visual interpretation of the results, the same color scale was applied as in Athens.

Table 4: Regression results and evaluation in Belgrade

season	N	R	R^2	a_0	a_1	a_2	a_3	a_4
Winter	10	0.788	0.62	-148.707	2210.443	-1.636	2	-2.014
Spring	58	0.555	0.308	-11.89	15459.162	-2.314	0.214	2.38
Summer	68	0.349	0.122	18.67	5524.633	-0.39	-0.122	-0.571
Autumn	62	0.714	0.51	-82.045	4360.644	4.424	1.295	-3.842

season	N	R	R^2	a_0	a_1	a_2	a_3	a_4	a_5
Winter	10	0.84	0.706	-72.482	-26.925	-10.381	-0.015	1.352	-0.898
Spring	58	0.496	0.246	-19.819	29.18	-1.386	0.003	0.309	1.211
Summer	68	0.343	0.118	19.386	9.535	-0.443	-0.003	-0.114	-0.324
Autumn	62	0.727	0.528	-65.165	-2.012	3.038	-0.019	1.189	-1.976

Regression results: Good, Relatively Good, Bad

Both methods had the best performance for winter (R=0.788 for AOD/PBL and R=0.84 for AOD, PBL) although during that period there was no good correlation between AOD and PM 2.5. Also good results were derived for autumn with R=0.714 and R=0.727. For spring, the results were relatively good, while for summer they were in both cases found to be bad results.

4.3.3 Nicosia

The following figure (Figure 15) presents the seasonal average of PM 2.5, AOD and AOD/PBL in Nicosia.

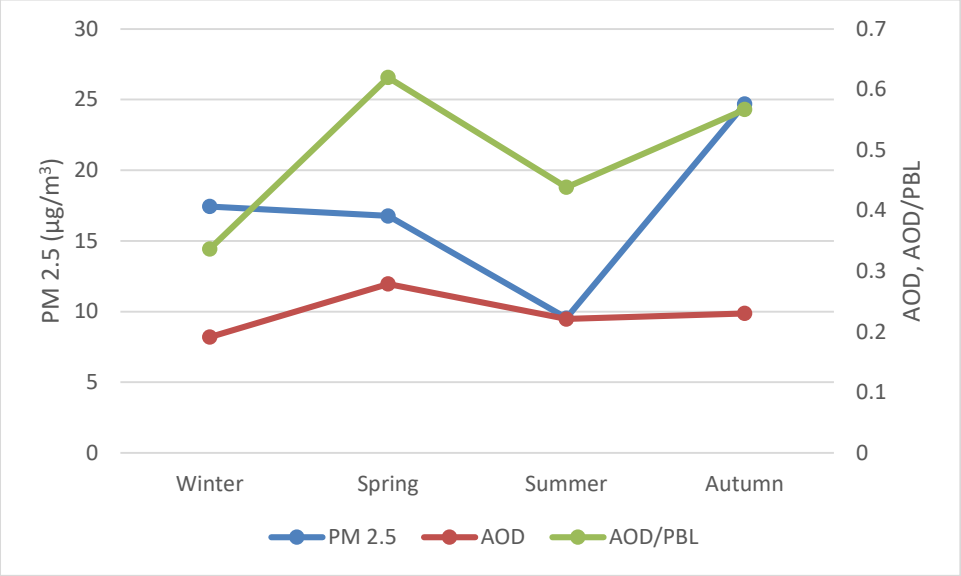

Figure 15: Time series of seasonal average of PM 2.5, AOD, AOD/PBL in Nicosia

PM 2.5 concentration shows a maximum during autumn and a minimum during summer for Nicosia, with winter and spring average concentration of about the same magnitude. AOD shows a maximum during spring and a minimum during winter. AOD/PBL shows a similar seasonal variation with AOD but with maximum during spring.

The seasonal correlation coefficients between PM 2.5, AOD and AOD/PBL are presented in the table below.

Table 5: correlation coefficients between PM 2.5, AOD and AOD/PBL in Nicosia

Season	Correlation coefficient of PM 2.5 with AOD	Correlation coefficient of PM 2.5 with AOD/PBL
Winter	**0.494**	0.424
Spring	**0.64**	0.446
Summer	**0.39**	0.39
Autumn	**0.514**	0.454

In all cases, PM 2.5 has a better correlation with AOD than with AOD/PBL for Nicosia, with a maximum correlation coefficient during spring (0.64) and a minimum during summer (0.39).

The next two figures (Figures 16 and 17) present the time series of daily average PM 2.5 concentration with AOD and AOD/PBL for Nicosia, respectively.

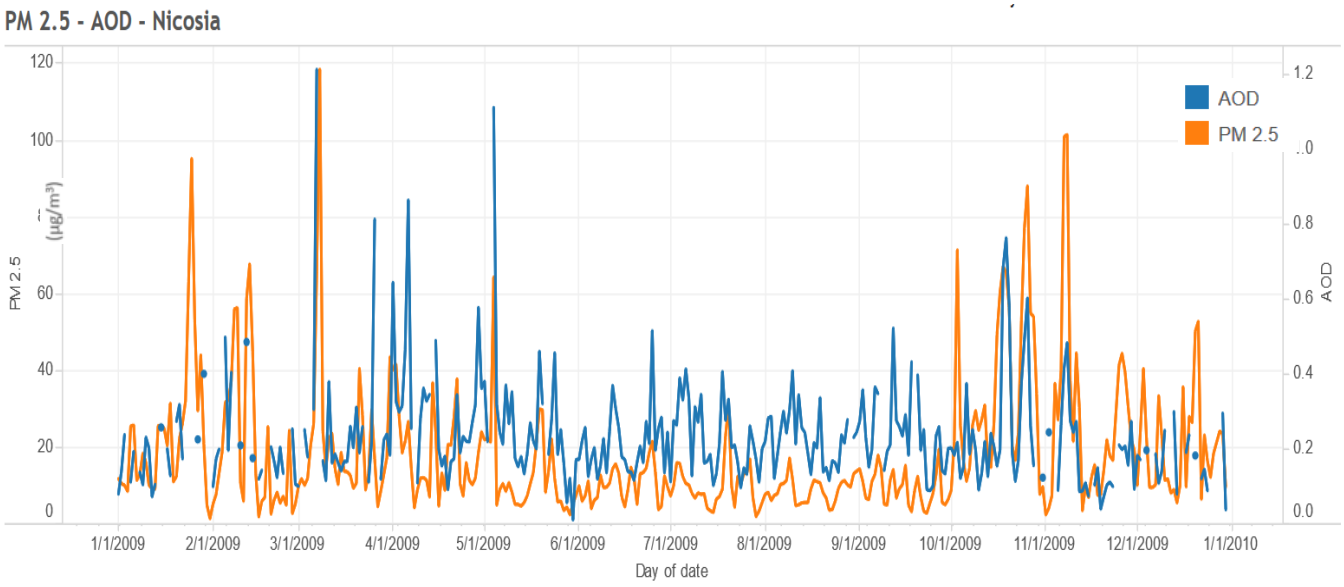

Figure 16: Time series of daily PM 2.5, AOD values in Nicosia

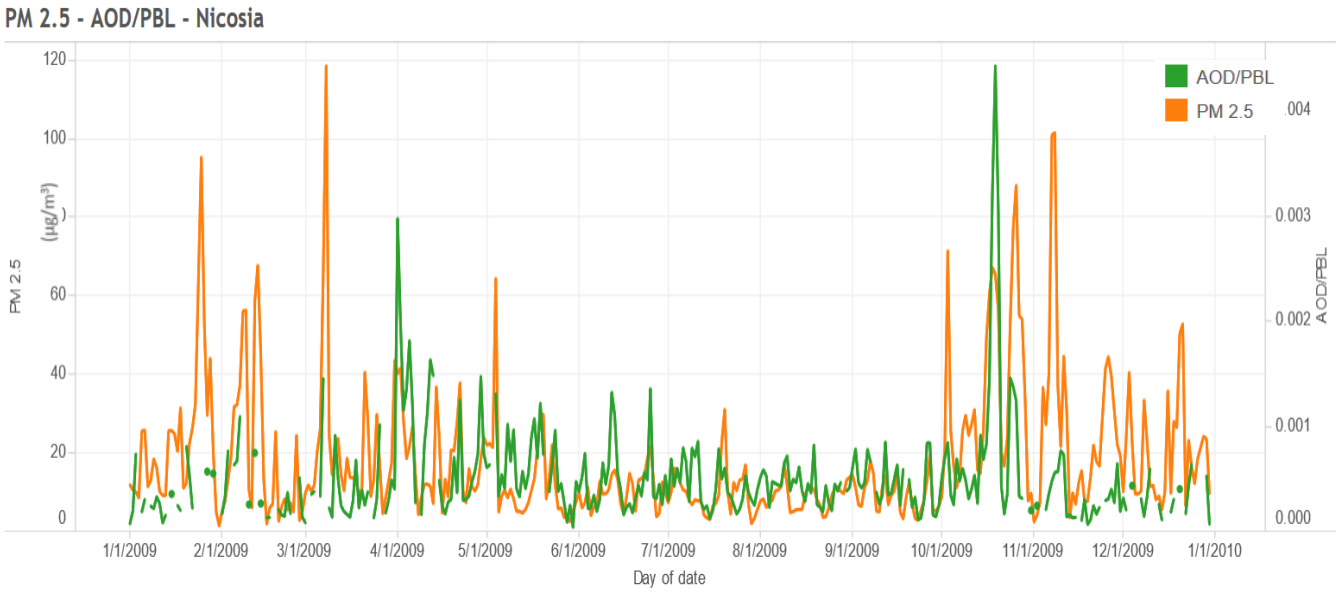

Figure 17: Time series of daily PM 2.5, AOD/PBL values in Nicosia

In both cases we can see periods with good correlation and periods with bad correlation.

The next table presents the regression results and coefficients for Nicosia using AOD/PBL as independent variable as well as both AOD and PBL as independent variables.

The regression equations are those presented in Equation 1 and Equation 2 in the earlier section.

Table 6: Regression results and evaluation in Nicosia

season	N	R	R^2	a_0	a_1	a_2	a_3	a_4
Winter	37	0.584	0.341	-64.709	15349.212	3.991	0.828	2.763
Spring	72	0.568	0.322	-7.494	14057.016	1.778	0.017	2.774
Summer	83	0.434	0.189	16.056	8402.34	-17.927	0.006	0.207
Autumn	69	0.591	0.349	-76.876	16054.777	3.074	1.092	2.748

season	N	R	R^2	a_0	a_1	a_2	a_3	a_4	a_5
Winter	37	0.644	0.414	-24.667	43.409	3.758	-0.027	0.439	3.567
Spring	72	0.659	0.434	0.507	41.722	10.433	-0.002	-0.041	0.342
Summer	83	0.462	0.214	20.53	20.271	-18.292	-0.007	-0.012	0.193
Autumn	69	0.607	0.369	-52.422	73.202	6.573	-0.024	0.798	2.569

Regression results: Good, Relatively Good, Bad

The regression analysis with both AOD and PBL as independent variables for Nicosia was the one with better results. The results were good for spring (0.659), winter (0.644) and autumn (0.607), and relatively good for summer. The regression with AOD/PBL gave relatively good results for all cases / seasons (R from 0.43 in summer to 0.59 in autumn).

4.3.4 Paris

The following figure (Figure 18) presents the seasonal average of PM 2.5, AOD and AOD/PBL in Paris.

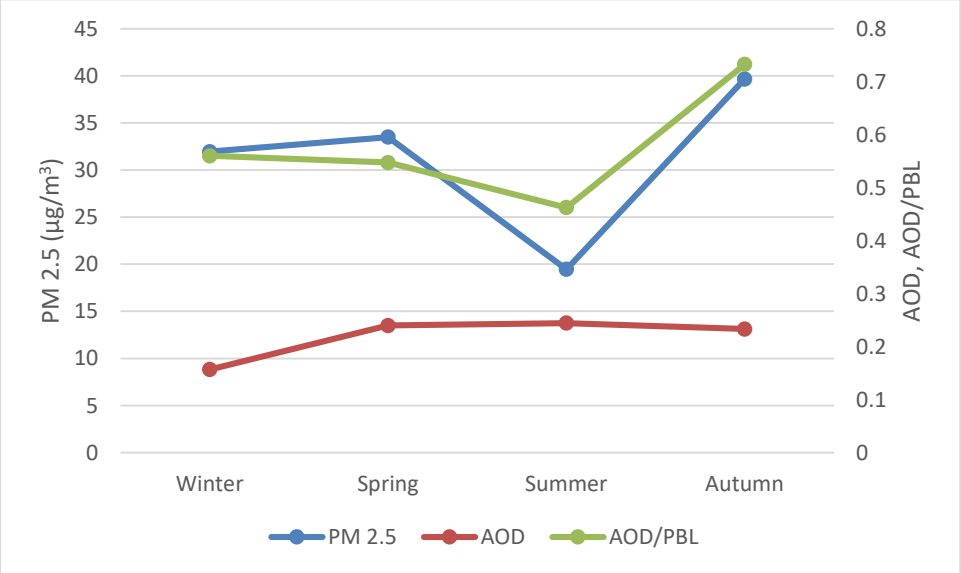

Figure 18: Time series of seasonal average of PM 2.5, AOD, AOD/PBL in Paris

PM 2.5 concentration shows a maximum during autumn and a minimum during summer, with winter and spring average concentration of about the same magnitude. AOD in Paris shows a minimum during winter and almost a constant value throughout the other seasons. AOD/PBL shows a very similar seasonal variation with PM 2.5 with maximum during autumn and minimum during summer.

The seasonal correlation coefficients between PM 2.5 and AOD, AOD/PBL are presented in the table below.

Table 7: correlation coefficients between PM 2.5, AOD and AOD/PBL in Paris

Season	Correlation coefficient of PM 2.5 with AOD	Correlation coefficient of PM 2.5 with AOD/PBL
Winter	0.203	**0.527**
Spring	-0.091	**0.138**
Summer	**-0.323**	-0.269
Autumn	**-0.285**	-0.177

PM 2.5 shows a relatively good correlation with AOD/PBL during winter for Paris, while for all other cases the correlation is not good. The seasonal scatter plots presented in Figure 19 show also the same relation.

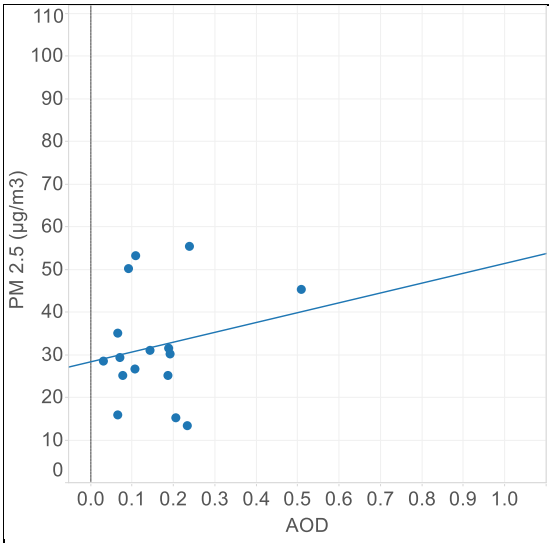

Winter

PM 2.5 = 23.0715*AOD + 28.331

R^2 = 0.45

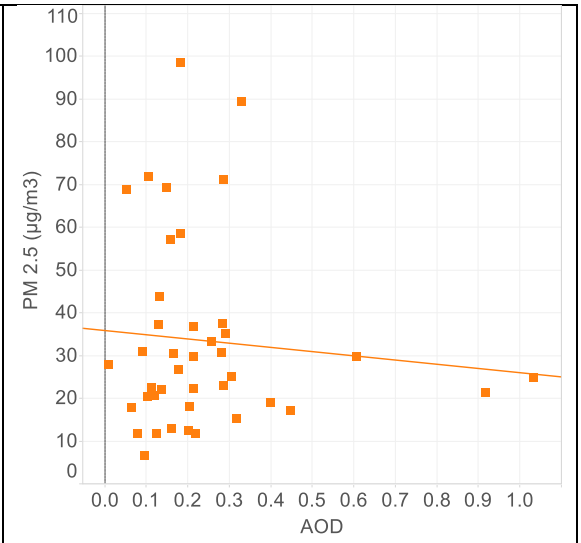

Spring

PM 2.5 = -9.86056*AOD + 35.8547

R^2 = 0.008

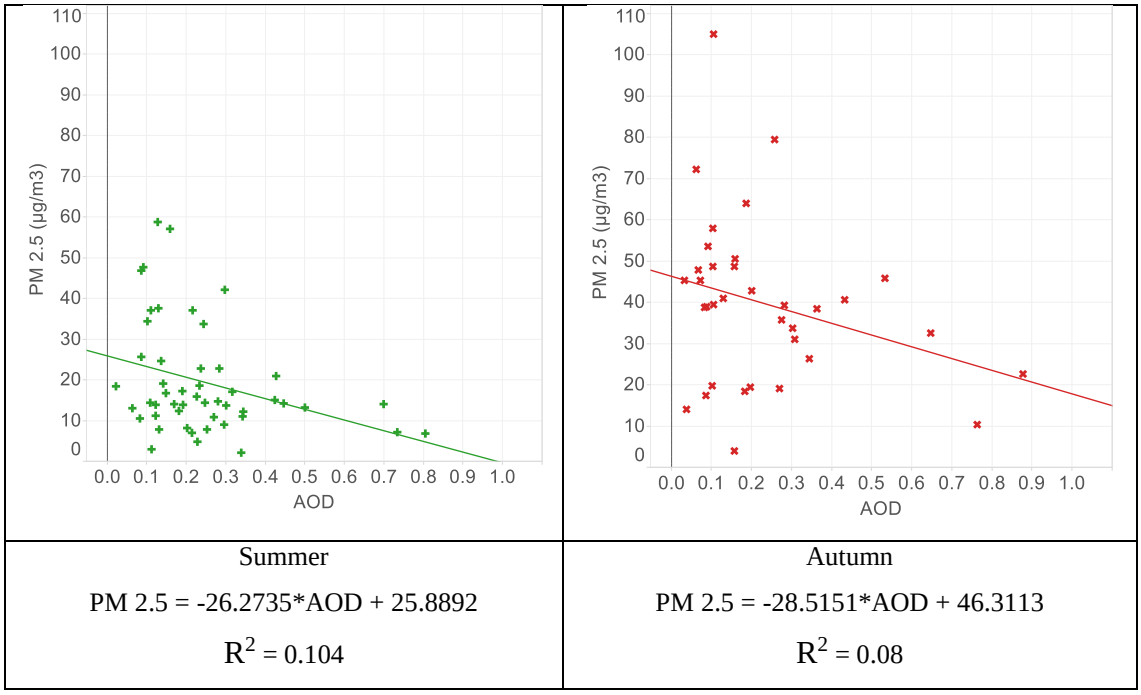

Summer	Autumn
PM 2.5 = -26.2735*AOD + 25.8892	PM 2.5 = -28.5151*AOD + 46.3113
R^2 = 0.104	R^2 = 0.08

Figure 19: Seasonal Scatter Plots of PM 2.5 and AOD values in Paris

The next table presents the regression results and coefficients for the two regression cases examined for Paris.

The regression equations are those presented in Equation 1 and Equation 2 in the earlier section.

Again, the same color scale was applied to the regression results in order to provide a visual interpretation of the regression performance.

Table 8: Regression results and evaluation in Paris

season	N	R	R^2	a_0	a_1	a_2	a_3	a_4
Winter	16	0.586	0.343	0.078	8956.725	-8.114	0.401	-0.917
Spring	41	0.625	0.39	-87.843	-5687.712	0.947	1.7	-7.12
Summer	50	0.426	0.181	72.031	-5732.915	0.093	-0.579	-1.421
Autumn	35	0.438	0.192	9.473	-7541.97	-14.045	0.667	-3.019

season	N	R	R^2	a_0	a_1	a_2	a_3	a_4	a_5
Winter	16	0.637	0.405	-3.987	-0.535	-2.237	0.053	0.591	-10.879
Spring	41	0.677	0.458	-23.221	-27.885	2.505	-0.047	1.016	0.097
Summer	50	0.452	0.204	70.84	-18.316	-1.031	0.005	-0.565	-1.464
Autumn	35	0.449	0.202	53.98	-31.836	-12.524	-0.029	0.114	2.292

Regression results: Good, Relatively Good, Bad

The regression analysis with both AOD and PBL as independent variables was the one with better results for Paris. The results were good for spring (0.677) and winter (0.637) and relatively good for the other seasons.

The regression with AOD/PBL gave good results for spring and relatively good results for all other seasons.

4.3.5 Zagreb

The following figure (Figure 20) presents the seasonal average of PM 2.5, AOD and AOD/PBL in Zagreb.

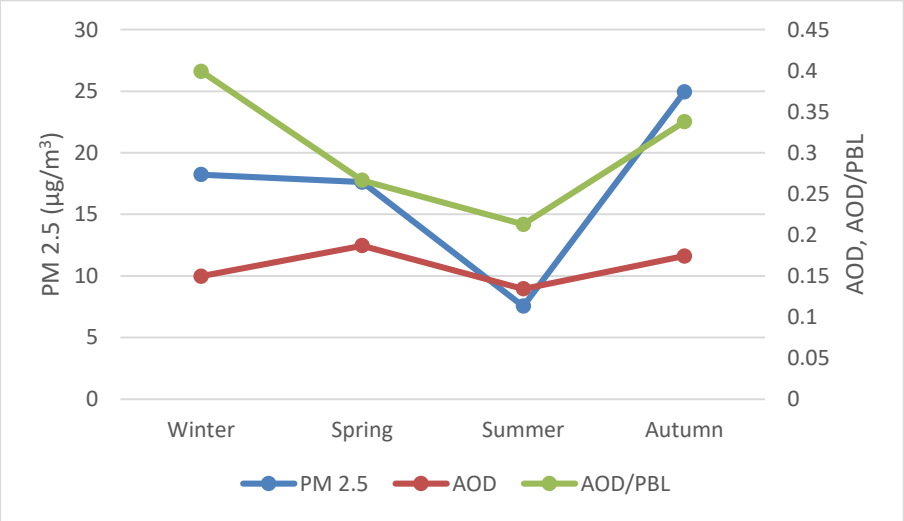

Figure 20: Time series of seasonal average of PM 2.5, AOD, AOD/PBL in Zagreb

PM 2.5 concentration in Zagreb shows a maximum during autumn and a minimum during summer. AOD shows a minimum during summer and a maximum during spring with a small variation. AOD/PBL shows a maximum during winter and a minimum during summer.

The seasonal correlation coefficients between PM 2.5 and AOD and PM 2.5 and AOD/PBL are presented in the table below.

Table 9: correlation coefficients between PM 2.5, AOD and AOD/PBL in Zagreb

Season	Correlation coefficient of PM 2.5 with AOD	Correlation coefficient of PM 2.5 with AOD/PBL
Winter	**0.508**	0.153
Spring	-0.171	**-0.172**
Summer	**0.132**	0.089
Autumn	**-0.258**	-0.122

PM 2.5 shows a relatively good correlation in Zagreb, with AOD during winter, while for all other cases the correlation is not good. The seasonal scatter plots presented in Figure 21 highlight also the same result.

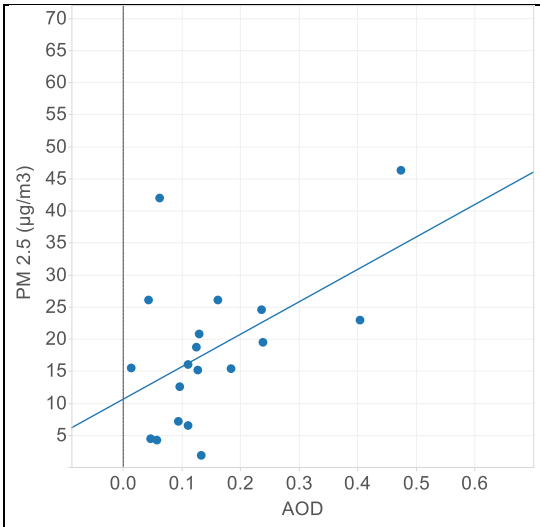

Winter

PM 2.5 = 50.5903*AOD + 10.6553

R^2 = 0.26

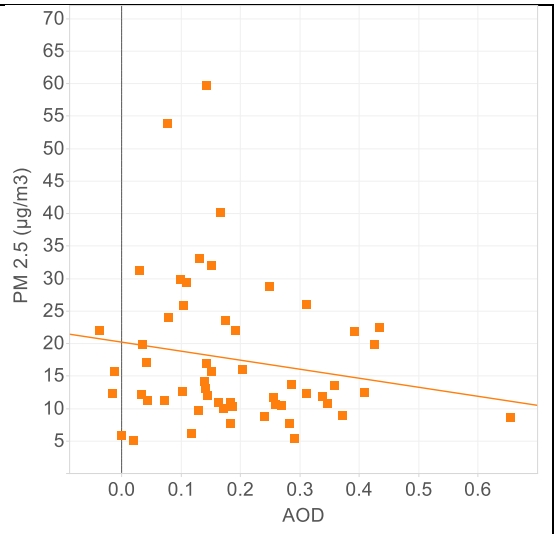

Spring

PM 2.5 = -13.8968*AOD + 20.2141

R^2 = 0.03

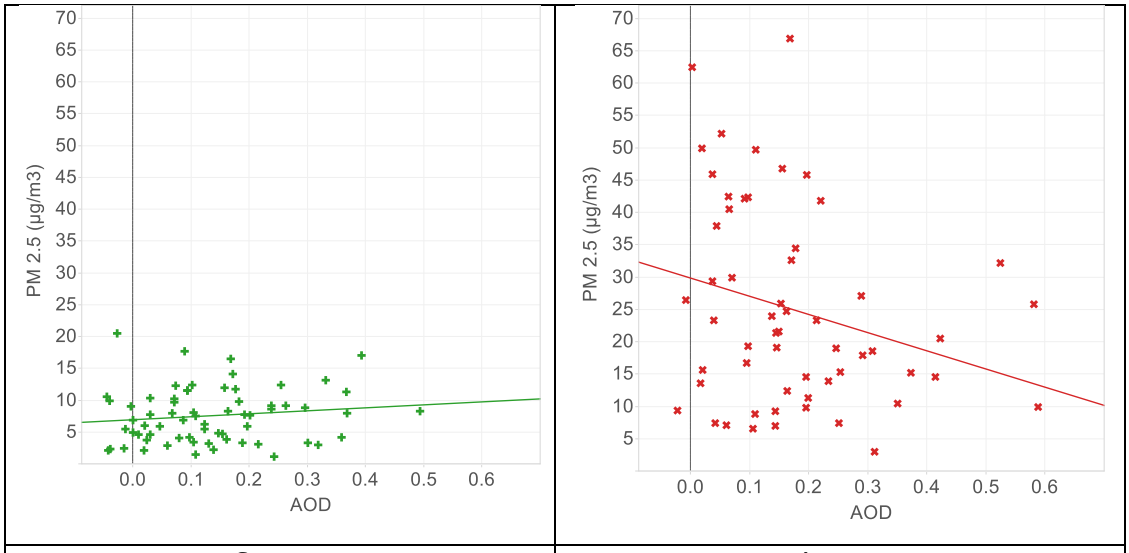

Summer	Autumn
PM 2.5 = 4.67512*AOD + 6.92539	PM 2.5 = -28.1235*AOD + 29.834
R^2 = 0.018	R^2 = 0.067

Figure 21: Seasonal Scatter Plots of PM 2.5 and AOD values in Zagreb

The next table presents the regression results and coefficients for Zagreb.

The regression equations and the performance evaluation color categories are the same with those presented in previous sections.

Table 10: Regression results and evaluation in Zagreb

season	N	R	R^2	a_0	a_1	a_2	a_3	a_4
Winter	19	0.417	0.174	8.273	-212.326	-2.371	0.237	-2.31
Spring	55	0.248	0.062	0.975	-12351.808	-1.912	0.309	-0.028
Summer	66	0.427	0.183	5.838	2347.961	-2.542	0.024	1.788
Autumn	57	0.638	0.407	-51.741	-13996.635	1.468	0.921	0.878

season	N	R	R^2	a_0	a_1	a_2	a_3	a_4	a_5
Winter	19	0.656	0.431	-26.829	53.908	2.837	0.005	0.469	-3.15
Spring	55	0.306	0.094	-14.335	-11.414	-0.053	0.013	0.387	-2.141
Summer	66	0.478	0.228	11.813	2.81	-2.917	-0.007	0.001	2.494
Autumn	57	0.693	0.481	-9.639	-28.994	-1.202	-0.022	0.464	6.702

Regression results: Good, Relatively Good, Bad

The regression analysis with both AOD and PBL for Zagreb among the independent variables was the one with better results. The results were good for autumn (0.693) and winter (0.656) and relatively good for summer. The regression with AOD/PBL gave good results for autumn and relatively good results for summer and winter. Both models gave bad results for spring.

4.3.6 Total evaluation

The following table shows an overall evaluation of the regression results for all seasons and all locations where regression analysis was performed. For each location the value of the best regression result is presented (as expressed using the R coefficient). The colors (green for good results, Yellow for relatively good results and red for bad results) represent the regression analysis performance evaluation as described in the previous sections where the detailed regression results in selected locations were presented.

Table 11: Regression results and evaluation in all locations (best result)

	Winter	Spring	Summer	Autumn
Amsterdam	-	0.387	0.378	0.855
Athens	0.82	0.266	0.613	0.72
Belgrade	0.84	0.555	0.349	0.727
Berlin	-	0.694	0.394	0.698
Berne	-	0.312	0.3	0.467
Brussels	-	0.544	0.338	0.362
Bucharest	0.571	0.562	0.302	0.787
Budapest	0.283	0.663	0.188	0.804
Copenhagen	-	0.576	0.295	0.415
Kiev	-	0.463	0.394	0.653
Madrid	0.65	0.25	0.221	0.701
Moscow	-	0.396	0.419	0.584
Nicosia	0.644	0.659	0.462	0.607
Oslo	-	0.379	0.577	0.601
Paris	0.637	0.677	0.452	0.449
Rome	0.419	0.154	0.326	0.474
Sofia	0.758	0.431	0.335	0.527
Stockholm	-	0.247	0.183	0.452
Vienna	0.921	0.638	0.313	0.525
Vilnius	-	0.579	0.443	0.683
Warsaw	-	0.477	0.212	0.666
Zagreb	0.656	0.306	0.478	0.693

Regression results: Good, Relatively Good, Bad

It is easy to see that regression results are in most cases (locations) good during winter and autumn, relatively good during spring and bad during summer.

This is also shown in Figure 22 below. This figure presents the total evaluation of the regression results for each season and for all locations, expressed as percentage of occurrence of each regression performance class. The best results are observed during winter with 73% good and 18% relatively good results, and for autumn with 59% good and 36% relatively good results. The performance is not good during spring (only 58% good and relatively good results

combined) and especially during summer (only 32 % good and relatively good results combined).

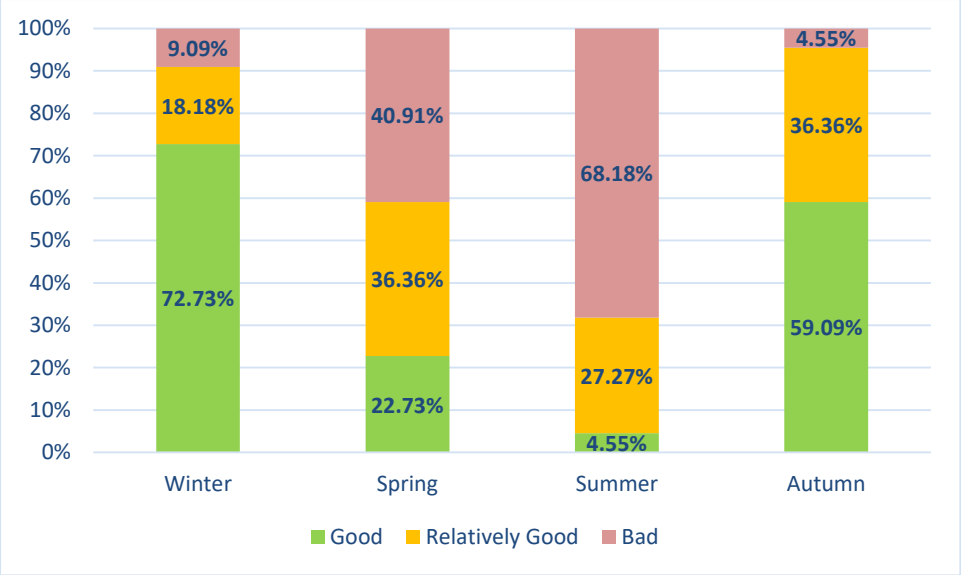

Figure 22: Overall regression analysis performance in all locations and seasons

In order to examine a possible spatial relation in the results, the following maps are provided for each season (Figure 23).

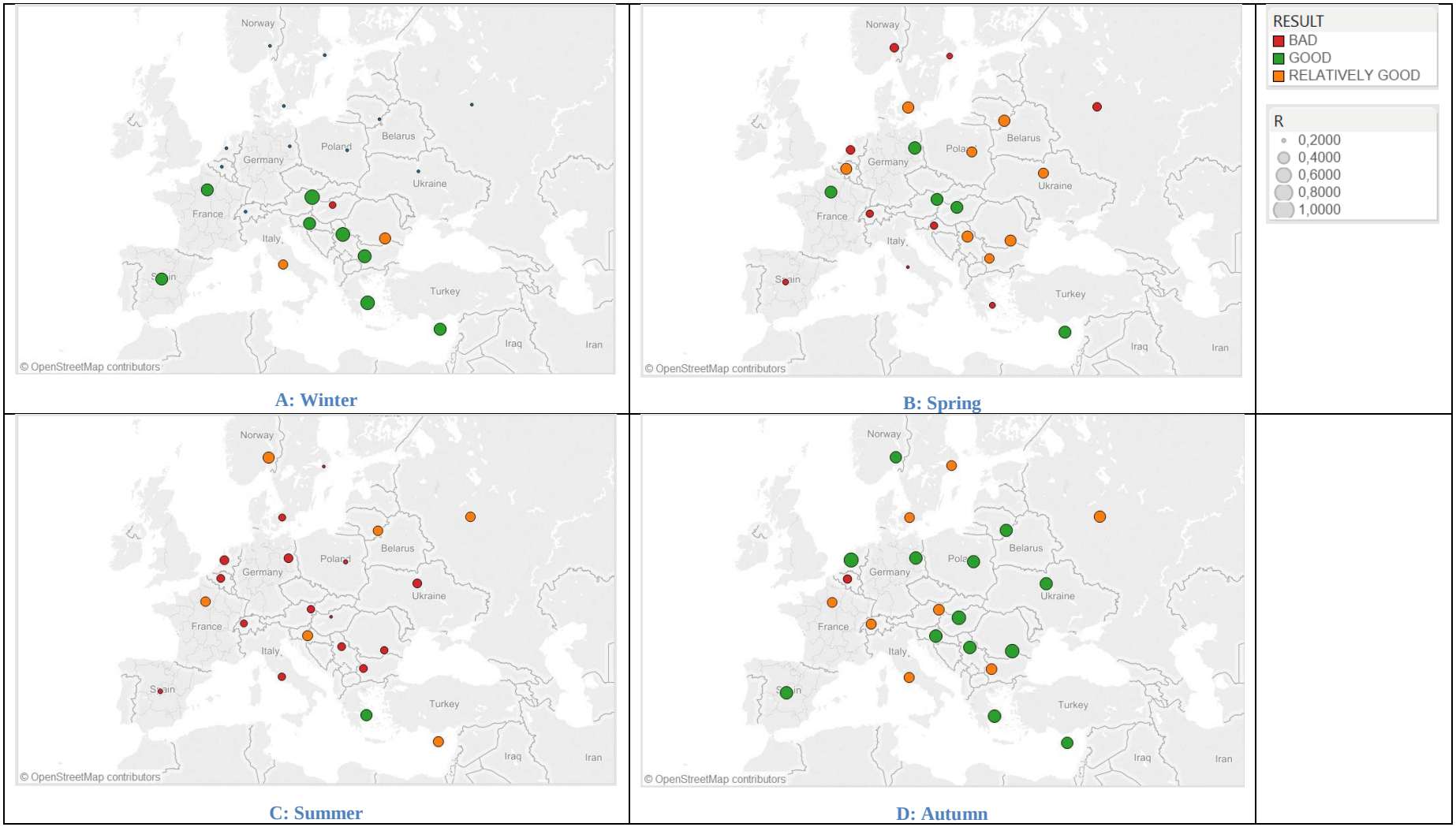

A: Winter **B: Spring**

C: Summer **D: Autumn**

Figure 23: Spatial relation of regression results

During winter we can see that in several locations, mostly in the northern parts of Europe, there are no regression results due to the limited days when valid AOD data are available. During that time, good results are shown in the southern areas around Mediterranean Sea (with the exception of Rome) and in the Balkan area.

During spring, the best results are located in central Europe. Most of the locations with good results during winter now show relatively good or even bad results for the following season.

During summer, the results are bad all over Europe, with the exception of those for Athens.

Finally, during autumn, the results are good in central Europe and several locations in southern Europe and the Balkans.

The maps show that, overall, best results are located in the Eastern Europe, but it is very difficult to establish any positive conclusion about their spatial pattern.

For that reason, the Morans index was calculated, which provides a measure of spatial autocorrelation. The corresponding values as well as the significance levels (p) and the critical values (z) are presented in Table 12, below.

Table 12: Morans index values for the examination of possible spatial autocorrelation in the regression results

Seasson	Morans Index	z-score	p-value	Spatial pattern
Winter	0.342532	4.119278	0.000038	Clustered
Spring	0.008664	0.599949	0.548540	Random
Summer	-0.071406	-0.258202	0.796251	Random
Autumn	-0.086810	-0.418931	0.675266	Random

The spatial pattern can be concluded according to the estimated critical values, as presented in Figure 24 below.

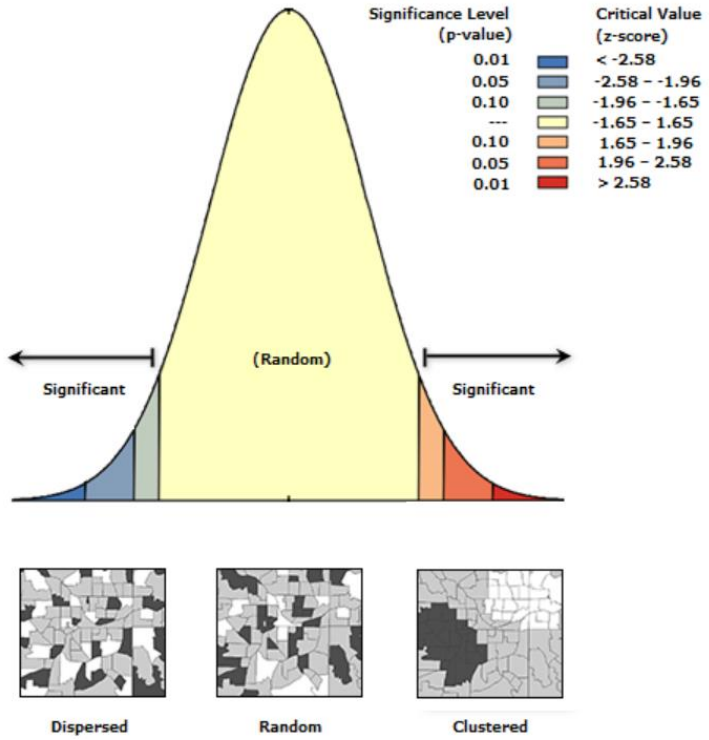

Figure 24: Interpretation of spatial pattern in the regression results

Thus, **a spatial autocorrelation appears only during winter**. **For all the other seasons, the spatial pattern of the results is random**.

Finally, in order to examine the dominant factor in the regression equation, and thus to understand which variable was most important in the prediction of the PM 2.5 concentration, the following tables are presented. Table 13 shows in each location and season, the most important factor in the regression equation (as well as the overall regression performance evaluation using again the same color classes). In addition, Table 14 shows the aggregated values of these dominant factors for cases where regression results were good or relatively good.

Table 13: Dominant variable in the regression equation

Location	Winter	Spring	Summer	Autumn
Amsterdam		RH	AE	AOD
Athens	AOD/PBL	AE	PBL,WS	RH
Belgrade	RH	AOD/PBL	AOD/PBL	RH
Berlin		AOD/PBL	RH	RH
Berne		RH	PBL	PBL
Brussels		RH	AOD	PBL
Bucharest	WS	PBL	PBL	PBL,WS
Budapest	WS	RH	AOD	RH
Copenhagen		RH	PBL	RH
Kiev		PBL	AOD/PBL	PBL
Madrid	AOD	AE	WS	RH
Moscow		WS	AE	PBL
Nicosia	WS	AOD	AOD	AOD
Oslo		RH	PBL	AOD/PBL
Paris	WS	AOD	RH	AOD
Rome	WS	WS	RH	RH
Sofia	PBL	RH	RH	PBL
Stockholm		WS	WS	PBL
Vienna	WS	RH	RH	AOD
Vilnius		PBL	PBL	WS
Warsaw		AOD/PBL	AOD	RH
Zagreb	AOD	PBL	WS	AOD

Regression results: Good, Relatively Good, Bad

Table 14: Statistics of the Dominant variable in the regression equation

variable / result	Good	Relatively Good
AOD or AOD/PBL	**38%**	**21%**
RH	35%	25%
WS	15%	13%
PBL	12%	38%
AE	0%	4%

Thus, only in 38% of the regression predictions with good performance AOD or AOD/PBL was the dominant variable. This value is even smaller in relatively good predictions (21%).

Relative Humidity was the most important factor in 35%, of the cases with good performance results. WS was the dominant factor in the regression equation in another 15% of these cases and PBL in 12%.

For cases with good regression results and AOD or AOD/PBL as the dominant variable, an additional regression analysis was performed with only AOD or AOD/PBL as the sole independent variable. The performance of this regression was compared to the one with all the other parameters considered, and the results are presented in Figure 25 below.

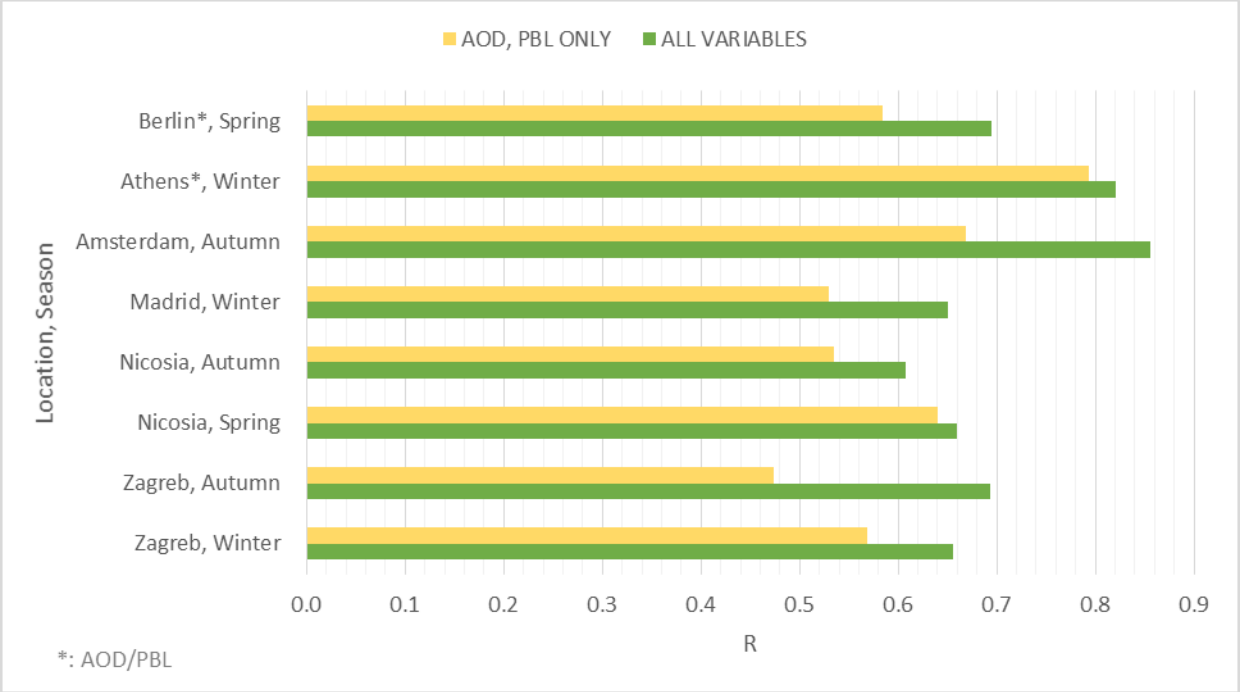

Figure 25: Regression results with only AOD, PBL as independent variables

The results of this analysis shows that, even in the cases where AOD or AOD/PBL was the most important parameter in the regression equation, the use of the other meteorological parameters improved the regression results from 3% to 32% (average difference 15%).

4.4 Statistical analysis of the relation of AOD – Stations PM concentration

4.4.1 Analysis of station PM 2.5 data

Before the investigation of the AOD – PM 2.5 relationship, the correlation between PM 2.5 measurements in the two stations was examined. Both stations are located at the north of the Athens city center and they are within the same cell of the AOD remote sensing data. Lykovrisi (LYK) is considered a suburban air quality monitoring station, while Agia Paraskevi (AGP) is a suburban / background station.

A descriptive statistics analysis was initially performed. The table below presents the yearly average value of PM 2.5 in these stations for year 2009.

Table 15: Descriptive Statistics of PM 2.5 concentration in AGP and LYK monitoring stations

	Mean (μg/m^3)	Std. Deviation (μg/m^3)	N
LYK	24.09	9.99	346
AGP	15.95	7.86	361

So, although both stations have similar characteristics, the average yearly PM 2.5 concentration is significant higher in LYK than in AGP.

The Pearson correlation coefficient between these 2 datasets is 0.59, which is significant at the 0.01 confidence level, but this is not a very high degree of confidence.

This relatively good correlation is presented also in the scatter plot below (Figure 25).

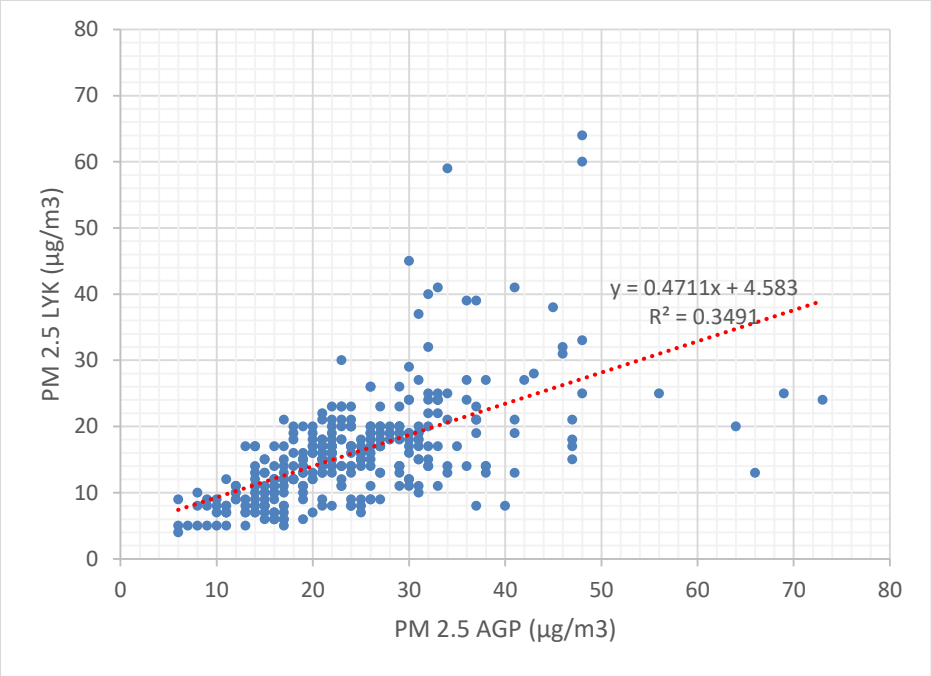

Figure 26: Stations PM 2.5 measurements scatter plot

Figure 26 below presents the monthly averages in both stations. Is interesting to note that LYK has overall greater PM 2.5 concentration than AGP, with different seasonal variability. PM 2.5 shows a maximum during July (which is difficult to explain) and a second maximum in November. At AGP, the maximum concentration was in April, and there were surprisingly low values during September to December.

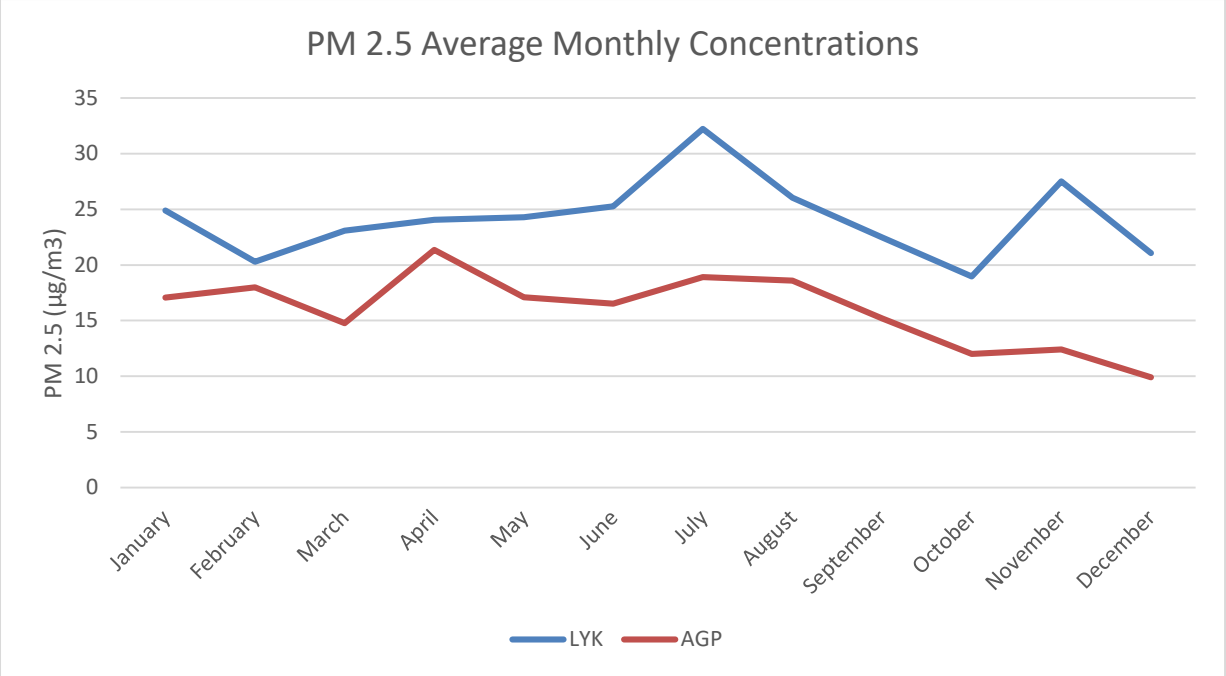

Figure 27: Stations monthly average PM 2.5 time series

Figure 34 below shows the time series of the daily concentrations observed at both stations. It can be easily seen that there are periods with good correlation between the measurements, as well as periods with low correlation.

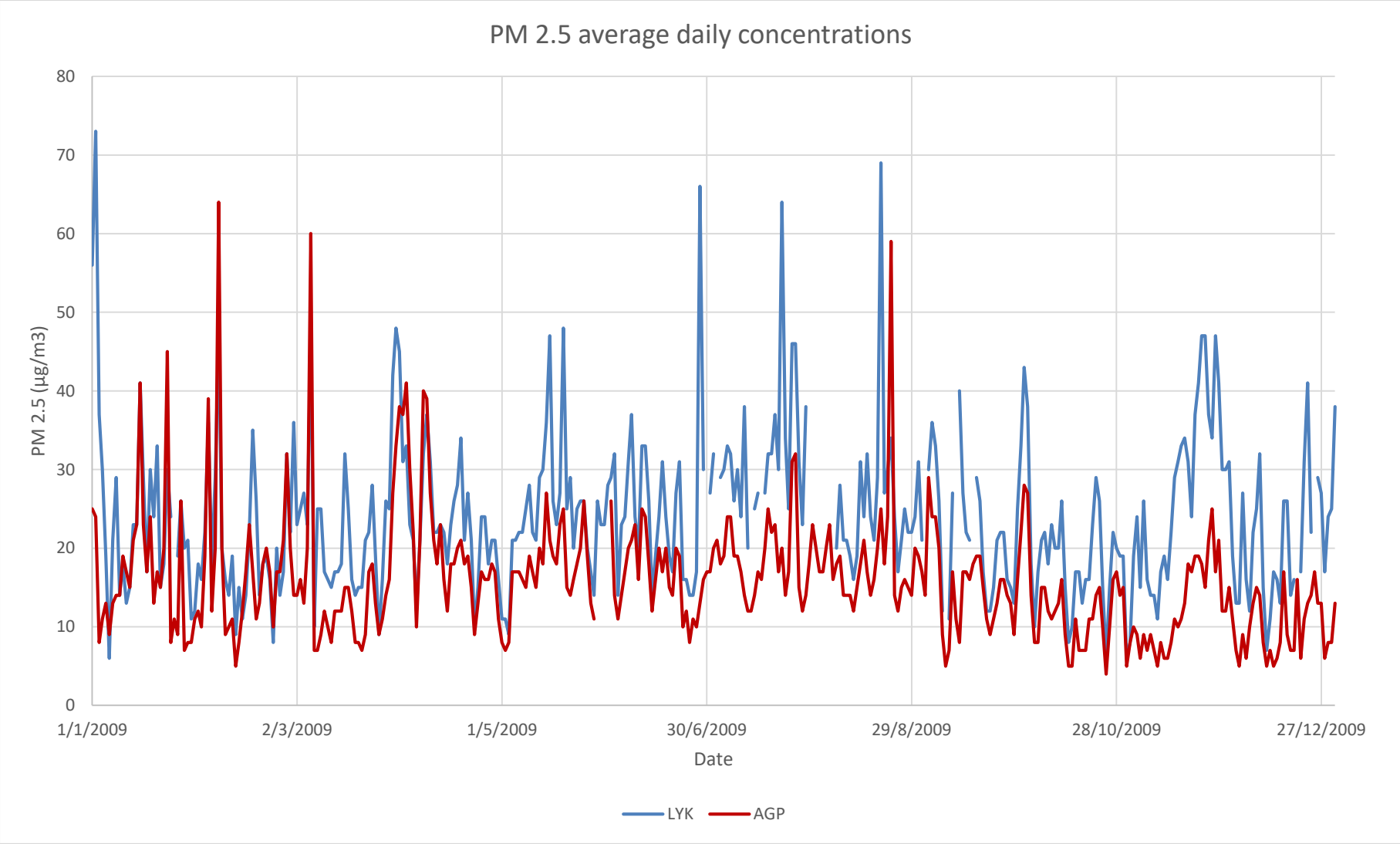

Figure 28: Stations average daily PM 2.5 time series

4.4.2 Regression Analysis

The following figure (Figure 28) presents the seasonal average of PM 2.5, AOD and AOD/PBL.

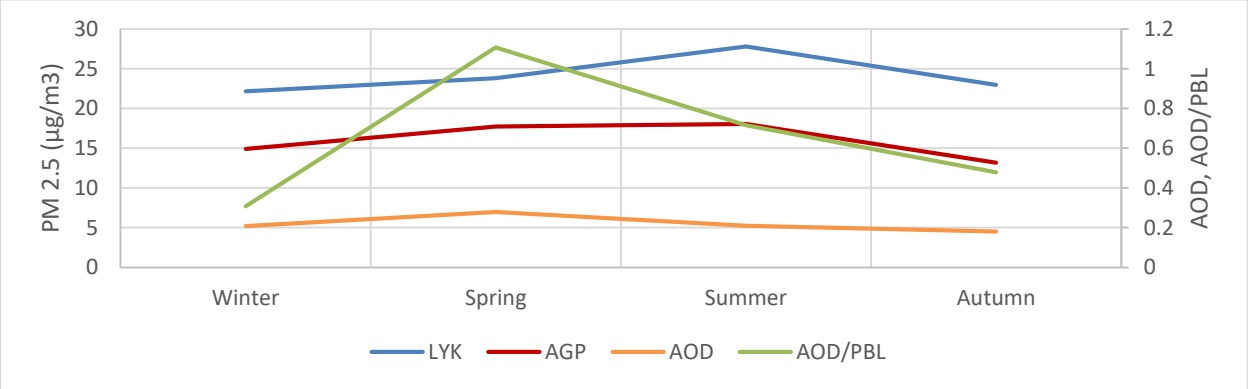

Figure 29: Time series of seasonal average of PM 2.5, AOD, AOD/PBL in Lykovrisi

PM 2.5 concentration in both LYK and AGP shows a maximum during summer and a minimum during winter and autumn respectively. AOD, which shows a small degree of variability, a maximum during spring, and values of the same magnitude during all other seasons. AOD/PBL has a maximum value during spring and a minimum during winter.

The next two figures (Figures 29 and 30) present the time series of daily average PM 2.5 concentration with AOD and AOD/PBL respectively.

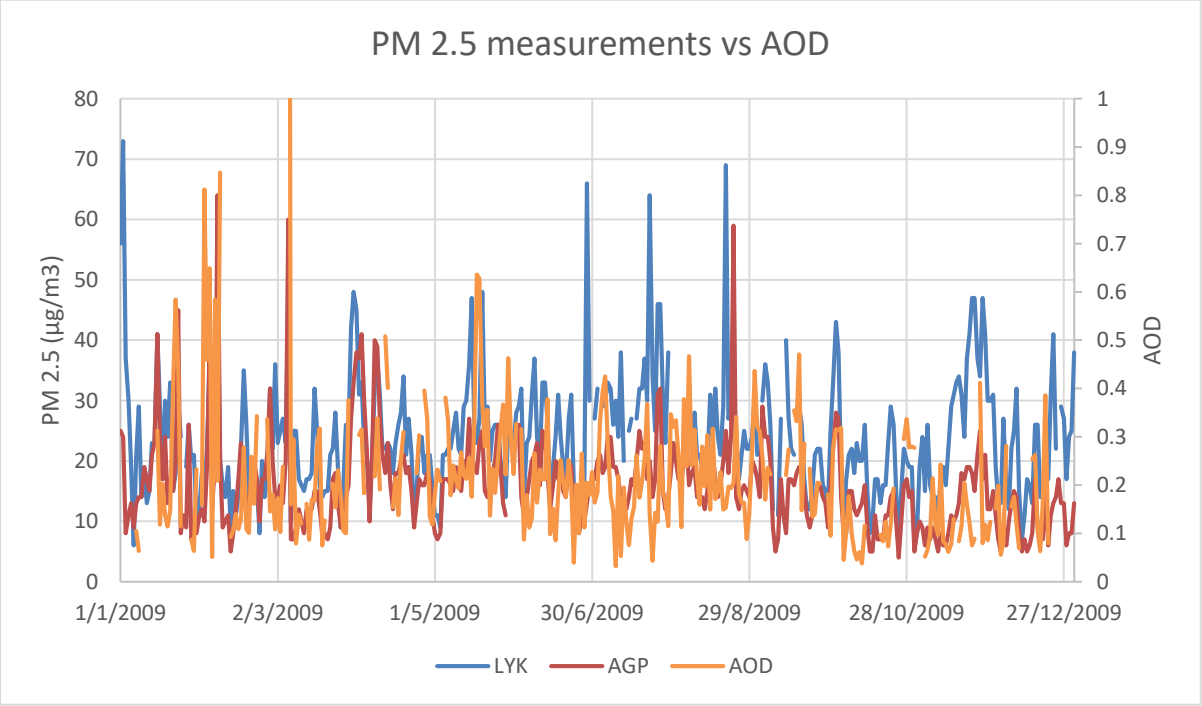

Figure 30: Time series of daily PM 2.5, AOD values

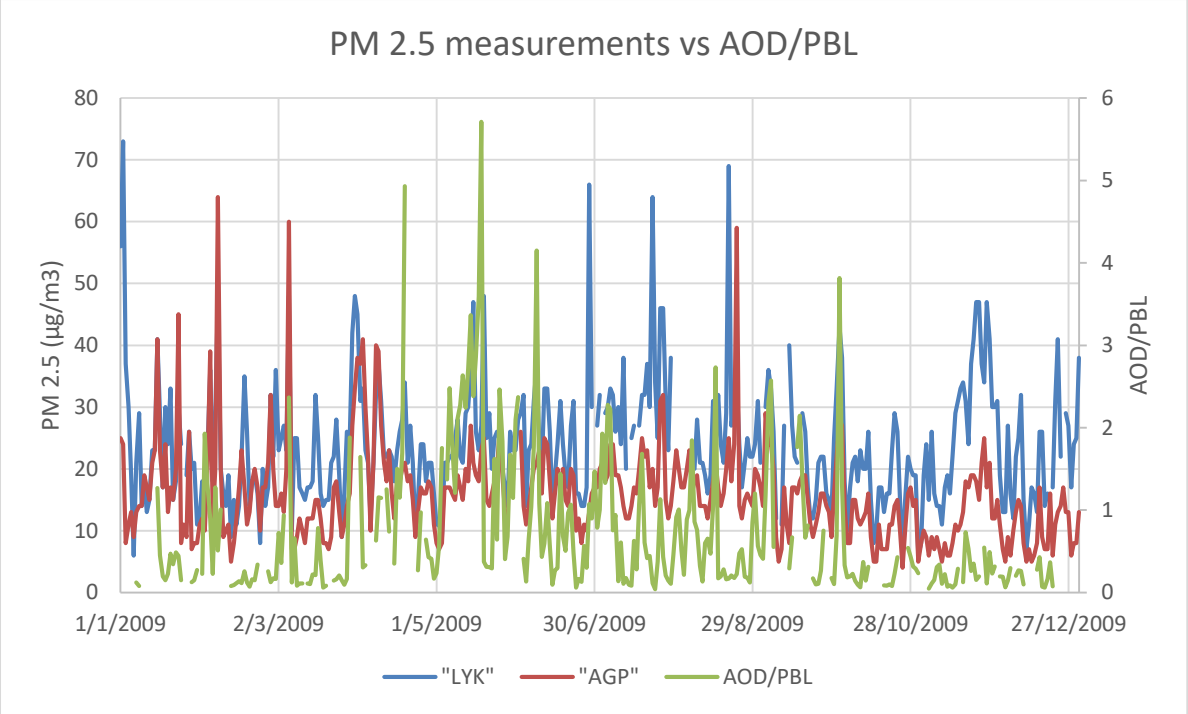

Figure 31: Time series of daily PM 2.5, AOD/PBL values

If we calculate the Pearson Correlation Coefficient for the two above time series, we can confirm that for LYK, the PM 2.5 concentration has a stronger correlation with AOD/PBL. The correlation coefficient between PM 2.5 and AOD is 0.094, while between PM 2.5 and AOD/PBL it is 0.167.

In contrast, for AGP the PM 2.5 concentration has a stronger correlation with AOD. The correlation coefficient between PM 2.5 and AOD is 0.421 while between PM 2.5 and AOD/PBL, it is 0.277.

This relation exists also when examined on a seasonal basis. The correlation coefficients for each season between the two stations PM 2.5 measurements and both AOD and AOD/PBL are presented in Figure 32 and Figure 33 below.

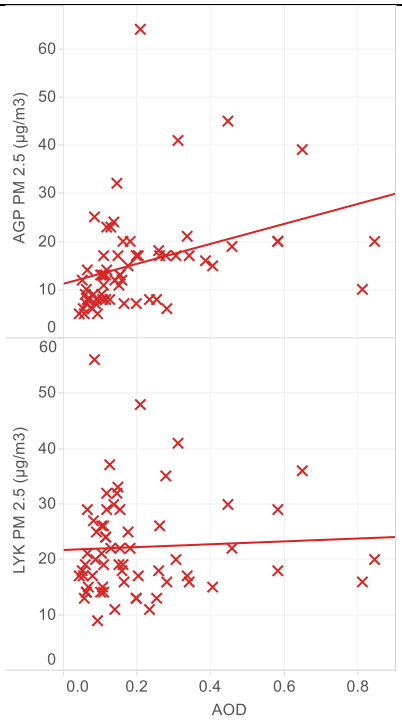

Winter

AGP: R^2 = 0.125 | LYK: R^2 = 0.003

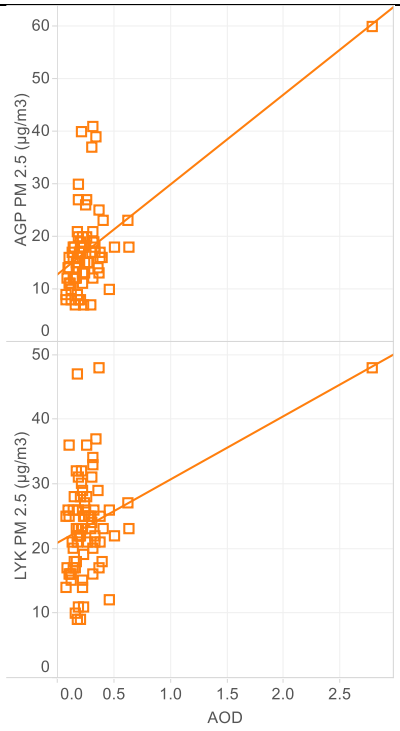

Spring

AGP: R^2 = 0.37 | LYK: R^2 = 0.14

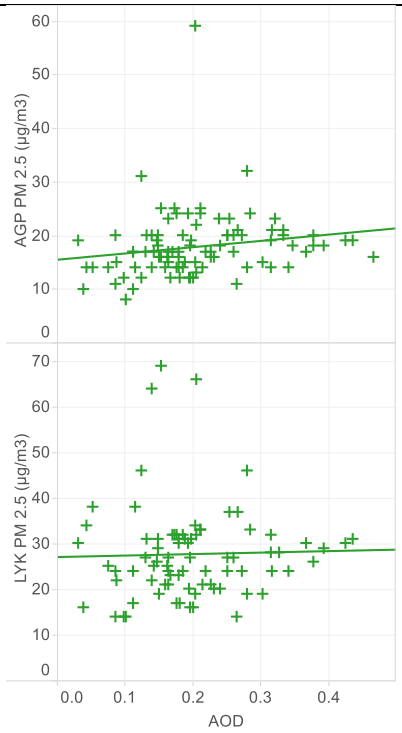

Summer

AGP: R^2 = 0.03 | LYK: R^2 = 0.0007

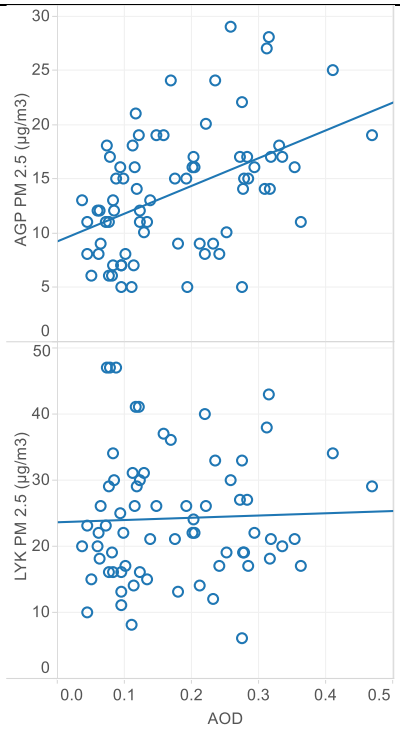

Autumn

AGP: R^2 = 0.21 | LYK: R^2 = 0.001

Figure 32: Seasonal Scatter plots of stations PM 2.5 data with AOD

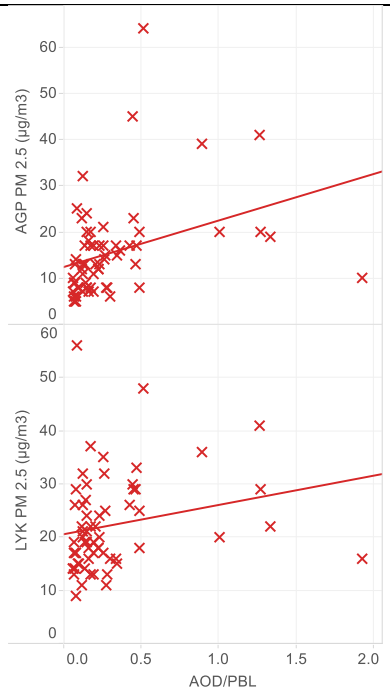

Winter

AGP: R^2 = 0.12 | LYK: R^2 = 0.05

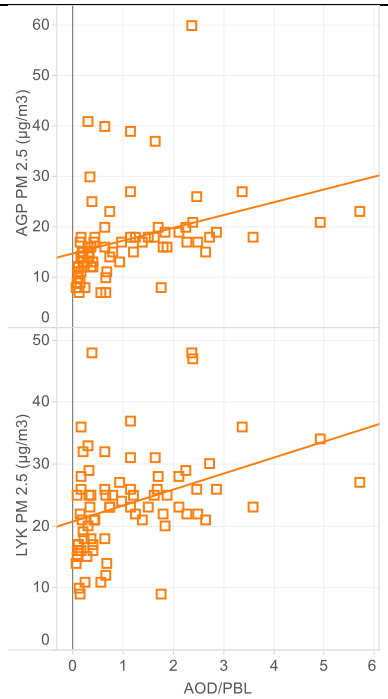

Spring

AGP: R^2 = 0.11 | LYK: R^2 = 0.14

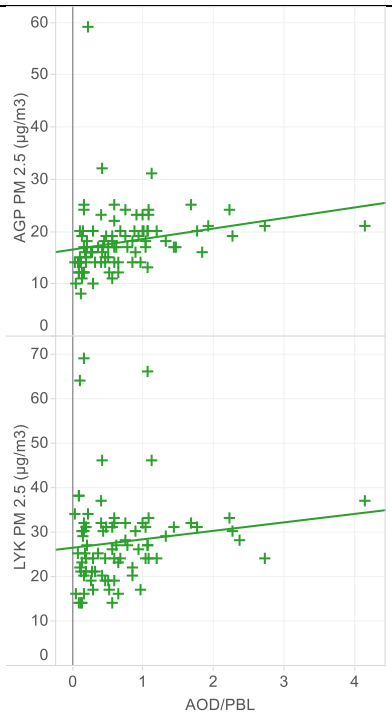

Summer

AGP: R^2 = 0.05 | LYK: R^2 = 0.016

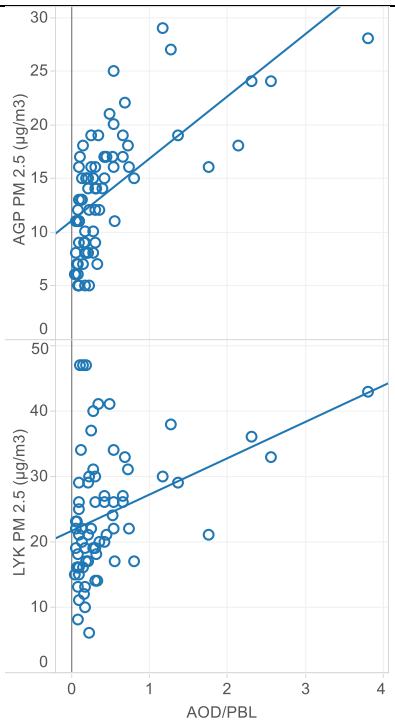

Autumn

AGP: R^2 = 0.42 | LYK: R^2 = 0.13

Figure 33: Seasonal Scatter plots of stations PM 2.5 data with AOD/PBL

Taking into account the estimated correlation coefficients for both stations, at LYK, the regression analysis was performed with AOD/PBL as independent variable, while at AGP both AOD and PBL were used as independent variables.

The results of the regression analysis at LYK station are presented in Table 16 below. The regression equation for LYK is expressed as:

Equation 3: PM 2.5 = a0 + a1 * AOD/PBL + a2 * AE + a3 * RH + a4 * WS (3)

Table 16: Regression results and evaluation at Lykovrisi

season	N	R	R^2	a_0	a_1	a_2	a_3	a_4
Winter	18	0.612	0.375	4.768	14411.79	2.732	0.212	-0.626
Spring	57	0.438	0.182	19.984	1679.23	-0.114	0.06	-0.546
Summer	45	0.561	0.213	45.298	7681.48	-1.975	-0.422	1.486
Autumn	49	0.58	0.336	0.857	3027.45	5.767	0.302	-1.09

Regression results: Good, Relatively Good, Bad

The best performance was for winter (R=0.612) while the results were relatively good for all the other seasons.

Table 17, presents the results of the regression analysis at AGP station. The regression equation for AGP was expressed as:

Equation 4: PM 2.5 = a_0 + a_1 * AOD + a_2 * AE + a_3 * PBL + a_4 * RH + a_5 * WS (4)

Table 17: Regression results and evaluation at Agia Paraskevi

season	N	R	R^2	a_0	a_1	a_2	a_3	a_4	a_5
Winter	18	0.675	0.455	-177.193	76.06	17.524	0.022	1.119	-0.959
Spring	57	0.543	0.294	-1.027	10.831	1.602	-0.013	0.153	1.619
Summer	45	0.467	0.219	49.901	6.649	-5.314	-0.021	-0.398	1.779
Autumn	49	0.791	0.625	27.911	35.259	1.205	-0.011	-0.167	0.002

Regression results: Good, Relatively Good, Bad

Both in autumn and winter, where the regression results were better, AOD was the dominant variable in the regression equation. For the other seasons, PBL was the most important variable in the regression equation.

Chapter 5: Conclusions

The understanding of the spatial distribution of the concentration of PM 2.5 over Europe is currently limited by the number and coverage of air quality stations. This study explored the possibility of using satellite-derived AOD as an estimator of ground level PM 2.5 concentration.

Daily AOD datasets from MODIS / TERRA were used for one year in order to examine the seasonal variability of data. The produced MODIS AOD maps indicated the major anthropogenic aerosol source areas located in Northern Italy, Southern Poland and Belgium / Netherlands, as well as the natural emission sources like sea salt and dust.

The seasonal variation of AOD reached a clear maximum value during spring and a minimum during autumn:

- Winter AOD values are generally low (below 0.1), with some higher values observed mostly over the sea in the East Mediterranean area and over populated or highly industrial areas like the valley of Po in Northern Italy or Paris in France.
- During spring, high AOD values are observed all over Europe (over 0.2). There is still evidence of high AOD values over the populated or industrial areas in Northern Italy, Germany, Poland and even Russia (over Moscow area during April), while high AOD values were also found over sea areas in the Mediterranean, especially during March and April.
- Lower AOD values are generally observed during summer. Higher AOD values can be seen over Poland (June and July), Holland (July), the Balkan area (especially during August), and during all summer period in northern Italy.
- During autumn, higher AOD values are observed during September and lower during October and November. The highest AOD values are found over areas in the Mediterranean and the Black Sea, whereas over the mainland, the higher values are observed over Turkey.

In this study, in contrast with most of the existing studies where ground station PM 2.5 measurements were used [Chu, 2006; Gupta et al, 2006; Li et al, 2003; Engel-Cox et al, 2004; Wang and Christopher, 2003; Liu et al, 2007; Donkelaar et al, 2010; Song et al, 2014], the

predictions of a photochemical air quality model were considered in order to provide PM 2.5 concentration information all over Europe. Such models were used to simulate complex atmospheric processes in order to estimate the ground level concentration of air pollutants. The decision to use model results in this study was also supported by the latest EU air quality legislation. In May 2008, the European Parliament and the Council of Europe adopted a new consolidated European Union Directive on ambient air quality and cleaner air for Europe — Directive 2008/50/EC. This Air Quality (AQ) Directive replaced earlier directives, simplifying and streamlining existing provisions, and introducing new provisions, in particular new objectives concerning PM 2.5. Whilst previous directives have based assessment and reporting largely on measurement data, the new AQ Directive **encourages the use of AQ models** in combination with monitoring in a range of applications.

Even though modelling is considered as being more uncertain than monitoring, there were two major reasons for using models:

- The spatial coverage of monitoring is limited. Modelling can provide complete spatial coverage of air quality.
- Modelling provides an improved understanding of the sources, causes and processes that determine air quality.

Modelling, however, does not provide all the answers, and there are a number of considerations regarding models, which include:

- Models require extensive input data that are not always reliable or easily acquired, particularly in relation to emissions and meteorology;
- model predictions remain uncertain; extensive validation is required by using monitoring data before models can be applied with confidence;
- models are only a representation of the reality; the ability of models to represent the real world is always limited by their spatial resolution and the quality of the representation of physical processes included in the models.

The modelling quality targets are described in Annex I of the AQ Directive. The quality objectives are given as a relative uncertainty percentage (%). For PM 2.5, for daily averages estimation the uncertainty is not yet defined, while for the annual estimation the uncertainty is 50 %. In order to understand the model acceptance limits we should mention that for SO_2, NO_2

and CO, the uncertainty for hourly, daily and annual estimations are 50%, 50% and 30% respectively.

The model data used originated from the CAMx model, and it was provided by the Laboratory of Atmospheric Physics of the Aristotle University of Thessaloniki. The analysis of these data showed that seasonal variation of PM 2.5 differed across Europe, and in many locations it was less obvious than that of AOD. In addition, the PM 2.5 monthly average maps showed the significant impact of the boundaries' conditions, especially in the western boundary of the model (Liora et al, 2013), as well as of the natural sea salt emissions, especially over the Atlantic Ocean area (Manders et al, 2010; Sofiev et al, 2011), upon the predicted concentration. In these areas, the PM 2.5 concentration calculated by the model was over 36 μg/m3, with high values up to 70 μg/m3 (only observed over oceanic areas). These high sea salt emissions can probably cause increased PM 2.5 values in countries like Ireland, UK, France or Portugal (up to 40 μg/m3 during winter, spring and autumn). Over the rest of Europe, higher PM 2.5 values were estimated during winter and autumn, due probably to greater anthropogenic emissions from central heating or other manmade activities. The lowest calculated PM 2.5 values were found during summer periods, when PM 2.5 was below 20 μg/m3 almost all over Europe.

The variation of the spatial distribution of PM 2.5 concentration over Europe could be explained if we consider the complexity of the physical and chemical procedures related to ambient PM pollution levels. There are several different conflicting factors that affect the PM 2.5 concentration at the local or regional scales. For example, high precipitation during autumn and winter might result in lower particulate matter air pollution (Textor, 2006), however this phenomenon cause either negligible or adverse effect to AOD (Gryspeerdt, 2015, Andreae, 2008), while at the same time, the lower boundary layer height results in higher ground level PM concentrations.

In this study, the relation between AOD and PM 2.5 was examined by performing regression analysis at 22 locations across Europe. Meteorological parameters were also used in the regression analysis, since it is well known from previous research that the relationship between AOD and PM 2.5 concentrations can be modified by meteorological parameters such as mixing height, relative humidity, air temperature, and wind speed (Koelemeijer et al. 2006; Liu et al. 2005, 2007; Pelletier et al. 2007; van Donkelaar et al. 2006). The meteorological data were also derived from a model; the weather forecasting model, WRF, was used.

The study confirmed a conclusion reached by other relevant studies, namely **that the relationship between AOD and PM 2.5 is highly variable for different regions and at different time scales** (Engel-Cox, 2004; Hu et al, 2013). Thus, a localized method was considered to be the most appropriate for the building of prediction models, in comparison to a uniform statistical regression analysis everywhere. The study also confirmed **that the use of meteorological data could improve the PM 2.5 to AOD correlation**.

A strong correlation of AOD – PM 2.5 was established for winter and autumn in most locations. During spring and, especially, summer the regression models did not produce good results for most of the places that were modelled.

A spatial autocorrelation in the regression results appeared only during winter. **For all the other seasons, the spatial pattern of the results was random**.

AOD or AOD/PBL was the most dominant factor in the regression analysis in only in 40% of the cases with good results. In 60% of cases, one of the meteorological factors (RH, WS or PBL) was the most important factor in the regression equation. Generally, the use of meteorological parameters, in addition to the use of satellite AOD in order to estimate the ground level concentration of PM 2.5, improved the results of the regression analysis between AOD and PM 2.5. Especially in cases where AOD or AOD/PBL was the most important parameter in the regression equation, it was observed that the use of meteorological parameters improved the regression performance from 3% to 32%.

Chapter 6: Discussion

Among the factors that should be considered in the evaluation of the results of this study are:

1. **Spatial accuracy of MODIS aerosols datasets.**

   The 1-degree spatial resolution of MODIS AOD dataset was very rough and thus it was very difficult to show local variations in the PM 2.5 concentration. In most studies where a good relationship between AOD and PM 2.5 was found, high-resolution remote sensing data was used (Yuanyu, 2015; Chudnovsky, 2013). The effect of AOD spatial resolution on PM 2.5 concentration prediction was also examined by Strandgren et al. (2014). According to their research, the correlation between PM 2.5 and AOD increased significantly with increasing spatial resolution of the AOD.

   The effect of local conditions in PM 2.5 concentration was demonstrated also in this study by the analysis of the air quality measurements collected at the two stations in Athens (LYK and AGP), which, although they were in the same AOD cell, showed significant differences in the PM 2.5 daily, monthly and yearly concentration values.

2. **The accuracy of the air quality model.**

   The produced PM 2.5 monthly average maps showed very high concentration of PM 2.5 in the west side boundary of the modelling domain. This was probably the result of the boundary conditions for natural emissions (calculated using the MOZART model) used in the air quality model, which were relatively high in that area due to high estimation of sea salt emissions from the Atlantic Ocean. Such evidence, of over estimation of sea salt emissions, can be found also in several other studies (Zhang et al., 2013; de Leeuw et al., 2011; Yang et al., 2011). A possible overestimation of the natural sea salt emissions could affect the PM 2.5 concentrations of the model and thus the results of the regression analysis between AOD and PM 2.5.

   Also, although the model results were validated and thus can be accepted, the magnitude of the accepted uncertainty percentage (50% in yearly average values) makes it difficult to perform such an analysis using only modelled values. Other datasets (such as the ENSEMBLE reanalysis dataset (MACC III Project, 2015) might be more suitable for this purpose, since it was created using both measurements from

several monitoring stations as well as model data, in order to provide a more accurate estimation of the pollution concentration in Europe.

3. **Daily averaged PM 2.5** values were used in the regression analysis, even though the AOD measurements were taken at a specific time, during the satellite overpass. Since PM 2.5 concentration shows a significant variation during the day, this might result in an additional error in the AOD/PM relation. PM 2.5 concentration in urban areas usually displays a bimodal pattern, with one morning and one evening peak. The morning peak is due to enhanced anthropogenic transport activity during rush hours. The decreases of boundary layer height in the afternoon, accompanied by increased transport activity during the afternoon rush hour, results in the second PM 2.5 peak (Xiujuan, 2009).

4. A drawback of the use of AOD as a PM 2.5 predictor is that it can only be measured under low cloud conditions, and thus it can provide indirect PM 2.5 estimation only for those days. This is the result of the AOD calculation algorithm, which screens out unwanted features like clouds, water, snow/ice pixels, discards the brightest 50% and darkest 20% of pixels, and then applies the retrieval algorithm only if sufficient pixels remain. Also, the quality of the MODIS AOD retrievals decreases when the underlying surface becomes bright and/or heterogeneous as is the case in many urban regions (Levy et al., 2010).

Nevertheless, this study demonstrated that remote sensing data like AOD can be used to provide air quality information, which is very useful because of its global coverage, especially in places with a lack of a sufficiently dense air quality measurement network. A regional approach is probably the most suitable approach because of the complex physical and chemical parameters that affect air pollution concentrations. In the future, improvements in satellite remote sensing of the atmosphere, as well as the use of higher spatial and temporal resolution data, will lead to more accurate predictions of PM 2.5 based on satellite observations of the atmosphere.

References

Afshar, H. and Delavar, M.R. (2007). A GIS based Air Pollution Modelling in Tehran, Environmental Informatics Archives, ISEIS Publication Number P002, Vol. 5, 557–566

Albrecht, B.A., (1989) Aerosols, cloud microphysics, and fractional cloudiness. Science, 245, pp. 1227-1230

Andreae, M. and Rosenfeld, D. (2008). Aerosol cloud precipitation inter-actions. Part 1. The nature and sources of cloud-active aerosols, Earth Sci. Rev., 89, 13–41, doi:10.1016/j.earscirev.2008.03.001Benas, N., Beloconi, A., Chrysoulakis, N. (2013). Estimation of urban PM10 concentration, based on MODIS and MERIS/AATSR synergistic observations. Atmospheric Environment, 79, 448 - 454.

Beuchle, R., Grecchi, R. C., Shimabukuro, Y. E., Seliger, R., Eva, H. D., Sano, E., Achard, F. (2015). Land cover changes in the Brazilian Cerrado and Caatinga biomes from 1990 to 2010 based on a systematic remote sensing sampling approach, Applied Geography, Volume 58, Pages 116-127

Boccardo, P., Tonolo, F. G. (2014). Remote Sensing Role in Emergency Mapping for Disaster Response. Engineering Geology for Society and Territory - Volume 5, Springer International Publishing, ISBN 978-3-319-09047-4 pp 17-24

Carmichael, G. R., Adhikary, B., Kulkarni, S., D'allura, A., Tang, Y., Streets, D., Zhang, Q., Bond, T. C., Ramanathan, V., Jamroensan, A., Marrapu, P. (2009). Asian aerosols: Current and year 2030 distributions and implications to human health and regional climate change. Environmental Science & Technology 43 (15) 5811-5817

Chin, M., Diehl, T., Ginoux, P. and Malm, W. (2007). Intercontinental transport of pollution and dust aerosols: implications for regional air quality. Atmospheric Chemistry and Physics, 7, 5501-5517.

Chin, M., Kahn, R., and Schwartz, S. (2009). Atmospheric Aerosol Properties and Climate Impacts: A Report by the U.S. Climate Change Science Program and the Subcommittee on Global Change Research. Washington, DC: NASA.

Chislock, M. F., Doster, E., Zitomer, R. A. & Wilson, A. E. (2013) Eutrophication: Causes, Consequences, and Controls in Aquatic Ecosystems. Nature Education Knowledge 4(4):10

Chu, D.A. (2006). Analysis of the relationship between MODIS aerosol optical depth and PM 2.5 over the summertime US. Proc. SPIE 6299 (29903-29903)

Chu, D.A., Kaufman, Y.J., Zibordi, G., Chern, J.D., Mao, J., Li, C. and Holben, B.N. (2003). Global Monitoring of Air Pollution over Land from the Earth Observing System-Terra Moderate Resolution Imaging Spectroradiometer (Modis). J. Geophys. Res. 108: 4661, doi: 10.1029/2002JD003179.

Chudnovsky, A., Tang, C., Lyapustin, A., Wang, Y., Schwartz, J., and Koutrakis, P. (2013). A critical assessment of high-resolution aerosol optical depth retrievals for fine particulate matter predictions. Atmos. Chem. Phys., 13, 10907–10917

Chylek, P., Wong, J. (1995). Effect of absorbing aerosols on global radiation budget. Geophysical research letters, 22(8), 929-931.

Copernicus (2016). Marine Environment Monitoring Service. [ONLINE] Available at: http://marine.copernicus.eu/training/education/observation/satellites/. [Accessed 1 December 2016].

Corcoran, J. M., Knight, J. F., Gallant, A. L. (2013). Influence of Multi-Source and Multi-Temporal Remotely Sensed and Ancillary Data on the Accuracy of Random Forest Classification of Wetlands in Northern Minnesota. Remote Sensing 5(7), 3212-3238; doi:10.3390/rs5073212

Daly, A. and Zannetti P. (2007). Air Pollution Modeling–An Overview. Chapter 2 of Ambient Air Pollution, Published by The Arab School for Science and Technology (ASST) and The EnviroCamp Institute.

de Leeuw, G., Andreas, E. L., Anguelova, M. D., Fairall, C. W., Lewis, E. R., O'Dowd, C., Schulz, M., and Schwartz, S. E. (2011). Production flux of sea spray aerosol, Reviews of Geophysics, 49, 10.1029/2010RG000349.

Dockery, D.W. and Stone, P.H. (2007) Cardiovascular Risks from Fine Particulate Air Pollution. The New England Journal of Medicine, 356, 511-513.

Dockery, D.W., Pope, C.A., Xu, X., (1993). An association between air pollution and mortality in six U.S. cities. N Engl J Med, 329, 1753-1759

Donkelaar, A., Martin, R.V., Brauer, M., Kahn, R., Levy, R., Verduzco, C. and Villeneuve, P.J. (2010). Global Estimates of Ambient Fine Particulate Matter Concentrations from Satellite-Based Aerosol Optical Depth: Development and Application. Environmental Health Perspectives volume 118 number 6, 847-855

Edussuriya, P. S. (2000). Impact of urban physical design attributes on urban air quality and microclimate: towards formulation of urban design guidelines for Mong Kok. University of Hong Kong, Pokfulam, Hong Kong.

El-Sharkawy, M. M., Sheta, A. S., Abd El-Washed, M. S., Arafat, S. M., El Bahiery, O. M. (2016). Precision Agriculture Using Remote Sensing and GIS for Peanut Crop Production in Arid Land. International Journal of Plants & Soil cience, 10(3): 1-9, Article no.IJPSS.20539

European Commission. (2016a). *Legislation - Air - Environment*. [ONLINE] Available at: http://ec.europa.eu/environment/air/legis.htm. [Accessed 1 December 2016].

European Commission. (2016b). *Existing Legislation - Air Quality - Environment*. [ONLINE] Available at: http://ec.europa.eu/environment/air/quality/legislation/existing_leg.htm. [Accessed 1 December 2016].

European Environmental Agency (EEA) (2013). Building our knowledge about air. [ONLINE] Available at: http://www.eea.europa.eu/signals/signals-2013/articles/building-knowledge-about-air. [Accessed 28 July 2016].

European Environmental Agency (EEA) (2015). Air quality in Europe – 2015 report. EEA report No 5/2015. ISBN 978-92-9213-702-1, doi:10.2800/62459

European Topic Centre on Air Pollution and Climate Change Mitigation (ETC/ACM) (2013). The European Exchange of information in 2012. ETC/ACM Technical Paper 2013/1

Engel-Cox, J.A., Holloman, C.H., Coutant, B.W. and Hoff, R.M. (2004). Qualitative and Quantitative Evaluation of MODIS Satellite Sensor Data for Regional and Urban Scale Air Quality. Atmos. Environ. 38: 2495–2509.

Engle-Cox, J.A., Holloman, C.H., & Coutant, B.W. (2004). Qualitative and quantitative evaluation of MODIS satellite sensor data for regional and urban scale air quality. Atmospheriv Environment 38, 2495-2509

Fabry, V. J., Seibel, B. A., Feely, R. A., and Orr, J. C. (2008). Impacts of ocean acidification on marine fauna and ecosystem processes. ICES Journal of Marine Science, 65, 414–432.

Flash Eurobarometer 360, (2013) ATTITUDES OF EUROPEANS TOWARDS AIR QUALITY

George, J., Harenduprakash, L. and Mohan, M., (2006) A study of the Spatial and Temporal Distribution of Aerosols over India and Surrounding Seas using TOMS and MODIS Data Products, Remote Sensing and Modeling of the Atmosphere, Oceans, and Interactions, edited by Tiruvalam N. Krishnamurti, B. N. Goswami, Toshiki Iwasaki, Proc. of SPIE Vol. 6404, 640413

Goddard Earth Sciences Data and Information Services Center (GES DISC), (2016). *Aerosol Angstrom Exponent*. [ONLINE] Available at: https://disc.gsfc.nasa.gov/data-holdings/PIP/aerosol_angstrom_exponent.shtml. [Accessed 1 December 2016].

Gryspeerdt, E., Stier, P., White, B. A., and Kipling, Z. (2015). Wet scavenging limits the detection of aerosol effects on precipitation. Atmos. Chem. Phys., 15, 7557–7570

Guo, J-P., Zhang, X-Y., Che, H-Z., Gong, S-L., An, X., Cao, C-X., Guang, J., Zhang, H., Wang, Y-Q., Zhang, X-C., Xue, M., Li, X-W. (2009). Correlation between PM concentrations and aerosol optical depth in eastern China. Atmospheric Environment, Vol 43, Issue 37, 5876–5886

Gupta, P. and Christopher, S.A. (2009). Particulate matter Air Quality Assessment Using Integrated Surface, Satellite, and Meteorological Products: Multiple Regression Approach. J. Geophys. Res. 114: D14205.

Gupta, P. and Christopher, S.A., 2009. Particulate matter air quality assessment using integrated surface, satellite and meteorological products: Multiple regression approach. Journal of Geophysical Research-Atmospheres, 114

Gupta, P., Christopher, S.A., Wang, J., Gehrig, R., Lee, Y. and Kumar, N. (2006). Satellite Remote Sensing of Particulate Matter and Air Quality Assessment over Global Cities. Atmos. Environ. 40: 5880–5892.

Gupta, P., Christopher, S.A., Wang, J., Gehrig, R., Lee, Y., Kuma,r N. (2006). Satellite remote sensing of particulate matter and air quality assessment over global cities. Atmos. Environ. 40 (30), 5880-5892

Hegazy, I. R., Kaloop, M. R. (2015). Monitoring urban growth and land use change detection with GIS and remote sensing techniques in Daqahlia governorate Egypt. International Journal of Sustainable Built Environment, Volume 4, Issue 1, June 2015, Pages 117–124

Hinds, W. C. (1999). Aerosol Technology: Properties, Behavior, and Measurement of Airborne Particles, 2nd Edition. ISBN: 978-0-471-19410-1

Hogan, C. (2012). Microclimate. [Online]. Available from: http://www.eoearth.org/view/article/160653

Hogan, C. (2012). Microclimate. Retrieved from http://www.eoearth.org/view/article/160653

Holben, B., Tanré, D., Smirnov, A., et al (2001). An emerging ground-based aerosol climatology: aerosol optical depth from AERONET. Journal of Geophysical Research, VOL. 106, NO. D11, PP. 12,067-12,097.

Hu, X., Waller, L.A., Al-Hamdan, M.Z., Crosson, W.L., Estes, M.G. Jr, Estes, S.M., Quattrochi, D.A., Sarnat, J.A., Liu, Y. (2013). Estimating ground-level PM(2.5) concentrations in the southeastern U.S. using geographically weighted regression. Environmental Research, 121, 1-10

Hu, Z. (2009). Spatial Analysis of MODIS Aerosol Optical Depth PM 2.5 and Chronic Coronary Heart Disease. Int. J. Health Geographics 8: 27, doi: 10.1186/1476-072X-8-*27*

ICF International. (2016). The UAM-V Photochemical Modeling System. [ONLINE] Available at: http://uamv.icfconsulting.com/overview.htm. [Accessed 1 December 2016].

Intergovernmental Panel on Climate Change (IPCC), (2001). Climate Change 2001: The Scientific Basis, Cambridge University Press, New York

Intergovernmental Panel on Climate Change (IPCC), (2007). Climate Change 2007: The Physical Science Basis, Cambridge University Press, New York

Intergovernmental Panel on Climate Change (IPCC), (2013). Climate Change 2013: The Physical Science Basis: Summary for Policymakers, Cambridge, UK, 2013

IUPAC, (1997). Compendium of Chemical Terminology, 2nd ed. (the "Gold Book"). Compiled by A. D. McNaught and A. Wilkinson. Blackwell Scientific Publications, Oxford

Kaufman, Y. J., Tanre, D. and Boucher, O., (2002) A satellite view of aerosols in the climate system, Nature, 419, 215–223

King, M.D. and Herring, D.D. (2000). Monitoring the Earth's Vital Signs, Sci. Am., 92-97

Koelemeijer, R.B.A., Homan, C.D., Matthijsen, J. (2006). Comparison of spatial and temporal variations of aerosol optical thickness and particulate matter over Europe. Atmos. Environ. Vol 40, Is. 27, 5304-5315

Koren, I., Kaufman, Y., Remer, L., and Martins, J. (2004). Measurement of the effect of Amazon smoke on inhibition of cloud formation. Science, 303, 1342

Kucera, V., Fitz, S. (1995). Direct and indirect air pollution effects on materials including cultural monuments. Water, Air, and Soil Pollution, Volume 85, Issue 1, pp 153-165

Kumar, N., Chu, A., Foster, A.D. (2007). An empiricl relationship between PM 2.5 and aerosol optical depth in Delhi Metropolitan. Atmos. Environ. 41, 4492-4503

Lee, H. J., Liu, Y., Coull, B. A., Schwartz, J., and Koutrakis, P. (2011). A novel calibration approach of MODIS AOD data to predict PM 2.5 concentrations. Atmos. Chem. Phys. Discuss., 11, 9769-9795

Levin, Z. and Cotton, W.R. (2008). Aerosol pollution impact on precipitation: A scientific review. Report from the WMO/IUGG International Aerosol Precipitation Science, Assessment Group (IAPSAG). Geneva, Switzerland: World Meteorological Organization.

Levy, R.C., Remer, L.A., Kleidman, R.G., Mattoo, S., Ichoku, C., Kahn, R., Eck, T.F.: Global evaluation of the collection 5 MODIS dark–target aerosol products over land Atmospheric Chemistry and Physics, 10, pp. 10399–10420, 2010

Li, C.C., Mao, J.T., Lau, A.K. et al (2003). Research on the air pollution in Beijing and its surroundings with MODIS AOD product. Chinese Journal of Atmospheric Science. 37, 869-880

Li, H., Faruque, F., Williams, W., Al-Hamdan, M., Luvall, J., Crosson, W., Rickman, D., Limaye, A. (2009). Optimal temporal scale for the correlation of AOD and ground

measurements of PM 2.5 in a real-time air quality estimation system. Atmos. Environ. 43, 4303-4310

Li, J., Cui, Y., Liu, J., Shi, W., Qin, Y. (2013). Estimation and analysis of net primary productivity by integrating MODIS remote sensing data with a light use efficiency model, Ecological Modelling, Volume 252, Pages 3-10

Liakos, V., Tagarakis, A., Foundas, S., Nanos, G. D., Tsiropoulos, Z., Gemtos, T. (2015). Use of NDVI to predict yield variability in a commercial apple orchard. Precision agriculture ´15. ISBN: 978-90-8686-267-2, DOI: http://dx.doi.org/10.3920/978-90-8686-814-8 Pages 553-560

Liora, N., Markakis, K., Poupkou, A., Dimopoulos, S., Giannaros, T., Melas, D. (2013). Particulate matter emissions from natural sources in Europe – A case study of the impact of natural sources on PM pollution levels, ACCENT Plus Symposium 2013 Urbino, Italy

Liu, Y., Koutrakis, P., Kahn, R., Turquety, S., Yantosca, R.M. (2007). Estimating fine particulate matter component concentrations and size distributions using satellite-retrieved fractional aerosol optical depth: pat 2 – a case study. J. Air Waste Manag. Assoc. 57 (11), 1360-1369

Liu, Y., Paciorek, C.J. and Koutrakis, P. (2009). Estimating Regional Spatial and Temporal Variability of PM Concentrations Using Satellite Data, Meteorology, and Land Use Information. Environmental Health Perspectives 117(6): 886-892.

Liu, Y., Park, R.J., Jacob, D.J., Li, Q., Kilaru, V. and Sarnat, J.A. (2004). Mapping annual mean ground-level PM 2.5 concentrations using Multiangle Imaging Spectroradiometer aerosol optical thickness over the contiguous United States. Journal of Geophysical Research 109. doi: 10.1029/2004JD005025. issn: 0148-0227

Liu, Y., Sarnat, J.A., Kilaru, V., Jacob, D.J. and Koutrakis, P. (2005). Estimating Ground-Level PM 2.5 in the Eastern United States Using Satellite Remote Sensing. Environ. Sci. Technol. 39: 3269–3278.

MACC Project. (2009). *Monitoring Atmospheric Composition & Climate*. [ONLINE] Available at: http://lap.physics.auth.gr/macc/. [Accessed 26 July 2016].

MACC III Project. (2011). *MACC Project-Verification of Regional Services*. [ONLINE] Available at: http://www.gmes-atmosphere.eu/services/aqac/regional_verification/. [Accessed 26 July 2016].

Macdonald, R. (2003). Theory and Objective of Air Dispersion Modelling, Modelling Air Emissions for Compliance, MME 474A, Wind Engineering

Malherbe, L., Schneider, P., Ung, A., Jimmink, B., de Leeuw, F. (2013). Analysis of station classification and network design. 18th EIONET meeting, Dublin.

Manders, A.M.M., Schaap, M., Querol, X., Albert, M.F.M.A., Vercauteren, J., Kuhlbusch, T.A.J., Hoogerbrugg, R. (2010). Sea salt concentrations across the European continent. Atmospheric Environment 44 2434-2442

Melesse, A., Weng, Q., Thenkabail, P.S. and Senay, G.B. (2007). Remote Sensing Sensors and Applications in Environmental Resources Mapping and Modelling, Sensors 2007, 7, 3209-3241

Michalakes, J., J. Dudhia, D. Gill, T. Henderson, J. Klemp, W. Skamarock, and W. Wang, 2004: "The Weather Reseach and Forecast Model: Software Architecture and Performance,"to appear in proceedings of the 11th ECMWF Workshop on the Use of High Performance Computing In Meteorology, 25-29 October 2004, Reading U.K.

Michalakes, J., S. Chen, J. Dudhia, L. Hart, J. Klemp, J. Middlecoff, and W. Skamarock (2001): *Development of a Next Generation Regional Weather Research and Forecast Model. Developments in Teracomputing: Proceedings of the Ninth ECMWF Workshop on the Use of High Performance Computing in Meteorology*. Eds. Walter Zwieflhofer and Norbert Kreitz. World Scientific, Singapore. pp. 269-276.

Miller, K.A., Siscovick, D.S., Sheppard, L. et al (2007). Long-term exposure to air pollution and incidence of cardiovascular events in women. N Engl J Med, 356, 447-458

Nammalwar, P., Satheesh, S., Ramesh, R. (2013). Applications of Remote Sensing in the validations of Potential Fishing Zones (PFZ) along the coast of North Tamil Nadu, India. Indian Journal of Geo-Marine Sciences, 42 (3). pp. 283-292

National Aeronautics and Space Administration (NASA), (2016a). *Terra Instruments*. [ONLINE] Available at: https://terra.nasa.gov/about/terra-instruments. [Accessed 1 December 2016].

National Aeronautics and Space Administration (NASA), (2016b). *Terra Spacecraft*. [ONLINE] Available at: https://www.nasa.gov/mission_pages/terra/spacecraft/index.html. [Accessed 1 December 2016].

National Aeronautics and Space Administration (NASA), (2016c). *Instruments Aqua Project Science*. [ONLINE] Available at: https://aqua.nasa.gov/content/instruments. [Accessed 1 December 2016].

National Aeronautics and Space Administration (NASA), (2016d). MODIS Atmosphere: Daily Global Products. [ONLINE] Available at: http://modis-atmos.gsfc.nasa.gov/MOD08_D3/. [Accessed 1 December 2016].

National Aeronautics and Space Administration (NASA), (2016e). *MODIS Terra*. [ONLINE] Available at: https://terra.nasa.gov/about/terra-instruments/modis. [Accessed 1 December 2016].

Nowak, D.J. (1994). Air pollution removal by Chicago's urban forest. In: McPherson, E.G, D.J. Nowak and R.A. Rowntree. Chicago's Urban Forest Ecosystem: Results of the Chicago Urban Forest Climate Project. USDA Forest Service General Technical Report NE-186. pp. 63-81

OpenWeatherMap (2016). *Models*. [ONLINE] Available at: https://openweathermap.org/models. [Accessed 1 December 2016].

Orr, J.C. et al (2005). Anthropogenic ocean acidification over the twenty-first century and its impact on calcifying organisms. Nature 437, 681-686

Paciorek, C.H., Liu, Y., Moreno-Macias, H. and Kondragunta, S. (2008). Spatiotemporal Associations between GOES Aerosol Optical Depth Retrievals and Ground-Level PM 2.5. Environ. Sci. Technol., 2008, 42 (15), 5800–5806

Park, M., Kim, M., Lee, M., Im, J., Park, S. (2016). Detection of tropical cyclone genesis via quantitative satellite ocean surface wind pattern and intensity analyses using decision trees, Remote Sensing of Environment, Volume 183, Pages 205-214

Pelletier, B., Sante,r R., Vidot, T. (2007). Retrieving of particulate matter from optical measurements: a semiparametric approach. Journal of Geophysical Research 112, D06208

Pérez, L., Sunyer, J., Künzli, N. (2009). Estimating the health and economic benefits associated with reducing air pollution in the Barcelona metropolitan area (Spain). Gac Sanit, 23 (4), pp. 287–294

Peters, A., Dockery, D.W., Muller, J.E. and Mittleman, M.A. (2001). Increased Particulate Air Pollution and the Triggering of Myocardial infarction. Circulation 103: 2810–2815

Petrenko, M., Ichoku, C. (2013). Coherent uncertainty analysis of aerosol measurements from multiple satellite sensors. Atmos. Chem. Phys., 13, 6777–6805

Pope, C.A. III. (2000). Epidemiology of Fine Particulate Air Pollution and Human Health: Biologic Mechanisms and Who's at Risk? Environ. Health Perspect. 108: 713–723.

Pope, C.A., Thun, M.J., Namboodiri, M.M., et al (1995). Particulate air pollution as a predictor of mortality in a prospective study of U.S. adults. Am J Respir Crit Care Med,151, 669-674

Prata, F., Bluth, G., Werner, C., Realmuto, V., Carn, S., Watson, M. (2015). Remote sensing of gas emissions from volcanoes. Monitoring Volcanoes in the North Pacific: Observations from space. Springer Berlin Heidelberg, ISBN 978-3-540-68750-4 DOI 10.1007/978-3-540-68750-4_6 pp 145-186

Qie, L., Li, Z,, Sun, X., Sun, B., Li, D., Liu, Z., Huang, W., Wang, H., Chen, X., Hou, W., and Qiao, Y. (2015). Improving Remote Sensing of Aerosol Optical Depth over Land by Polarimetric Measurements at 1640 nm: Airborne Test in North China. Remote Sens. 2015, 7(5), 6240-6256; doi:10.3390/rs70506240

Ramboll Environ. (2016). *CMAx Overview*. [ONLINE] Available at: http://www.camx.com/about/default.aspx. [Accessed 1 December 2016].

Saiz-Jimenez (ed.), (2004). Air pollution and cultural heritage. Taylor and Francis Group, ISBN 90 5809 682 3

Schaap, M., Apituley, A., Timmermans, R.M.A., Koelemeijer, R.B.A., Leeuw, G. (2009). Exploring the relation between aerosol optical depth and PM 2.5 at Cabauw, the Nederlands. Atmos. Chem. Phys. 9, 909-925

Sharma, N., Choudhary, K.K. and Rao, C.V.C. (2004). Vehicular Pollution Prediction Modelling: A Review of Highway Dispersion Models", Transport Reviews, Vol. 24, No. 4, 409–435

Shen, L., Xu, H., Guo, X. (2012). Satellite Remote Sensing of Harmful Algal Blooms (HABs) and a Potential Synthesized Framework. Sensors (Basel). 12(6): 7778–7803

Sofiev, M., Soares, J., Prank, M., Leeuw de, M. and Kukkonen J. (2011). A regional - to - global model of emission and transport of sea salt particles in the atmosphere. JOURNAL OF GEOPHYSICAL RESEARCH, VOL. 116, D21302, doi:10.1029/2010JD014713

Solomon, S. (1999). Stratospheric ozone depletion: a review of concepts and history. Rev. Geophysics 37, 275-316

Song, W., Jia, H., Huang, J., Zhang, Y. (2014). A satellite-based geographically weighted regression model for regional PM 2.5 estimation over the Pearl River Delta region in China. Remote Sensing of Environment, Volume 154, 1–7

Strandgren, J., Mei, L., Vountas, M., Burrows, J. P., Lyapustin, A., and Wang, Y. (2014). Study of satellite retrieved aerosol optical depth spatial resolution effect on particulate matter concentration prediction. Atmos. Chem. Phys. Discuss., 14, 25869–25899

Textor, C., Schulz, M., Guibert, S., Kinne, S., Balkanski, Y., Bauer, S., Berntsen, T., Berglen, T., Boucher, O., Chin, M., Dentener, F., Diehl, T., Easter, R., Feichter, H., Fillmore, D., Ghan, S., Ginoux, P., Gong, S., Grini, A., Hendricks, J., Horowitz, L., Huang, P., Isaksen, I., Iversen, I., Kloster, S., Koch, D., Kirkevåg, A., Kristjansson, J. E., Krol, M., Lauer, A., Lamarque, J. F., Liu, X., Montanaro, V., Myhre, G., Penner, J., Pitari, G., Reddy, S., Seland, Ø., Stier, P., Takemura, T., and Tie, X. (2006). Analysis and quantification of the diversities of aerosol life cycles within AeroCom, Atmos. Chem. Phys., 6, 1777–1813, doi:10.5194/acp-6-1777-2006

Tian, J., Chen, D. (2010). A semi-empirical model for predicting hourly ground-level fine particulate matter (PM 2.5) concentration in southern Ontario from satellite remote sensing and ground-based meteorological measurements. Remote Sensing of Environment, Volume 114, Issue 2, 221–229

Toth, T.D., Zhang, J., Campbell, J.R., Hyer, E.J., Reid, J.S., Shi, Y. and Westphal, D.L. (2014). Impact of Data Quality and Surface-to-Column Representativeness on the PM 2.5 /Satellite

Aod Relationship for the Contiguous United States. Atmos. Chem. Phys.14: 6049–6062, doi:10.5194/acp-14-6049-2014.

Tourville, N., Stephens, G., DeMaria, M., Vane, D. (2015). Remote Sensing of Tropical Cyclones: Observations from CloudSat and A-Train Profilers. Bulletin of the American Meteorological Society, Vol 96 No. 4, pp 609-622

Twomey, S., (1977) Developments in Atmospheric Science, Atmospheric Aerozols (Amsterdam: Elsevier Scientific Publications)

UCAR. (2016). *MM5 Community Model*. [ONLINE] Available at: http://www2.mmm.ucar.edu/mm5/mm5-home.html. [Accessed 1 December 2016].

UNC. (2016). *CMAS: Community Modeling and Analysis System*. [ONLINE] Available at: https://www.cmascenter.org/cmaq/. [Accessed 1 December 2016]

Van Donkelaar, A., Martin, R.V. and Park, R.J. (2006). Estimating ground-level PM 2.5 using aerosol optical depth determined from satellite remote sensing. Journal of Geophysics Research, Vol. 111, D21201, doi:10.1029/2005JD006996

Van Donkelaar, A., Martin, R.V., Brauer, M., Kahn, R., Levy, R., Verduzco, C. and Villeneuve, P.J. (2010). Global Estimates of Ambient Fine Particulate Matter Concentrations from Satellite-Based Aerosol Optical Depth: Development and Application. Environ. Health Perspect. 118: 847–855.

Wang, J., & Christopher, A. (2003). Intercomparison between satellite-derived aerosol optical thickness and PM 2.5 mass: Implications for air quality studies. Geophysics Research Letters, 30, 1-4

Wang, Z., Chen, L., Tao, J., Zhang, Y. and Su, L. (2010). Satellite-Based Estimation of Regional Particulate Matter (PM) in Beijing Using Vertical-and-Rh Correcting Method. Remote Sens. Environ. 114: 50–63.

Xiujuan Zhao, Xiaoling Zhang, Xiaofeng Xu, Jing Xu, Wei Meng, Weiwei Pu (2009). Seasonal and diurnal variations of ambient PM 2.5 concentration in urban and rural environments in Beijing. Atmospheric Environment Volume 43, Issue 18, Pages 2893–2900

Yang, Q., W. I. Gustafson, J., Fast, J. D., Wang, H., Easter, R. C., Morrison, H., Lee, Y. N., Chapman, E. G., Spak, S. N., and Mena - Carrasco, M. A. (2011). Assessing regional scale

predictions of aerosols, marine stratocumulus, and their interactions during VOCALS-REx using WRF-Chem, Atmos. Chem. Phys., 11, 11951-11975, 10.5194/acp-11-11951-2011.

Yap, X.Q., Hashim, M. (2013). A robust calibration approach for PM 10 prediction from MODIS aerosol optical depth. Atmos. Chem. Phys., 13, 3517–3526

Yuanyu Xie, Yuxuan Wang, Kai Zhang, Wenhao Dong, Baolei Lv, and Yuqi Bai (2015). Daily Estimation of Ground-Level PM 2.5 Concentrations over Beijing Using 3 km Resolution MODIS AOD. Environ. Sci. Technol., 49 (20), pp 12280–12288

Zanchetta, A., Bitelli, G., Karnieli, A. (2016). Monitoring desertification by remote sensing using the Tasselled Cap transform for long-term change detection. Natural Hazards, Vol 83, Supplement 1, pp 223-237

Zhang, Y., Sartelet, K., Zhu, S., Wang, W., Wu, S. Y., Zhang, X., Wang, K., Tran, P., Seigneur, C., and Wang, Z. F. (2013). Application of WRF/Chem-MADRID and WRF/Polyphemus in Europe – Part 2: Evaluation of chemical concentrations and sensitivity simulations, Atmos. Chem. Phys., 13, 6845-6875, 10.5194/acp-13-6845-2013

Zhao, N., Yang, Y. H., & Zhou, X. Y. (2010). Application of geographically weighted regression in estimating the effect of climate and site conditions on vegetation distribution in Haihe Catchment, China. Plant Ecology, 209, 349–359

Zhao, X., Chan, P. (2014). NOAA Climate Data Record (CDR) of AVHRR Daily and Monthly Aerosol Optical Thickness over Global Oceans, Version 2.0. NOAA National Centers for Environmental Information. doi:10.7289/V5SB43PD

List of previous published master thesis reports

Series from Lund University:

Department of Physical Geography and Ecosystem Science

Master Thesis in Geographical Information Science

1. *Anthony Lawther:* The application of GIS-based binary logistic regression for slope failure susceptibility mapping in the Western Grampian Mountains, Scotland (2008).
2. *Rickard Hansen:* Daily mobility in Grenoble Metropolitan Region, France. Applied GIS methods in time geographical research (2008).
3. *Emil Bayramov:* Environmental monitoring of bio-restoration activities using GIS and Remote Sensing (2009).
4. *Rafael Villarreal Pacheco:* Applications of Geographic Information Systems as an analytical and visualization tool for mass real estate valuation: a case study of Fontibon District, Bogota, Columbia (2009).
5. *Siri Oestreich Waage:* a case study of route solving for oversized transport: The use of GIS functionalities in transport of transformers, as part of maintaining a reliable power infrastructure (2010).
6. *Edgar Pimiento:* Shallow landslide susceptibility – Modelling and validation (2010).
7. *Martina Schäfer:* Near real-time mapping of floodwater mosquito breeding sites using aerial photographs (2010).
8. *August Pieter van Waarden-Nagel:* Land use evaluation to assess the outcome of the programme of rehabilitation measures for the river Rhine in the Netherlands (2010).

9. *Samira Muhammad:* Development and implementation of air quality data mart for Ontario, Canada: A case study of air quality in Ontario using OLAP tool. (2010).

10. *Fredros Oketch Okumu*: Using remotely sensed data to explore spatial and temporal relationships between photosynthetic productivity of vegetation and malaria transmission intensities in selected parts of Africa (2011).

11. *Svajunas Plunge:* Advanced decision support methods for solving diffuse water pollution problems (2011).

12. *Jonathan Higgins:* Monitoring urban growth in greater Lagos: A case study using GIS to monitor the urban growth of Lagos 1990 - 2008 and produce future growth prospects for the city (2011).

13. *Mårten Karlberg:* Mobile Map Client API: Design and Implementation for Android (2011).

14. *Jeanette McBride:* Mapping Chicago area urban tree canopy using color infrared imagery (2011).

15. *Andrew Farina:* Exploring the relationship between land surface temperature and vegetation abundance for urban heat island mitigation in Seville, Spain (2011).

16. *David Kanyari*: Nairobi City Journey Planner: An online and a Mobile Application (2011).

17. *Laura V. Drews:* Multi-criteria GIS analysis for siting of small wind power plants - A case study from Berlin (2012).

18. *Qaisar Nadeem:* Best living neighborhood in the city - A GIS based multi criteria evaluation of ArRiyadh City (2012).

19. *Ahmed Mohamed El Saeid Mustafa:* Development of a photo voltaic building rooftop integration analysis tool for GIS for Dokki District, Cairo, Egypt (2012).

20. *Daniel Patrick Taylor*: Eastern Oyster Aquaculture: Estuarine Remediation via Site Suitability and Spatially Explicit Carrying Capacity Modeling in Virginia's Chesapeake Bay (2013).

21. *Angeleta Oveta Wilson:* A Participatory GIS approach to *unearthing* Manchester's Cultural Heritage '*gold mine'* (2013).

22. *Ola Svensson:* Visibility and Tholos Tombs in the Messenian Landscape: A Comparative Case Study of the Pylian Hinterlands and the Soulima Valley (2013).

23. *Monika Ogden:* Land use impact on water quality in two river systems in South Africa (2013).

24. *Stefan Rova:* A GIS based approach assessing phosphorus load impact on Lake Flaten in Salem, Sweden (2013).

25. *Yann Buhot:* Analysis of the history of landscape changes over a period of 200 years. How can we predict past landscape pattern scenario and the impact on habitat diversity? (2013).

26. *Christina Fotiou:* Evaluating habitat suitability and spectral heterogeneity models to predict weed species presence (2014).

27. *Inese Linuza:* Accuracy Assessment in Glacier Change Analysis (2014).

28. *Agnieszka Griffin:* Domestic energy consumption and social living standards: a GIS analysis within the Greater London Authority area (2014).

29. *Brynja Guðmundsdóttir:* Detection of potential arable land with remote sensing and GIS - A Case Study for Kjósarhreppur (2014).

30. *Oleksandr Nekrasov:* Processing of MODIS Vegetation Indices for analysis of agricultural droughts in the southern Ukraine between the years 2000-2012 (2014).

31. *Sarah Tressel:* Recommendations for a polar Earth science portal

    in the context of Arctic Spatial Data Infrastructure (2014).

32. *Caroline Gevaert:* Combining Hyperspectral UAV and Multispectral Formosat-2 Imagery for Precision Agriculture Applications (2014).

33. *Salem Jamal-Uddeen:* Using GeoTools to implement the multi-criteria evaluation analysis - weighted linear combination model (2014).

34. *Samanah Seyedi-Shandiz:* Schematic representation of geographical railway network at the Swedish Transport Administration (2014).

35. *Kazi Masel Ullah:* Urban Land-use planning using Geographical Information System and analytical hierarchy process: case study Dhaka City (2014).

36. *Alexia Chang-Wailing Spitteler:* Development of a web application based on MCDA and GIS for the decision support of river and floodplain rehabilitation projects (2014).

37. *Alessandro De Martino:* Geographic accessibility analysis and evaluation of potential changes to the public transportation system in the City of Milan (2014).

38. *Alireza Mollasalehi:* GIS Based Modelling for Fuel Reduction Using Controlled Burn in Australia. Case Study: Logan City, QLD (2015).

39. *Negin A. Sanati:* Chronic Kidney Disease Mortality in Costa Rica; Geographical Distribution, Spatial Analysis and Non-traditional Risk Factors (2015).

40. *Karen McIntyre:* Benthic mapping of the Bluefields Bay fish sanctuary, Jamaica (2015).

41. *Kees van Duijvendijk:* Feasibility of a low-cost weather sensor network for agricultural purposes: A preliminary assessment (2015).

42. *Sebastian Andersson Hylander:* Evaluation of cultural ecosystem services using GIS (2015).

43. *Deborah Bowyer:* Measuring Urban Growth, Urban Form and Accessibility as Indicators of Urban Sprawl in Hamilton, New Zealand (2015).

44. *Stefan Arvidsson:* Relationship between tree species composition and phenology extracted from satellite data in Swedish forests (2015).

45. *Damián Giménez Cruz*: GIS-based optimal localisation of beekeeping in rural Kenya (2016).

46. *Alejandra Narváez Vallejo:* Can the introduction of the topographic indices in LPJ-GUESS improve the spatial representation of environmental variables? (2016).

47. *Anna Lundgren:* Development of a method for mapping the highest coastline in Sweden using breaklines extracted from high resolution digital elevation models (2016).

48. *Oluwatomi Esther Adejoro:* Does location also matter? A spatial analysis of social achievements of young South Australians (2016).

49. *Hristo Dobrev Tomov:* Automated temporal NDVI analysis over the Middle East for the period 1982 - 2010 (2016).

50. *Vincent Muller:* Impact of Security Context on Mobile Clinic Activities A GIS Multi Criteria Evaluation based on an MSF Humanitarian Mission in Cameroon (2016).

51. *Gezahagn Negash Seboka:* Spatial Assessment of NDVI as an Indicator of Desertification in Ethiopia using Remote Sensing and GIS (2016).

52. *Holly Buhler:* Evaluation of Interfacility Medical Transport Journey Times in Southeastern British Columbia. (2016).

53. *Lars Ole Grottenberg*: Assessing the ability to share spatial data between emergency management organisations in the High North (2016).

54. *Sean Grant:* The Right Tree in the Right Place: Using GIS to Maximize the Net Benefits from Urban Forests (2016).

55. *Irshad Jamal:* Multi-Criteria GIS Analysis for School Site Selection in Gorno-Badakhshan Autonomous Oblast, Tajikistan (2016).

56. *Fulgencio Sanmartín:* Wisdom-volkano: A novel tool based on open GIS and time-series visualization to analyse and share volcanic data (2016).

57. *Nezha Acil:* Remote sensing-based monitoring of snow cover dynamics and its influence on vegetation growth in the Middle Atlas Mountains (2016).

58. *Julia Hjalmarsson:* A Weighty Issue: Estimation of Fire Size with Geographically Weighted Logistic Regression (2016).

59. *Mathewos Tamiru Amato:* Using multi-criteria evaluation and GIS for chronic food and nutrition insecurity indicators analysis in Ethiopia (2016).

60. *Karim Alaa El Din Mohamed Soliman El Attar:* Bicycling Suitability in Downtown, Cairo, Egypt (2016).

61. *Gilbert Akol Echelai:* Asset Management: Integrating GIS as a Decision Support Tool in Meter Management in National Water and Sewerage Corporation (2016).

62. *Terje Slinning:* Analytic comparison of multibeam echo soundings (2016).

63. *Gréta Hlín Sveinsdóttir:* GIS-based MCDA for decision support: A framework for wind farm siting in Iceland (2017).

64. *Jonas Sjögren:* Consequences of a flood in Kristianstad, Sweden: A GIS-based analysis of impacts on important societal functions (2017).

65. *Nadine Raska:* 3D geologic subsurface modelling within the Mackenzie Plain, Northwest Territories, Canada (2017).